RESEARCH REPORT

HEALTH EFFECTS INSTITUTE

Number 117
December 2003

Peroxides and Macrophages in the Toxicity of Fine Particulate Matter in Rats

Debra L Laskin, Lisa Morio, Kimberly Hooper, Tsung-Hung Li, Brian Buckley, and Barbara Turpin

Includes a Commentary by the Institute's Health Review Committee

HEALTH
EFFECTS
INSTITUTE

The Health Effects Institute, established in 1980, is an independent and unbiased source of information on the health effects of motor vehicle emissions. HEI supports research on all major air pollutants, including regulated pollutants (such as carbon monoxide, ozone, nitrogen dioxide, and particulate matter) and unregulated pollutants (such as diesel engine exhaust, methanol, and aldehydes). To date, HEI has supported more than 220 projects at institutions in North America and Europe and has published over 140 research reports.

Typically, HEI receives half its funds from the US Environmental Protection Agency and half from 28 manufacturers and marketers of motor vehicles and engines in the US. Occasionally, funds from other public and private organizations either support special projects or provide a portion of the resources for an HEI study. Regardless of funding sources, HEI exercises complete autonomy in setting its research priorities and in reaching its conclusions. An independent Board of Directors governs HEI. The Institute's Health Research and Health Review Committees serve complementary scientific purposes and draw distinguished scientists as members. The results of HEI-funded studies are made available as Research Reports, which contain both the Investigators' Report and the Review Committee's evaluation of the work's scientific quality and regulatory relevance.

HEI STATEMENT
Synopsis of Research Report 117

Peroxides and Macrophages in Toxicity of Fine Particulate Matter

Epidemiologic studies have established an association between short-term increases in ambient levels of particulate matter and increases in morbidity and mortality. The biological mechanisms underlying these associations are not well understood, however. Dr Debra Laskin of Rutgers University and colleagues tested the hypothesis that oxidants in ambient air, such as hydrogen peroxide, may be transported by fine particulate matter into the lungs and thus contribute to lung tissue injury. HEI funded this study because the project could provide insight into transportation of volatile compounds into the lung and provide valuable information on the health effects of particles and peroxides.

APPROACH

The investigators proposed to use ammonium sulfate particles because of their prevalence in the ambient air of the eastern United States and their reportedly low toxicity in animals and humans. Rats inhaled ammonium sulfate (450 μg/m^3; particle size 0.45 ± 0.1 μm), hydrogen peroxide (10, 20 or 100 ppb), or combinations thereof, for 2 hours on a single occasion. Concentrations of hydrogen peroxide and ammonium sulfate were approximately one to two and two orders of magnitude greater than concentrations in ambient air, respectively. The investigators assessed lung tissue injury and presence of inflammatory markers in the lung. They also assessed activation of alveolar macrophages, which are involved in the first line of defense against foreign materials that enter the lung. Exposures with ^{18}O-labeled hydrogen peroxide were conducted to measure deposition in the lung. Additional experiments assessed lung injury and inflammation, after rats inhaled an organic peroxide (cumene hydroperoxide), and investigated hydrogen peroxide formation in an indoor environment.

RESULTS AND INTERPRETATION

Laskin and colleagues found little evidence for lung inflammation in rats exposed to ammonium sulfate, confirming its low toxicity. They did find some evidence for lung inflammation and activation of alveolar macrophages in rats exposed to hydrogen peroxide gas alone. They consistently found increased neutrophil influx into the lung and increased neutrophil adherence as well as increased tumor necrosis factor α expression in lung tissue in rats exposed to hydrogen peroxide gas. Less consistent changes were observed in other inflammatory endpoints, such as superoxide anion and nitric oxide production and heat shock protein expression by alveolar macrophages. Many other inflammatory endpoints were not changed, however.

After exposure to hydrogen peroxide in combination with ammonium sulfate, the investigators also observed increased neutrophil influx and adherence as well as increased tumor necrosis factor α expression. They presented some evidence that the inflammatory effects of combined exposure might have been greater than exposure to hydrogen peroxide alone. Caution is needed in interpreting these data, however, due to a lack of quantification of certain endpoints, such as neutrophil influx into lung tissue and heat shock protein expression by alveolar macrophages, and a lack of dose-response relations for other endpoints, such as superoxide anion and nitric oxide production by alveolar macrophages.

These results were supported by the presence of ^{18}O in cells and fluid from bronchoalveolar lavage after exposure to ^{18}O-labeled hydrogen peroxide alone and, to a greater extent, in combination with ammonium sulfate. These results suggest that ammonium sulfate particles can transport hydrogen peroxide into the lower airways and induce inflammation.

This Statement, prepared by the Health Effects Institute, summarizes a research project funded by HEI and conducted by Dr Debra L Laskin at Environmental and Occupational Health Sciences Institute, Rutgers University, and the University of Medicine and Dentistry of New Jersey–Robert Wood Johnson Medical School, Piscataway, New Jersey. The following Research Report contains both the detailed Investigators' Report and a Commentary on the study prepared by the Institute's Health Review Committee.

Exposure to cumene hydroperoxide had fewer effects than hydrogen peroxide exposure on inflammatory endpoints, but it is not clear whether these results are generalizable to other organic peroxides, which may have different chemical reactivity and toxicity. Finally, the investigators demonstrated that low levels of hydrogen peroxide may form in indoor environments under highly polluted conditions.

SUMMARY

Laskin and colleagues have shown that hydrogen peroxide reaches the lower lung when inhaled alone and in combination with particles, leading to some inflammatory changes in lung tissue at concentrations that are one to two orders of magnitude greater than concentrations in ambient air. Caution is needed in interpreting these data, however, owing to a lack of quantification of certain endpoints and a lack of dose-response relations for other endpoints. Whether ammonium sulfate or other particles indeed promote transport of peroxides and other oxidants into the lung at ambient concentrations, thereby increasing the possibility for adverse health effects, is still uncertain and remains to be investigated further.

Library of Congress Catalog Number for the HEI Report Series: WA 754 R432.
The paper in this publication meets the minimum standard requirements of the ANSI Standard Z39.48-1984 (Permanence of Paper) effective with Report 21 in December 1988; and effective with Report 92 in 1999 the paper is recycled from at least 30% postconsumer waste with Reports 25, 26, 32, 51, 65 Parts IV, VIII, and IX, 91, and 105 excepted. These excepted Reports are printed on acid-free coated paper.

HEI

CONTENTS

Research Report 117

HEALTH EFFECTS INSTITUTE

Peroxides and Macrophages in the Toxicity of Fine Particulate Matter in Rats

Debra L Laskin, Lisa Morio, Kimberly Hooper, Tsung-Hung Li, Brian Buckley, and Barbara Turpin

Environmental and Occupational Health Sciences Institute, Rutgers University, and the University of Medicine and Dentistry of New Jersey–Robert Wood Johnson Medical School, Piscataway, New Jersey

HEI STATEMENT

This Statement is a nontechnical summary of the Investigators' Report and the Health Review Committee's Commentary.

INVESTIGATORS' REPORT

When an HEI-funded study is completed, the investigators submit a final report. The Investigators' Report is first examined by three ouside technical reviewers and a biostatistician. The report and the reviewers' comments are then evaluated by members of the HEI Health Review Committee, who had no role in selecting or managing the project. During the review process, the investigators have an opportunity to exchange comments with the Review Committee and, if necessary, revise the report.

Continued

COMMENTARY Health Review Committee

The Commentary about the Investigators' Report is prepared by the HEI Health Review Committee and staff. Its purpose is to place the study into a broader scientific context, to point out its strengths and limitations, and to discuss remaining uncertainties and implications of the findings for public health.

RELATED HEI PUBLICATIONS

Publishing History: This document was posted as a preprint on *www.healtheffects.org* and then finalized for print.

Citation for whole document:

Laskin DL, Morio L, Hooper K, Li T-H, Buckley B, Turpin B. 2003. Peroxides and Macrophages in the Toxicity of Fine Particulate Matter in Rats. Research Report 117. Health Effects Institute, Boston MA.

When specifying a section of this report, cite it as a chapter of the whole document.

INVESTIGATORS' REPORT

Peroxides and Macrophages in the Toxicity of Fine Particulate Matter in Rats

Debra L Laskin, Lisa Morio, Kimberly Hooper, Tsung-Hung Li, Brian Buckley, and Barbara Turpin

ABSTRACT

Epidemiologists have observed a positive association between human morbidity and mortality and the atmospheric concentrations of fine particulate matter (PM*), but the mechanisms underlying the toxic effects of PM have not been elucidated. Various components of ambient PM have been implicated in toxicity (including ultrafine particles, transition metals, organics and oxidants). Our research focused on hydrogen peroxide (H_2O_2). We speculated that fine PM transports H_2O_2 into the lower lung, leading to tissue injury and to accumulation and activation of macrophages in these regions. The macrophages release cytotoxic mediators and proinflammatory cytokines that contribute to the pathogenesis of tissue injury.

To test this hypothesis, we conducted studies to determine (1) whether tissue injury induced by aerosols is mediated by cytotoxic H_2O_2 carried into the lower lung by fine particles and (2) whether exposure of rats to fine PM leads to accumulation of activated macrophages in the lung.

For our studies, systems were designed to generate model atmospheric fine PM and atmospheric peroxides consisting of an ammonium sulfate [$(NH_4)_2SO_4$] aerosol (mass median diameter, 0.46 ± 0.14 μm) and H_2O_2. We also constructed a 6-port nose-only exposure chamber. Female Sprague Dawley rats were exposed for 2 hours to aerosols consisting of $(NH_4)_2SO_4$ (430 $\mu g/m^3$), $(NH_4)_2SO_4$ + 10, 20 or 100 ppb H_2O_2, vapor-phase H_2O_2 (10, 20 or 100 ppb), or particle-free air. Studies using oxygen-18 (^{18}O)-labeled H_2O_2 were conducted to validate the transport of H_2O_2 into the lower lung with $(NH_4)_2SO_4$. Rats were killed immediately (0 hours) or 24 hours after exposure.

Compared with control animals, inhalation of $(NH_4)_2SO_4$ and H_2O_2, alone or in combination, had no major effect on cell number or viability, protein content, or lactate dehydrogenase (LDH) levels in bronchoalveolar lavage (BAL) fluid collected either immediately or 24 hours after exposure. However, electron microscopy revealed that a larger number of neutrophils in pulmonary capillaries adhered to the vascular endothelium, especially in lungs of rats exposed to $(NH_4)_2SO_4$ + H_2O_2. Inhalation of $(NH_4)_2SO_4$ + H_2O_2 was also found to be associated with altered macrophage functional activity. Thus, exposing rats to $(NH_4)_2SO_4$ + 20 ppb H_2O_2 or 20 ppb H_2O_2 alone caused a level of tumor necrosis factor α (TNF-α) production by lung macrophages that was higher than in controls. This higher level was observed immediately after exposure and persisted for at least 24 hours. Greater TNF-α production was also detected 24 hours after exposure to $(NH_4)_2SO_4$ + 10 ppb H_2O_2. Immediately after rats inhaled $(NH_4)_2SO_4$ + 10 ppb H_2O_2 or 20 ppb H_2O_2 alone, we also observed a transiently higher production of superoxide anion (O_2^-) by alveolar macrophages. Macrophages isolated 24 hours after exposure to 20 ppb H_2O_2 also produced larger quantities of superoxide anion. In contrast, immediately after exposure, macrophages from rats exposed to $(NH_4)_2SO_4$ + 10 ppb H_2O_2 or to 20 ppb H_2O_2 alone generated less nitric oxide (NO). Reduced nitric oxide production was also observed 24 hours after exposure to $(NH_4)_2SO_4$ + 10 ppb H_2O_2 or to 10 or 20 ppb H_2O_2 alone. Reduced nitric oxide production may have been due to superoxide anion-driven formation of peroxynitrite ($ONOO^-$) anions. In this regard, nitrotyrosine, an in vivo marker of peroxynitrite, was detected in lung tissue immediately after rats were exposed to $(NH_4)_2SO_4$ + H_2O_2 or to H_2O_2 alone (10 or 20 ppb). We also found that alveolar macrophages from rats exposed to $(NH_4)_2SO_4$ + H_2O_2 showed a greater expression of the antioxidant enzyme heme oxygenase-1 (HO-1) when stimulated with lipopolysaccharide (LPS) and interferon-γ (IFN-γ). Similar results were observed after exposure of rats to an organic peroxide aerosol (cumene hydroperoxide).

* A list of abbreviations and other terms appears at the end of the Investigators' Report.

This Investigators' Report is one part of Health Effects Institute Research Report 117, which also includes a Commentary by the Health Review Committee, and an HEI Statement about the research project. Correspondence concerning the Investigators' Report may be addressed to Dr Debra L Laskin, Rutgers University, Environmental and Occupational Health Sciences Institute, 170 Frelinghuysen Road, Piscataway NJ 08854-8020.

Although this document was produced with partial funding by the United States Environmental Protection Agency under Assistance Award R82811201 to the Health Effects Institute, it has not been subjected to the Agency's peer and administrative review and therefore may not necessarily reflect the views of the Agency, and no official endorsement by it should be inferred. The contents of this document also have not been reviewed by private party institutions, including those that support the Health Effects Institute; therefore, it may not reflect the views or policies of these parties, and no endorsement by them should be inferred.

Taken together, the results of our studies demonstrate that biological effects of inhaled H_2O_2 are augmented by fine PM. Moreover, tissue injury induced by $(NH_4)_2SO_4 + H_2O_2$ may be related to altered production of cytotoxic mediators by alveolar macrophages. Determining the relevance of these toxicologic results to human health will be important in future studies for evaluating the risk of exposure.

INTRODUCTION

Epidemiologic studies have demonstrated a positive association between PM concentrations and human morbidity and mortality (Dockery et al 1992; Gouveia and Fletcher 2000; Klemm et al 2000; Moolgavkar 2000; Pope et al 1992; Samet et al 2000a). Of particular concern is fine PM (< 2.5 μm in aerodynamic diameter), which comprises particles that readily penetrate the lower respiratory tract and induce injury (Wilson and Suh 1997). A number of studies have demonstrated that individuals with chronic cardiopulmonary disease, influenza, or asthma are particularly susceptible to serious effects from acutely elevated, short-term PM exposures (Goldsmith and Kobzik 1999; Pope 2000). Although toxicity may be due to a direct action of fine PM on respiratory tissue, particle composition varies extensively and toxicologic effects may also be mediated by compounds present in or associated with fine PM. These include semivolatile organics and water-soluble oxidants that partition into atmospheric PM by adsorption and absorption. Understanding the mechanisms mediating the toxicity of fine PM is critical for designing therapeutic strategies for abrogating or preventing tissue injury and for establishing exposure limits.

Fine PM is formed through combustion and through atmospheric vapor-to-particle conversion. The major constituents are sulfates, nitrates, carbonaceous compounds, water, and trace metals. Inhalation of fine PM is associated with increased microvascular permeability, pulmonary edema, inflammation, and in some instances, damage to alveolar epithelial cells (reviewed by Environmental Protection Agency [EPA] 1996a). Current mechanistic hypotheses have implicated acid aerosols, ultrafine particles, transition metals, and organics in association with the particles as mediators of tissue injury (EPA 1996b). Friedlander and Yeh (1998) also suggested that short-lived water-soluble reactive chemical species (including peroxides and free radicals) may be involved in PM-induced toxicity. According to these investigators, these species are absorbed into particle-associated water and transported to the lower respiratory tract where they induce injury.

Water is a major component of fine atmospheric aerosols in amounts that strongly depend on the relative humidity. For example, at 80% to 90% relative humidity, greater than 50% of fine particle mass is water (Zhang et al 1994). Moreover, the amount of particle-associated water is likely to increase as particles are inhaled because the relative humidity in the respiratory tract approaches 100%. As the water content of fine PM increases, its ability to absorb water-soluble oxidants, to transport them to the lower respiratory tract, and to induce injury also increases. During transport into the lung, particles are exposed to saturated water vapor, which increases particle-phase water concentrations and promotes mass transfer of additional water-soluble vapors into the particle phase. This effect competes with decreasing vapor-phase concentrations of water-soluble compounds, including H_2O_2, as these vapors diffuse to and are removed by the water-coated surfaces (ie, vapor deposition).

Vapor deposition reduces vapor-phase concentrations of water-soluble compounds, which creates a driving force for volatilization of particle-associated concentrations of water-soluble compounds. The alveolar regions of the lung are the recipients of water-soluble oxidants in deposited particles plus vapor-phase material released by the particles entering these regions. Thus, as suggested by Friedlander and Yeh (1998), the adverse health effects of inhaled fine PM may be a response to atmospheric peroxides associated with the particles. The presence of oxidants such as H_2O_2 in the atmosphere at concentrations known to induce cytotoxicity and tissue injury (Hyslop et al 1988; LaCagnin et al 1990; Kim and Suh 1993) supports this hypothesis. Biological concentrations of H_2O_2 (20–120 μM) produced by inflammatory cells as a defense against foreign substances and microorganisms (Oosting et al 1990) are lower than atmospheric concentrations (Gunz and Hoffman 1990; Kok et al 1990). These biological H_2O_2 concentrations are effective in destroying bacteria, in inducing DNA strand breaks, lipid peroxidation and mutations, and in activating the hexose monophosphate shunt and glutathione redox cycle (Oosting et al 1990; Schraufstatter and Cochrane 1991). Thus H_2O_2 can cause cell damage, and inhalation of H_2O_2 may be toxic to the lung.

FORMATION OF ATMOSPHERIC H_2O_2 AND ORGANIC PEROXIDES

Atmospheric H_2O_2 is mainly formed through photochemical reactions in the presence of ozone, nitrogen oxides (NO_X), volatile organic compounds (VOCs), and carbon monoxide (CO) and plays an important role in converting sulfur dioxide (SO_2) to sulfate (SO_4^{2-}) aerosol in

clouds and rain drops (Calvert et al 1985). Atmospheric, ground-level H_2O_2 concentrations range from 0.1 to 5.0 ppb (Lee et al 2000) and are highest in the summer due to strong photochemical activity (Sakugawa and Kaplan 1989). Organic peroxides such as methylhydroperoxide (MHP) and hydroxymethylhydroperoxide (HMHP) are also present in the atmosphere. Ambient vapor-phase HMHP concentrations, as high as 5 ppb, have been reported on a hot, humid, and hazy day in Georgia (Lee et al 1993).

A major pathway of H_2O_2 formation is the self-reaction of hydroperoxyl (HO_2) radicals (Finlayson-Pitts and Pitts 1986). These radicals are primarily produced from the photolysis of ozone followed by reactions with water and carbon monoxide (Lee et al 2000). H_2O_2 can also be generated by the ozonolysis of alkenes such as isoprene, isobutene and terpene under humid conditions (Becker et al 1990, 1993; Hewitt and Kok 1991; Simonaities et al 1991; Sauer et al 1999). Recently, Tobias and Ziemann (2000) showed that the major products formed by reactions of 1-tetradecene and ozone in the presence of alcohols and carboxylic acids in smog chamber studies are the organic peroxides, α-methoxytridecyl hydroperoxide [$CH_3(CH_2)_{11}CH(OOH)OCH_3$] and α-isoproxytridecyl hydroperoxide [$CH_3(CH_2)_{11}CH(OOH)$-$OCH(CH_3)_2$]. These are low-volatility compounds that are expected to be in the particle phase. Formation of these organic peroxides is consistent with a mechanism involving reactions of the alcohols and carboxylic acids with Criegee biradicals (generic formula: RR′COO) generated in alkene–ozone reactions.

VAPOR-PARTICLE PARTITIONING

Wexler and Sarangapani (1998) showed that water-soluble organics (with Henry law constants greater than about 0.1 M/atm), present in the vapor phase, are rapidly removed by deposition in the upper airways. Semivolatile chemical compounds can partition into particles through adsorption, absorption, or condensation. While low-polarity, semivolatile organic compounds are expected to partition into particulate organic matter (Pankow 1994; Liang et al 1997), water-soluble compounds partition into aerosol water. H_2O_2 is highly soluble in water; hence, its Henry law constant and the presence of available aerosol water govern H_2O_2 partitioning between vapor and particle phases. If the atmosphere contained no liquid water, H_2O_2 would be present entirely in the vapor phase. As the water content of an aerosol increases, however, more H_2O_2 will be present in the particle phase (aqueous phase).

Particle-phase H_2O_2 concentrations could be expected to decrease in the airways because removal of the vapor phase by diffusion to surfaces promotes volatilization of particle-phase H_2O_2. However, the modeling results of Wexler and Sarangapani (1998) show that the particle-phase concentration of H_2O_2 is relatively stable in the bronchial regions of the upper lung. Water rapidly condenses on the particles because of the elevated humidity in the airways. This results in rapid particle growth and dilution of the H_2O_2 concentration in the particle. The dilution reduces the partial pressure of H_2O_2 over the particle, leading to additional absorption of H_2O_2 into the particle. These two competing effects (ie, reduced vapor concentration and increased aerosol water concentration) are about equal in the bronchial region. In the lower lung, where the lumen vapor concentration is an order of magnitude lower, evaporation of particle-phase H_2O_2 becomes significant and the released H_2O_2 rapidly diffuses to the surfaces. The decrease in particle-phase H_2O_2 concentration is a function of particle size: H_2O_2 in particles smaller than 0.1 μm in diameter evaporates before the particles reach the lower lung, while particles larger than 1.0 μm in diameter retain H_2O_2. Thus, the dose of H_2O_2 delivered to the lower lung is expected to include H_2O_2 volatized from small particles (0.1–1.0 μm) in the lower lung as well as H_2O_2 present in the fraction of particles that actually deposit in the lower lung.

PM constituents such as $(NH_4)_2SO_4$ and ammonium nitrate may influence the solubility of H_2O_2 in water. Lind and Kok (1986, 1994) demonstrated that the solubility of H_2O_2 in a saturated $(NH_4)_2SO_4$ solution is almost a factor of two greater than its solubility in pure water. H_2O_2 behaves as an ionizing solvent because its dielectric constant is about the same as water. Hydrated $(NH_4)_2SO_4$ ions, both positive and negative, can react with H_2O_2 to form adducts that augment H_2O_2 absorption. As a result, the particle-phase concentration of H_2O_2 is enhanced in ambient aerosols in which $(NH_4)_2SO_4$ and ammonium nitrate are major components.

The vapor and particle distribution of H_2O_2 in ambient aerosols can be predicted as follows: given a concentration (C_{ppb}) of vapor-phase H_2O_2 in air, the particle-phase H_2O_2 concentration (μg/m^3) is equal to:

$$C_{ppb} \times H \times 10^{-9} \times W \times M_r(1/\rho_w)$$

where

H = the Henry law constant for H_2O_2 in water (M/atm),

W = aerosol water content (μg/m^3),

M_r = molecular weight of H_2O_2 (g/mol), and

ρ_w = water density (g/cm^3).

Thus, once concentrations of total H_2O_2 and aerosol water content are known, the H_2O_2 partitioning between the vapor and particle phases can be calculated assuming equilibrium.

Atmospherically relevant, ground-level concentrations of total H_2O_2 are between 0.1 and 5.0 ppb (Tanner et al 1986; Sakugawa and Kaplan 1989, Hewitt and Kok 1991; Lee et al 1993; Das and Aneja 1994; Tanner and Schorran 1995; Watkins et al 1995; Lee et al 2000). Aerosol water concentrations are 10 to 50 $\mu g/m^3$ (Friedlander and Yeh 1998). At 298 K, the Henry law constant is 7.36×10^4 M/atm (Lind and Kok 1986) and the particle-phase concentration of H_2O_2 is 0.04 to 1.0 ng/m^3. As indicated above, however, the Henry law constant for H_2O_2 in an aqueous $(NH_4)_2SO_4$ solution is greater by a factor of two than the Henry law constant for H_2O_2 in water at saturation. Thus, 0.08 to 2.0 ng/m^3 is a better estimate for particle-phase H_2O_2 concentrations when $(NH_4)_2SO_4$ is a major PM component.

The vapor-phase and particle-phase partitioning of H_2O_2 and other water-soluble peroxides must be predicted in order to assess dose and health effects because lung deposition patterns differ substantially for vapors and particles. The preceding equation predicts that most H_2O_2 will be in the vapor phase. Thus, measurement of particle-phase H_2O_2 is difficult because levels should be expected to be very low. Moreover, particle collection can alter equilibrium conditions (eg, for aerosol water), resulting in sampling artifacts. Collected particles are also likely to react with other constituents in the sample stream. Thus, collection of particle-phase H_2O_2 on a filter over time is not practical; the amount of H_2O_2 in the particle phase can only be estimated.

EFFECTS OF FINE PM ON LUNG TISSUES

Exposure to inhaled PM is known to result in pulmonary inflammation, which is generally characterized by an influx of neutrophils and macrophages into the lung. These cells release mediators aimed at destroying inhaled materials and initiating wound repair. However, these mediators are nonspecific and many have the capacity to potentiate tissue injury (Laskin and Pendino 1995). Alveolar macrophages are the primary host defense against respiratory insults. Inhaled particles and infectious agents are phagocytized in the lower airways by alveolar macrophages, while both alveolar macrophages and epithelial cells remove smaller particles and soluble materials by endocytosis (Kreyling 1992). After injury to the lung, alveolar macrophages become activated and release soluble mediators with proinflammatory and/or cytotoxic activity (Laskin and Pendino 1995). These mediators include reactive oxygen intermediates, reactive nitrogen intermediates, and various cytokines such as TNF-α and interleukin 1β. Although the activity of alveolar macrophages and their biological mediators in normal host defense has been well established, the role of these cells in PM-induced tissue injury is largely unknown. The observation that expression of receptors important for phagocytosis of opsonized microbes (CD11b, CD11c) and for extracellular matrix interaction decreases in alveolar macrophages exposed to PM suggests that exposure to PM may impair host defense functions of these cells (Becker and Soukop 1998). Damage to lung macrophages is an important factor in increased host susceptibility to airborne bacterial infection (Kaplan 1981). In this regard, alveolar macrophage-regulated chemokine production in response to infection with respiratory syncytial virus, a frequent cause of viral pneumonia in infants and the elderly, has been reported to be lower after exposure to PM (Becker and Soukup 1999).

Lung inflammation has been observed in animals exposed to various types of particles, including silica (Bruch et al 1993), carbon black (Driscoll et al 1996), titanium dioxide (TiO_2), and barium sulfate ($BaSO_4$) (Cullen et al 2000). Other types of PM elicit changes in inflammatory cell function, such as reduced phagocytic activity and altered cytokine or chemokine expression (Clarke et al 2000; Nadadur et al 2000). For example, although the number of recoverable BAL cells and differential cell counts were unchanged after exposure of mice to acid sulfate-coated carbon black particles, alveolar macrophages isolated from these animals exhibited decreased Fc receptor-mediated phagocytosis and bactericidal activity (Clarke et al 2000). Using microarray technology, Nadadur and colleagues (2000) reported increased pulmonary expression of several genes involved in inflammation [including interleukin 6, tissue inhibitor of matrix metalloproteinases-1, fibronectin, intercellular adhesion molecule-1, interleukin 1β, and inducible nitric oxide synthase (NOS II)] after exposure of rats to residual oil fly ash. Thus, alterations in inflammatory mediator production appear to be a highly sensitive indicator of tissue injury induced by inhaled PM.

SELECTION OF MODEL AEROSOL COMPONENTS AND DOSES

For the majority of the studies described in this report, $(NH_4)_2SO_4$ with a mass median diameter of 0.45 ± 0.14 μm was used as a model atmospheric aerosol. $(NH_4)_2SO_4$ is a major component of atmospheric fine PM in northeastern United States and is highly hygroscopic. The water content of $(NH_4)_2SO_4$ particles as a function of relative humidity is also well characterized. We used a relative humidity of 85% to provide a known amount of particle-associated water, near the upper limit of what would be

expected in the atmosphere. The particle size used falls in the middle of the accumulation mode, where most of the fine particle mass is found in atmospheric particles. It should be recognized that atmospheric $PM_{2.5}$ is somewhat less hygroscopic than $(NH_4)_2SO_4$ because it includes some less hygroscopic organic and mineral species as well as hygroscopic organics, nitrate, and sulfate. H_2O_2 partitions between the vapor phase and particle-associated water.

The concentrations of $(NH_4)_2SO_4$ and H_2O_2 used in our animal exposure studies were extrapolated from concentrations in the atmosphere. The 24-hour average National Ambient Air Quality Standard for $PM_{2.5}$ is 65 $\mu g/m^3$, and atmospheric ground-level peak concentrations of H_2O_2 range from 0.1 to 5.0 ppb (Lee et al 2000). In addition, research described in Appendix B suggests that peak indoor H_2O_2 concentrations are comparable to peak outdoor concentrations. Dosimetry studies after ozone inhalation indicate that structural differences between the rat and human respiratory tracts cause about a 10-fold decrease in the efficiency of inhaled materials to reach the lower lung of rats (Hatch et al 1994). To compensate for these differences in the present studies, we selected $(NH_4)_2SO_4$ (430 $\mu g/m^3$; 215 $\mu g/m^3$) and H_2O_2 (10 ppb; 20 ppb; 100 ppb), levels approximately tenfold higher than atmospheric concentrations.

We also conducted pilot studies with an aerosol consisting of a commercially available organic peroxide (cumene hydroperoxide). This compound is similar to two particle-phase organic peroxides, identified in smog chamber experiments, that are expected to be present in atmospheric particles (Tobias and Ziemann 2000).

To accomplish our aims, it was first necessary to develop and characterize an aerosol generation and exposure system for rodents. We developed a real-time peroxide detector to monitor H_2O_2 concentrations in the exposure system. This instrument was also used to measure H_2O_2 concentrations in a realistic but manipulated indoor environment (Appendix B).

SPECIFIC AIMS

The respiratory tract is unique in that it is directly linked to the external environment. As a consequence, it is particularly susceptible to damage induced by inhaled agents. For example, inhalation of fine atmospheric aerosols by humans and experimental animals results in increased microvascular permeability, pulmonary edema, and in some instances, damage to epithelial cells. These changes are associated with an accumulation of macrophages in the tissue. Although numerous epidemiologic studies have demonstrated that inhalation of atmospheric fine PM is associated with morbidity and mortality, the mechanisms underlying the toxic effects of relatively low levels of these materials are unknown (Moolgavkar and Luebeck 1996). Moreover, there appears to be a discrepancy between the results of epidemiologic studies associating atmospheric particles with human health and the results of toxicity studies using laboratory-generated particles and animal models. Peroxides carried by fine particles may be one of the factors contributing to the adverse health effects observed after exposure to ambient PM.

The overall objective of the present set of studies was to analyze the role of particle-associated H_2O_2 and inflammatory macrophages in fine PM-induced tissue injury (Table 1). We hypothesized that fine PM transports water-soluble peroxides into the lower lung, leading to tissue injury and to accumulation and activation of macrophages in these regions. Once activated, the macrophages release cytotoxic mediators and proinflammatory cytokines that contribute to the pathogenesis of tissue injury. To test this hypothesis, experiments were conducted to: (1) determine if tissue injury induced by aerosols is mediated by cytotoxic H_2O_2 carried into the lower airways by fine particles, and (2) assess whether exposure of rats to fine PM and H_2O_2 results in activation of lung macrophages (which contribute to tissue injury).

Specific aim 1 was addressed by comparing the effects of inhalation of H_2O_2-containing $(NH_4)_2SO_4$ (215 or 430 $\mu g/m^3$) aerosols with inhalation of particle-free air, $(NH_4)_2SO_4$ aerosols, or vapor-phase H_2O_2 (10, 20, or 100 ppb) alone on markers of lung injury and inflammation. Measurements were made of BAL fluid protein and LDH levels as well as inflammatory cell accumulation in the lung. Histologic sections of lung were also examined for evidence of structural alterations and inflammation. Dose response and time course studies are described in Section 3 of this report. Studies using ^{18}O-labeled H_2O_2, which are described in Appendix A, provided information on the transport of H_2O_2 into the lower lung, the response of the lower lung to H_2O_2, and the doses of H_2O_2 that induce biological responses.

Specific aim 2 was addressed by analyzing the effects of inhaling $(NH_4)_2SO_4$ or $(NH_4)_2SO_4 + H_2O_2$ aerosols on alveolar macrophages. Histologic sections of lungs from control and exposed rats were assessed for changes in the number and morphology of macrophages and neutrophils in the alveolar regions. Immunohistochemistry was used to quantify production of several inflammatory mediators and their pattern of localization. We also isolated alveolar macrophages from exposed and control animals and measured inflammatory mediator production. The effects of inhibiting macrophage function on mediator production and tissue injury were also evaluated. These studies,

Table 1. Overview of Specific Aims and Study Design

	Study Design
Methods: Generate and Characterize Model Atmospheric Fine PM and Peroxides; Establish Animal Exposure System	
• Develop and characterize a system to model atmospheric fine PM and atmospheric H_2O_2	$(NH_4)_2SO_4$, H_2O_2, and particle-free atmosphere generation; exposure monitoring (Section 1)
• Develop an exposure system for rodents	Construction of a 6-port nose only exposure chamber (Section 1)
• Quantitative real-time measurement of H_2O_2 concentration	Develop a real-time H_2O_2 detector; select collection devices; determine detection units, validate collection efficiencies; apply to the animal exposure system (Section 2)
• Develop and characterize a system to model an organic peroxide aerosol	Generation of cumene hydroperoxide (Section 1)
Aim 1: Determine Whether Tissue Injury Induced by Fine PM is Mediated by Cytotoxic Peroxides Carried Into Lower Airways by Fine Particles	
• Compare the effects of inhaled $(NH_4)_2SO_4 + H_2O_2$ to the effects of inhaled particle-free air, $(NH_4)_2SO_4$, or gas-phase H_2O_2 alone on lung injury and inflammation.	Inhalation exposure of rats to particle-free air, $(NH_4)_2SO_4$, H_2O_2 or $(NH_4)_2SO_4 + H_2O_2$; lung lavage analysis; lung histology (Section 3)
Aim 2: Evaluate Effect of Inhalation Exposure of Rats to Fine PM and Peroxides on Lung Macrophages	
• Assess changes in the structural properties of lung macrophages after inhalation of $(NH_4)_2SO_4 + H_2O_2$ aerosols by rats	Inhalation exposure of rats to particle-free air, $(NH_4)_2SO_4$, H_2O_2, or $(NH_4)_2SO_4 + H_2O_2$; isolation of alveolar macrophages; cell number; morphology (Section 3)
• Evaluate alterations in inflammatory mediator release by lung macrophages after inhalation of $(NH_4)_2SO_4 + H_2O_2$ aerosols by rats	Inhalation exposure of rats to particle-free air, $(NH_4)_2SO_4$, H_2O_2, or $(NH_4)_2SO_4 + H_2O_2$; isolation of alveolar macrophages; functional assays (TNF-α, superoxide anion, nitric oxide); NOS II, COX-2 expression (Section 3)
• Analyze altered expression of heat shock proteins by lung macrophages after inhalation of $(NH_4)_2SO_4 + H_2O_2$ aerosols by rats	Inhalation exposure of rats to particle-free air, $(NH_4)_2SO_4$, H_2O_2, or $(NH_4)_2SO_4 + H_2O_2$; isolation of alveolar macrophages; heat shock protein expression (Section 3)
• Evaluate the effects of inhalation exposure of rats to a particle-phase organic peroxide	Inhalation exposure of rats to solvent control or particle-phase cumene hydroperoxide; lung lavage analysis; isolation of alveolar macrophages; functional assays (TNF-α, superoxide anion, nitric oxide); NOS II, COX-2 expression; heat shock protein expression (Section 3)
Appendix A: Assess Pulmonary Deposition of Particle-Phase and Vapor-Phase H_2O_2	
• Validate the transport of $(NH_4)_2SO_4 + H_2O_2$ into the lower lung	Inhalation exposure of rats to $(NH_4)_2SO_4 + {}^{18}O$-labeled H_2O_2 or ${}^{18}O$-labeled H_2O_2 alone; lung lavage and alveolar macrophage isolation; detection of ${}^{18}O$ in samples
Appendix B: Assess Indoor H_2O_2 Formation	
• Assess the possible impact of ozone chemistry on indoor residential concentrations of H_2O_2	

described in Section 3, provided information on secretory products released by macrophages after exposure of rats to $(NH_4)_2SO_4$ fine PM + H_2O_2.

Addressing our specific aims required the design and construction of systems to generate stable and reproducible test atmospheres. A real-time H_2O_2 detector was also developed to monitor exposure conditions during animal experiments. These systems are described in Sections 1 and 2.

Several additional studies were ancillary to our original goals but provided useful insights into the human relevance of our results. These included measuring H_2O_2 concentrations in a realistic but manipulated indoor environment and assessing the likelihood that indoor particle concentrations could exceed the $PM_{2.5}$ standard under certain conditions. These studies are described in Appendix B.

SECTION 1. DEVELOPMENT OF ANIMAL EXPOSURE AND AEROSOL GENERATION SYSTEMS

INTRODUCTION

The first part of our studies involved the design, construction, and characterization of animal exposure and aerosol generation systems. The water uptake of $(NH_4)_2SO_4$ aerosol has been previously described (Lind and Kok 1986, 1994). The vapor-particle partitioning of H_2O_2 was calculated on the basis of the aerosol water content, total peroxide concentration, and the Henry law constant for H_2O_2. Four test atmospheres were generated: an aerosol containing $(NH_4)_2SO_4$ + H_2O_2; an $(NH_4)_2SO_4$ aerosol; vapor-phase H_2O_2; and particle-free air. The aerosol generation system was adapted in later experiments to produce an atmosphere consisting of cumene hydroperoxide and a particle-free solvent control.

METHODS

Exposure Chamber Design

A nose-only exposure chamber was constructed to ensure that individual animals received a fixed dose of test material. Moreover, lower flow rates could be used with this design because emissions from animal waste would not contribute to the exposure. The exposure chamber was constructed from a stainless steel cylindrical pipe, 2 inches in diameter, 0.25 inches in wall thickness, 36 inches long, and capped on one end. Test atmospheric particles were pushed from the exposure chamber into 6 nose-only exposure ports (Lab Products, Maywood NJ) through stainless steel tubes (0.25 inches in diameter and 4 inches in length) protruding from the stainless steel chamber. A total of 3.2 L/min of test atmosphere was pushed into the exposure chamber. Under these conditions, each individual exposure port was found to receive approximately 0.5 L/min of the test atmosphere. Excess and exhaled aerosol traveled through a polyvinyl chloride (PVC) exhaust manifold 1 inch in diameter (Figure 1). Exposure conditions were monitored in real time in one of the nose-only exposure ports.

Aerosol Generation

To generate the aerosol, an aqueous solution of $(NH_4)_2SO_4$ was prepared in high purity deionized water from an ultrapurification system (resistivity > 18 MΩ/cm; Millipore, Bedford MA). $(NH_4)_2SO_4$ particles were generated from the solution using a Collison nebulizer (Raabe 1976) operated at 35 psi (Figure 2). This nebulizer uses capillary action to pull the aqueous solution into a high-pressure air stream, where the solution is atomized into aqueous particles. The resulting particles travel through a diffusion dryer, which reduces the particle water content, particle size, and aerosol relative humidity by exchanging water vapor with a flow of dry sheath air across an annular membrane (48 inches long; MD-110-48, Perma Pure, Toms River NJ). The particles were then given a Boltzmann charge distribution in a ^{210}Po neutralizer (NRD, Grand Island NY) and, for 430 μg/m^3 exposures, pushed directly into the nose-only exposure chamber. The relative humidity and water content of the $(NH_4)_2SO_4$ particles were controlled by changing the flow rate of countercurrent sheath air in the diffusion dryer. The relation between achieved relative humidity and sheath airflow rate is shown

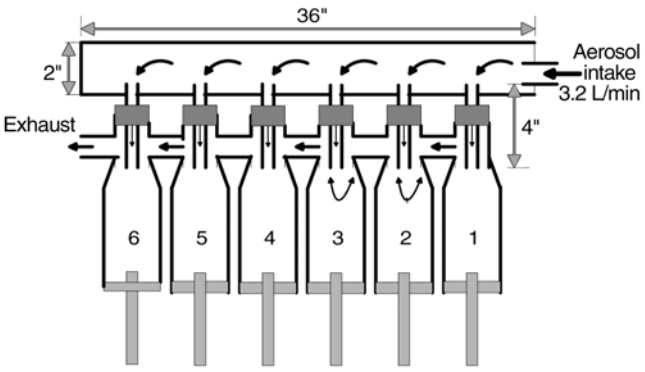

Figure 1. Nose-only exposure chamber. Aerosol enters the chamber at 3.2 L/min and flows into the animal exposure ports as indicated by the arrows. Exhaled air and remaining aerosol are pushed out the exhaust manifold.

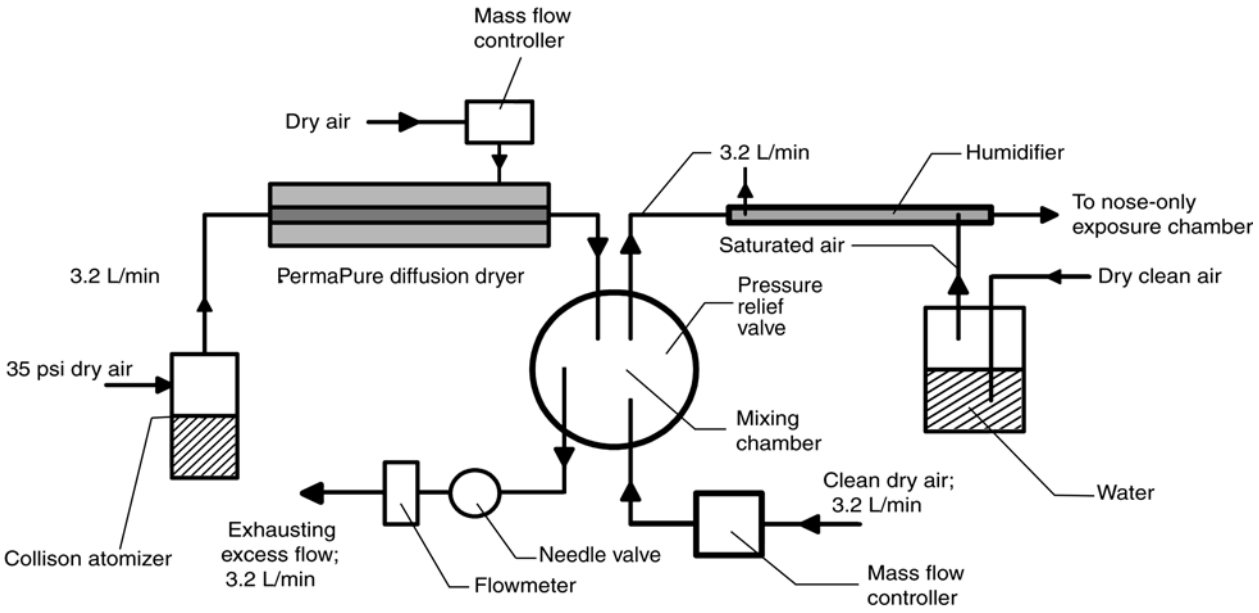

Figure 2. Generation of test aerosols.

in Figure 3. A 1.5 L/min countercurrent sheath airflow rate resulted in 85 ± 2% relative humidity.

Reduced aerosol concentrations were achieved by adding a mixing chamber and humidifier immediately upstream of the exposure chamber (Figure 2). In the mixing chamber, the aerosol was diluted 1:1 with dry, particle-free air to achieve a concentration of 215 μg/m^3. Particles were mixed dry to reduce coagulation and to prevent them from sticking to the wall of the chamber. The resulting particles were adjusted to 85% relative humidity in a diffusion humidifier (24 inches long; MH-110-24S, Perma Pure) with saturated countercurrent sheath air. The total flow rate into the exposure chamber was maintained at 3.2 L/min by exhausting excess flow. The particle size

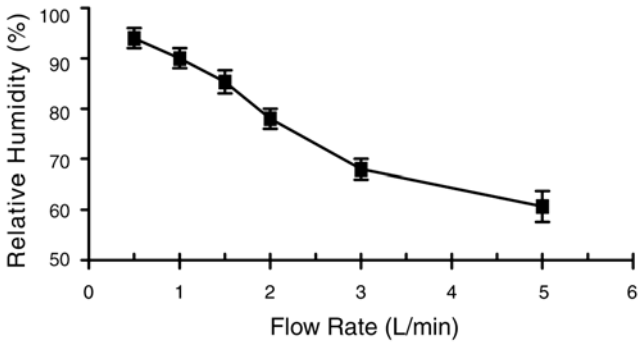

Figure 3. Relation between aerosol relative humidity and sheath air flow rate in a 48-inch diffusion dryer. Each flow rate had three measurements. Error bars indicate measurement uncertainty expressed as ± 1 SD from the measurement mean.

distribution was controlled by the solution strength in the nebulizer and relative humidity.

An aerosol containing $(NH_4)_2SO_4 + H_2O_2$ was generated by adding H_2O_2 to the nebulizer solution. The total H_2O_2 concentration was varied by changing the concentration of H_2O_2 in the nebulizer solution. Partitioning of H_2O_2 between the vapor and particle phases is a function of the mass concentration of $(NH_4)_2SO_4$ and the relative humidity. Together, these factors determine the water content of the particles as discussed in detail in the section on Calculation of Aerosol Properties later in this report. The particle-phase H_2O_2 concentrations decrease with decreasing aerosol water content, meaning that they decrease with decreasing relative humidity and with decreasing concentrations of $(NH_4)_2SO_4$ in the nebulizer solution (ie, smaller particle size). This effect occurs because the particle-associated H_2O_2 partitions by absorption into the aerosol water. The concentration of particle-phase H_2O_2 (mass/m^3 air) can be changed independently of particle size by changing the total H_2O_2 concentration or changing the relative humidity and thus the aerosol water content.

Generation of Particle-Free Atmospheres

Vapor-phase H_2O_2 test atmospheres (relative humidity, 85%) were generated by bubbling 2.8 L/min of clean compressed air through a 250-mL glass washing bottle containing 150 mL of an aqueous H_2O_2 solution (Figure 4). An additional 0.4 L/min of clean dry air was added to adjust the

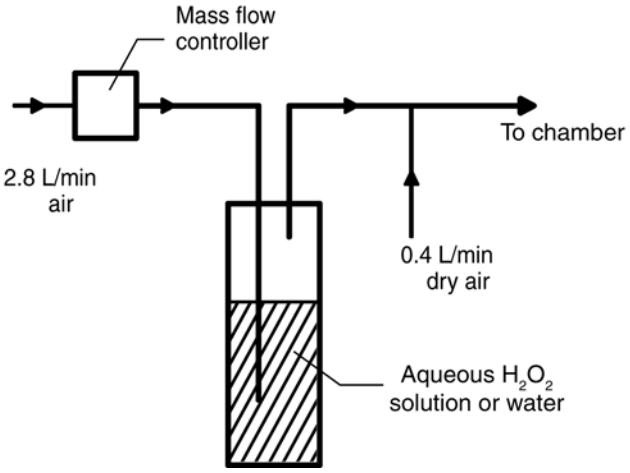

Figure 4. Generating vapor-phase H_2O_2 at 85% relative humidity. Particle-free air is also generated using this system.

relative humidity to 85%. The particle-free control atmosphere (relative humidity, 85%) was generated by using high purity deionized water from a Millipore ultrapurification system (resistivity, >18 MΩ/cm) in the bubbler.

Exposure Monitoring

Exposure conditions were monitored continuously in a nose-only exposure port during each experiment. A meter (model 625, Testo, Flanders NJ) was used to measure relative humidity and temperature. Particle size distribution and number concentration were monitored using an 8-channel laser particle counter (model PMS-LASAIR1002, Particle Measuring Systems, Boulder CO) calibrated with latex particles having a refractive index of 1.6. Total and integrated H_2O_2 were measured in one of the exposure ports in real time using the automated fluorometric method described in Section 2 of this report.

Generation of Cumene Hydroperoxide Aerosol

Cumene hydroperoxide particles were generated in the same manner as $(NH_4)_2SO_4$ particles, except that the diffusion dryer shown in Figure 2 was replaced with an activated charcoal diffusion dryer to remove the solvent in which the cumene hydroperoxide was dissolved. The nebulizer contained a solution of 1.2 mL of 88% cumene hydroperoxide [$C_6H_5C(CH_3)_2OOH$] in 180 mL methanol (Aldrich Chemical, Milwaukee WI). During the two animal experiments, 102 ± 23 and 106 ± 21 μg/m^3 of cumene hydroperoxide PM were measured in the exposure chamber. The PM comprised solely cumene hydroperoxide and was equilibrated at 44% to 46% relative humidity (temperature: 22.4°C and 18.2°C). The mass median particle diameter was 0.45 μm ± 0.10. Solvent controls were produced by generating the same aerosol but removing the particles by filtration before they reached the exposure chamber. Thus, if any solvent remained in the airstream after the diffusion dryer, its effect would be detected in the solvent blank. Less than 1 particle/cm^3 was measured in the chamber during solvent blank runs. Particle number concentrations of 15,720/cm^3 and 14,280/cm^3 were measured during cumene hydroperoxide experiments.

RESULTS AND DISCUSSION

Exposure Chamber Characterization

Particle number concentrations at 85% relative humidity in each individual port were measured to ensure particles were evenly distributed. Mass concentrations were calculated from numbered size distributions as explained in Calculation of Aerosol Properties. Table 2 shows number and mass concentrations by particle size across each individual port over 3 hours. No significant difference in particle number or mass concentration was observed between ports at a 95% confidence level according to a paired *t* test.

Aerosol Generation System Characterization

Atomization of an aqueous $(NH_4)_2SO_4$ solution yielded aqueous $(NH_4)_2SO_4$ particles suspended in humid air. The effect of $(NH_4)_2SO_4$ solution strength on the particle mass size distribution at 85% relative humidity is shown in Figure 5. $(NH_4)_2SO_4$ mass concentrations of 96 ± 28 to 440 ± 30 μg/m^3 and number concentrations of 24,000 ± 720 to 27,000 ± 1300 particles/cm^3 were obtained by atomizing 0.125% to 0.5% $(NH_4)_2SO_4$ solutions. For example, a 0.5% $(NH_4)_2SO_4$ solution yielded particles with a mass median diameter of 0.45 ± 0.14 μm and a mass concentration of 440 ± 30 μg/m^3 of $(NH_4)_2SO_4$.

The effect of diffusion humidifier sheath airflow rate on aerosol relative humidity is shown in Figure 6. The total flow rate into the exposure chamber was maintained at 3.2 L/min by exhausting excess flow. For example, 3.2 L/min of particle-free air was mixed with dried $(NH_4)_2SO_4$ aerosol [from a 0.5% $(NH_4)_2SO_4$ solution] in the mixing chamber to dilute the aerosol by approximately 50%. A 1 L/min flow of saturated sheath air in the diffusion humidifier downstream was needed to adjust the aerosol to 86% ± 2% relative humidity. The $(NH_4)_2SO_4$ number and mass concentrations were reduced to 14,000 ± 1500 particles/cm^3 and 230 ± 20 μg/m^3, respectively. This is a 48% reduction in number and mass concentrations. The mass median diameter was unchanged (0.45 ± 0.15 μm).

Table 2. Number and Mass Concentrations of $(NH_4)_2SO_4$ Particles in Exposure Chamber Ports[a]

*D*p (μm)[b]	Port 1	Port 2	Port 3	Port 4	Port 5	Port 6
Number Concentrations						
0.1–0.2	1330 ± 350	1340 ± 800	1100 ± 310	930 ± 280	820 ± 510	640 ± 510
0.2–0.3	1030 ± 160	920 ± 110	1050 ± 260	1720 ± 2130	840 ± 100	1720 ± 2120
0.3–0.4	14,730 ± 1830	13,200 ± 1580	13,700 ± 2820	14,380 ± 260	14,500 ± 450	15,370 ± 2490
0.4–0.5	7380 ± 1920	8260 ± 1360	7800 ± 870	8140 ± 940	7590 ± 2630	8060 ± 860
0.5–0.7	1540 ± 620	1800 ± 1350	1810 ± 1020	970 ± 690	1980 ± 700	860 ± 600
0.7–1.0	24 ± 8	30 ± 30	23 ± 22	44 ± 41	45 ± 19	120 ± 190
Total	26,000 ± 700	25,500 ± 1950	25,450 ± 2370	26170 ± 2390	25,800 ± 1880	26,760 ± 2280
Mass Concentrations (mg/m^3)						
0.1–0.2	1.1 ± 0.3	1.2 ± 0.8	0.9 ± 0.3	0.8 ± 0.2	0.7 ± 0.4	0.5 ± 0.4
0.2–0.3	4.0 ± 0.6	3.8 ± 0.7	4.1 ± 1.0	6.8 ± 8.4	3.3 ± 0.4	6.4 ± 8.7
0.3–0.4	160 ± 20.0	150 ± 27.0	148 ± 30.0	155 ± 3.0	157 ± 5.0	166 ± 27.0
0.4–0.5	170 ± 44.0	200 ± 35.0	180 ± 20.0	187 ± 22.0	174 ± 60.0	185 ± 20.0
0.5–0.7	84 ± 34.0	98 ± 72.0	98 ± 55.0	72 ± 6.0	108 ± 38.0	66 ± 6.0
0.7–1.0	0.3 ± 0.1	4.6 ± 4.0	3.6 ± 3.5	6.8 ± 6.4	7 ± 3.0	18 ± 30.0
Total	420 ± 60.0	454 ± 32.0	434 ± 31.0	429 ± 25.0	450 ± 16.0	443 ± 20.0

[a] Particles were generated by atomizing a 0.5% aqueous $(NH_4)_2SO_4$ solution over 3 hours. Three measurements were made in each port. Data represent mean ± SD of at least 10 experiments.

[b] *D*p = particle diameter.

The relation between the H_2O_2 solution strength in the nebulizer and total (vapor plus particle phase) H_2O_2 concentration in the exposure chamber is shown in Figure 7. Total H_2O_2 concentrations as low as 9 ± 0.7 ppb (13 ± 1 μg/m^3) and as high as 930 ± 150 ppb (1290 ± 210 μg/m^3) were achieved by atomizing solutions containing H_2O_2 and $(NH_4)_2SO_4$. For example, an H_2O_2 concentration of 0.01 M in a 0.5% aqueous $(NH_4)_2SO_4$ solution produced particles containing 424 ± 22 μg/m^3 of $(NH_4)_2SO_4$ and approximately 34 ng/m^3 of H_2O_2. The particle-phase H_2O_2 concentration reported here was calculated from the aerosol water content and the measured concentration of total (vapor plus particle phase) H_2O_2 (ie, 13 ± 1 μg/m^3 or 9.4 ± 0.7 ppb), as described in Calculation of Aerosol Properties.

A bubbler was used for H_2O_2-only experiments (Figure 4). The concentration of vapor-phase H_2O_2 was linearly related to the H_2O_2 solution strength in the bubbler for the range of concentrations generated (eg, 5 to 50 ppb in the exposure chamber [Figure 8]). For example, a 3 mM H_2O_2 bubbler solution yielded 11 ± 1 ppb H_2O_2 in the exposure chamber.

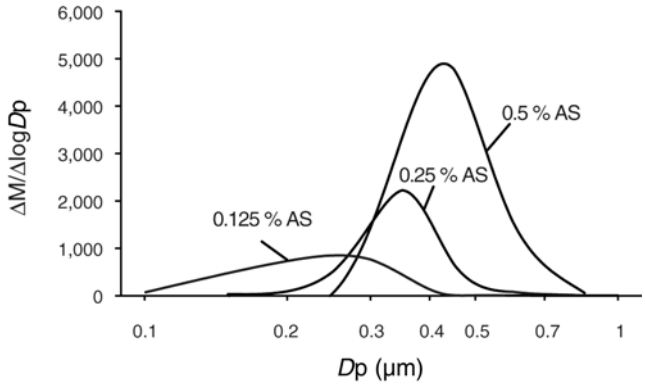

Figure 5. Particle mass distribution by size (85% relative humidity) for 0.125%, 0.25%, and 0.5% aqueous $(NH_4)_2SO_4$ nebulizer solutions. AS = $(NH_4)_2SO_4$; M = mass concentration; *D*p = particle diameter; y-axis displays the mass size distribution function.

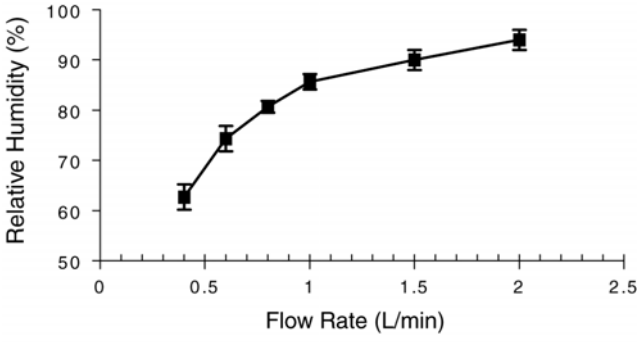

Figure 6. Effects of air flow rate through diffusion humidifier sheath on relative humidity. Sheath air is saturated. Three measurements were made at each flow rate. Error bars indicate measurement uncertainty expressed as ± 1 SD of the measurement mean.

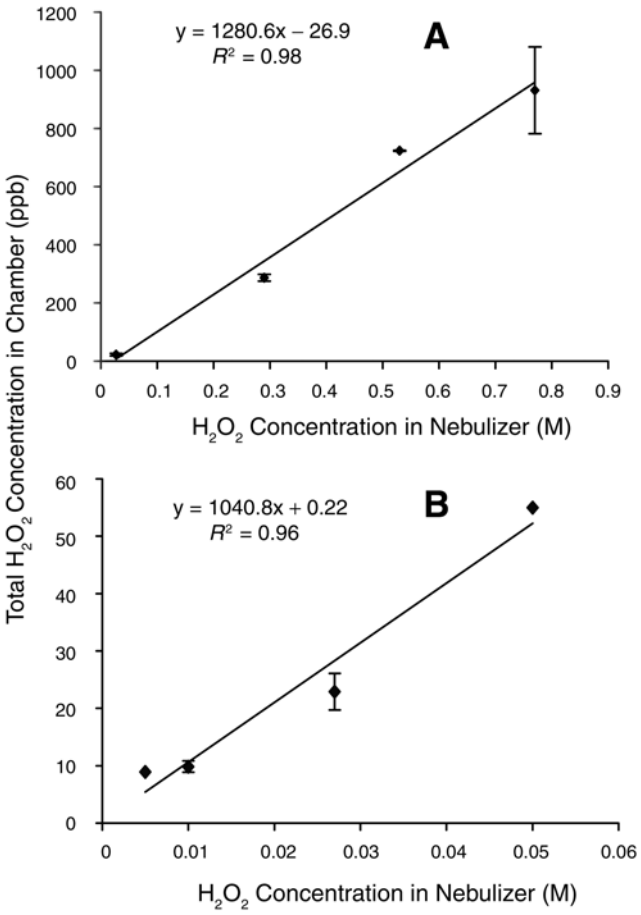

Figure 7. Total (vapor plus particle) H_2O_2 concentration in the exposure chamber as a function of H_2O_2 in the nebulizer: (***A***) 0 to 1200 ppb and (***B***) 0 to 60 ppb. H_2O_2 vapor was generated by bubbling an H_2O_2 solution. Vapor and particles were generated by atomizing aqueous $(NH_4)_2SO_4$ + H_2O_2 nebulizer solutions. The line shows the least squares fit.

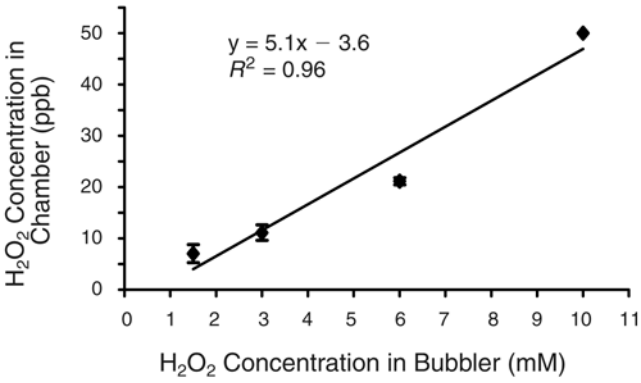

Figure 8. Vapor-phase H_2O_2 concentration in the exposure chamber as function of H_2O_2 solution strength in bubbler. H_2O_2 vapor was generated by bubbling an H_2O_2 solution. The line shows the least squares fit.

Figure 9 shows the $(NH_4)_2SO_4$ mass concentration in the exposure chamber over 2 hours of $(NH_4)_2SO_4$ aerosol generation [0.5% aqueous $(NH_4)_2SO_4$ solution in nebulizer]. The total H_2O_2 concentration in the chamber during vapor-phase H_2O_2 generation using the bubbler (3 mM H_2O_2 in bubbler) is also shown. Particle number concentrations measured by the laser particle counter were below 1 particle/cm^3 during generation of vapor-phase H_2O_2 and particle-free air. H_2O_2 concentrations measured by the automated H_2O_2 analyzer were below detection limits during the operation of particle-free air test atmospheres. The generation systems produced stable, reproducible test atmospheres over 2 hours. The addition of a syringe feed could extend operation considerably.

Calculation of Aerosol Properties

$(NH_4)_2SO_4$ Aerosol Particle mass concentrations were calculated from particle number concentrations measured with the laser particle counter assuming a particle density (ρ_p) of 1.3 g/cm^3. The density is the mass-weighted density of $(NH_4)_2SO_4$ ($\rho_{(NH4)2SO4}$ = 1.8 g/cm^3) and water (ρ_w = 1.0 g/cm^3) at 85% relative humidity:

$$\rho_p = (mf_{(NH4)2SO4}) \times (\rho_{(NH4)2SO4}) + (mf_w) \times (\rho_w) \quad (1)$$

where mf is mass fraction. The mass fractions of $(NH_4)_2SO_4$ and water in the aerosol were calculated using the empirical equation of Chan and associates (1992) for the $(NH_4)_2SO_4$ and water system:

$$mf_{(NH4)2SO4} = 2.27515 - 11.147\ RH + 36.3369\ RH^2 - 64.213\ RH^3 + 56.8341\ RH^4 - 20.0953\ RH^5 \quad (2)$$

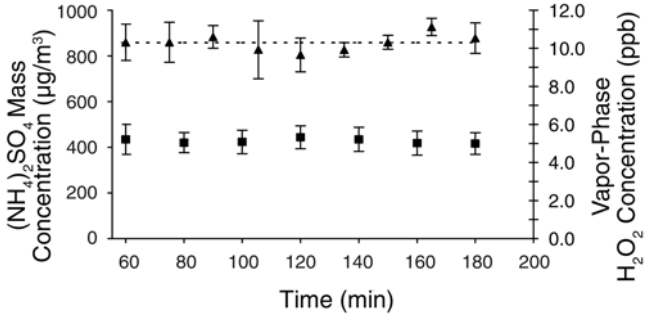

Figure 9. Exposure chamber $(NH_4)_2SO_4$ mass concentration [0.5% aqueous $(NH_4)_2SO_4$ solution in nebulizer] and vapor-phase H_2O_2 concentration (3 mM H_2O_2 in bubbler) measured over 2 hours (85% RH). ■, $(NH_4)_2SO_4$; ▲, H_2O_2; dotted line, average value. Measurements were made after system was conditioned for 1 hour (time = 60 minutes). Error bars indicate measurement uncertainty expressed as 1 SD.

where RH is relative humidity. At 85% RH, the aqueous $(NH_4)_2SO_4$ aerosol is 37% $(NH_4)_2SO_4$ and 63% water by mass.

Note that the particle counter was calibrated with latex particles having a refractive index of 1.59. The refractive index of $(NH_4)_2SO_4$ particles is 1.53 (Zhang et al 1994); the refractive index of water is 1.0. The refractive index of model aerosol (i) can be calculated as a volume average of species as follows:

$$i = \frac{i_1 V_1 + i_2 V_2 + \ldots + i_n V_n}{V_1 + V_2 + \ldots V_n} \quad (3)$$

where i_n and V_n are the refractive index and volume for the nth species in the model aerosol. For example, the refractive index of a solution of 37% $(NH_4)_2SO_4$ with 63% water by mass, calculated as a volume average of the two species, is approximately 1.38.

Particle sizes are not adjusted to account for the refractive index for the measurements presented here. This results in an underestimation of approximately 13% in particle diameter and 44% in mass concentration.

$(NH_4)_2SO_4$ + H_2O_2 Aerosol Adding H_2O_2 to the aqueous $(NH_4)_2SO_4$ nebulizer solution yielded aqueous particles containing H_2O_2 and $(NH_4)_2SO_4$ suspended in air containing H_2O_2 and water vapor. The Henry law constant, vapor-phase H_2O_2 concentration, and water content of the particles were used to calculate the particle-phase concentration of H_2O_2. The measured relative humidity and equations 1 and 2 were used to calculate the mass fractions of water and $(NH_4)_2SO_4$ and the particle material density. The mass fractions and particle density, together with measured particle size distributions, were used to calculate the particle mass, $(NH_4)_2SO_4$, and water concentrations (Table 3). The Henry law constant for H_2O_2 in water and the total H_2O_2 concentration were used to calculate the particle-phase H_2O_2 concentration. For example, at 85% relative humidity, an atomizer solution of 0.01 M H_2O_2 and 0.5% (wt/vol) $(NH_4)_2SO_4$ yields a total particle mass concentration of 1146 ± 59 μg/m^3 and total H_2O_2 concentration of 13 ± 1 μg/m^3 (Table 3). This aerosol is 37% sulfate and 63% water according to equation 2. Thus the aerosol water content is 722 ± 37 μg/m^3. At a temperature of 298 K (vapor constant 0.0821 atm L/K), the fraction of H_2O_2 in the particle phase, $F_{\text{particle-phase}}$, is

$$F_{\text{particle-phase}} \cong 2.5\times10^{-11} HW \quad (4)$$

where H is the Henry law constant for H_2O_2 (7.36×10^4 M/atm; Lind and Kok 1986) and W is aerosol water content (μg/m^3)(Wexler and Sarangapani 1998). In this example, $F_{\text{particle-phase}}$ is 0.0013 ± 0.0001, resulting in a particle-phase H_2O_2 concentration of 17 ± 2 ng/m^3.

Lind and Kok (1986) showed that H_2O_2 solubility increases in concentrated $(NH_4)_2SO_4$ solutions and that the Henry law constant for H_2O_2 in an aqueous $(NH_4)_2SO_4$ solution is greater than the Henry law constant for H_2O_2 in water by a factor of 2 for 2.5 M of $(NH_4)_2SO_4$ solutions. The $(NH_4)_2SO_4$ concentration is approximately 2.8 M in these aerosols. Thus, 34 ng/m^3 is a better estimate of particle-phase H_2O_2 in the H_2O_2 + $(NH_4)_2SO_4$ test atmosphere. Table 3 shows the H_2O_2 concentration in the nebulizer, the measured total (vapor plus particle) H_2O_2 concentration in exposure chamber, and the predicted particle-phase H_2O_2

Table 3. Measured Total and Calculated Particle-Phase Concentrations of H_2O_2[a]

Aqueous H_2O_2 in Nebulizer (M)	$(NH_4)_2SO_4$ Mass Concentration (μg/m^3)	Total H_2O_2 Concentration in Exposure Chamber		Particle-phase H_2O_2 Concentration in Exposure Chamber (μg/m^3)
		(μg/m^3)	(ppb)	
0.010	424 ± 22	13 ± 1[b]	9 ± 0.7	0.034 ± 0.002
0.027	435 ± 18	31 ± 6[b]	22 ± 4	0.082 ± 0.008
0.11	434 ± 17	145 ± 3[b]	104 ± 2	0.41 ± 0.02
0.29	420 ± 30	400 ± 17[c]	288 ± 12	1.04 ± 0.02
0.53	420 ± 30	1,000 ± 3[c]	719 ± 2	2.6 ± 0.004
0.77	420 ± 30	1,290 ± 210[c]	928 ± 151	3.36 ± 0.27

[a] Data represent means ± SD of at least 10 experiments.

[b] Total H_2O_2 was measured by the online automated analyzer. Conditions were 85% relative humidity and 298 K.

[c] Total H_2O_2 concentration was collected and measured by the integrated method.

concentration at 85% relative humidity in the exposure chamber. The addition of H_2O_2 to the aqueous $(NH_4)_2SO_4$ solution at these levels had a negligible influence on the resulting particle mass and size distribution. H_2O_2 concentrations of 0.027 and 0.01 M in 0.5% $(NH_4)_2SO_4$ solutions produced 435 ± 18 and 424 ± 22 μg/m^3 of $(NH_4)_2SO_4$, which are not significantly different according to a paired *t* test.

Only a small fraction of the H_2O_2 is in the particle phase. However, particle-phase concentrations of H_2O_2 in the atmosphere during photochemical smog episodes are likely to be similar to particle-phase concentrations of individual organic compounds (eg, benzo[*a*]pyrene). Moreover, the transport, fate and, therefore, effects of particle-phase atmospheric compounds are different from those in the vapor phase.

Equilibrium Partitioning Assumption An $H_2O_2 + (NH_4)_2SO_4$ aerosol consists of particles containing water, H_2O_2, and $(NH_4)_2SO_4$ in an atmosphere containing vapor-phase H_2O_2 and water. We assumed that the partitioning of H_2O_2 between vapor and particle phases was in equilibrium when calculating the particle-phase H_2O_2 concentration. The results of our evaluation of the validity of this assumption are shown in equation 5. The characteristic time required to reach equilibrium as derived in this equation is based on the work of Seinfeld and Pandis (1998).

The vapor-phase equilibrium concentration of H_2O_2 (c_{eq}) at the particle surface is related to the aqueous-phase molality of H_2O_2 (m_A) by

$$c_{eq} = K_A \gamma_A m_A \quad (5)$$

where

K_A = equilibrium constant for H_2O_2 (kg/m^3) and
γ_A = activity coefficient of H_2O_2.

The rate of change of the H_2O_2 molality in the aqueous phase is related to the rate of change of the concentration at the particle surface by

$$\frac{dc_{eq}}{dt} = K_A \gamma_A \frac{dm_A}{dt} . \quad (6)$$

Note that

$$m_A = n_A / (0.018 n_w) \quad (7)$$

where n_A and n_w are the molar concentrations of H_2O_2 and water in the aerosol per cubic meter of air. Because the mass transfer of H_2O_2 is small,

$$\frac{dm_A}{dt} \cong \frac{1}{0.018 n_w} \frac{dn_A}{dt} . \quad (8)$$

The rate of change of the molar concentration of H_2O_2 in the aerosol phase (dn_A/dt) equals the total flux (J) of H_2O_2 out of the aerosol. Thus,

$$\frac{dc_{eq}}{dt} \cong \frac{K_A \gamma_A J}{0.018 n_w} . \quad (9)$$

The flux from the surface of a single particle to the bulk vapor is given by

$$J_1 = 4\pi R_p D_A f(\mathrm{Kn}, \alpha)(c_{eq} - c_\infty) \quad (10)$$

where

R_p = particle radius,
D_A = vapor-phase diffusivity of H_2O_2,
c_{eq} = vapor-phase equilibrium concentration of H_2O_2 at particle surface (mol/m^3),
c_∞ = H_2O_2 concentration in the bulk vapor (mol/m^3),
$f(\mathrm{Kn},\alpha)$ = correction due to noncontinuum effects and imperfect accommodation (Fuchs and Sutugin 1971),
Kn = Knudsen number, and
α = mass accommodation coefficient on aqueous surfaces:

$$f(\mathrm{Kn}, \alpha) = \frac{0.75\alpha(1 + \mathrm{Kn})}{\mathrm{Kn}^2 + \mathrm{Kn} + 0.283\mathrm{Kn}\alpha + 0.75\alpha} . \quad (11)$$

For a monodisperse aerosol with a number concentration of N (particles/cm^3), the total flux away from the surface of the aerosol (J) is

$$J = NJ_1 = 4\pi R_p D_A N f(\mathrm{Kn}, \alpha)(c_{eq} - c_\infty) . \quad (12)$$

Thus, substituting for J,

$$\frac{dc_{eq}}{dt} = \frac{4\pi K_A \gamma_A R_p D_A N f(\mathrm{Kn}, \alpha)(c_{eq} - c_\infty)}{0.018 n_w} . \quad (13)$$

Because the fraction of H_2O_2 in the particle phase is small, c_∞ remains essentially constant and the time scale (τ_a) for establishing equilibrium between the vapor and aerosol phases is given by

$$\tau_a = \frac{C_w}{4\pi K_A \gamma_A R_p D_A N f(\mathrm{Kn}, \alpha)} \quad . \tag{14}$$

The time scale for a polydisperse aerosol can be approximated by replacing R_p by the actual number mean particle radius in equation 14 and in the calculation of Kn (Seinfeld and Pandis 1998).

Using values typically encountered in the exposure chamber:

N = 14,000 particles/cm^3,
R_p = 0.2 μm,
$K_A = 5.5 \times 10^5$ μg/m^3 air (Henry law constant),
γ_A = 1,
D_A = 0.18 cm^2/sec,
α = 0.12 (Seinfeld and Pandis 1998), and
C_w = 730 μg/m^3 (maximum chamber concentration),

the characteristic time to achieve equilibrium between vapor and particle-phase H_2O_2 concentrations is approximately 0.007 seconds, which is faster than the 0.73-second residence time of particles in the aerosol generation system. Thus, vapor–particle equilibrium is a reasonable assumption.

CONCLUSIONS

An inhalation exposure chamber was designed to study the effects of H_2O_2 and other water-soluble gases in animal models in order to understand mechanisms underlying toxicity associated with fine PM. The aerosol generation system was evaluated through repeated generation and measurement of four test atmospheres. We found that the aerosol generation system produced stable test atmospheres over a range of concentrations in the exposure chamber. Real-time chamber conditions were characterized by an automated H_2O_2 analyzer (see next section), a laser particle counter, and a relative humidity and temperature meter. Particle-phase H_2O_2 concentrations can be calculated using equilibrium assumptions. Interestingly, the rapid time to equilibrium (0.007 seconds) suggested that separate collection of particle-phase H_2O_2 using a diffusion denuder to strip the vapor phase was impractical. Overall, this system allowed for the generation of reproducible test atmospheres and facilitated mechanistic inhalation studies of PM-induced toxicity.

SECTION 2. DEVELOPMENT OF REAL-TIME H_2O_2 DETECTOR

INTRODUCTION

Quantitative measurement of H_2O_2 in the atmosphere is considered important because of the role H_2O_2 plays in oxidation of sulfur dioxide (SO_2) to sulfuric acid (H_2SO_4) aerosol in cloud droplets. In addition, knowledge of H_2O_2 concentrations is needed to assess human exposure. Generally, the concentration of H_2O_2 is determined by stripping H_2O_2 from the air into a solution followed by chemiluminescence or fluorescence of the H_2O_2 content.

Kok and coworkers (1978) used a chemiluminescent method to quantify H_2O_2 concentrations in solution. Their analytic system is based on the oxidation of 5-amino-2,3-dihydro-1,4-phthalazinedione (luminol) by H_2O_2 in the presence of a Cu(II) catalyst. The sensitivity for vapor-phase H_2O_2 is better than 1 ppb and the detection limit is about 0.5 ppb. Lazrus and colleagues (1986) developed an automated fluorometric method to measure H_2O_2 in real time; their method was based on peroxidase-mediated decomposition of H_2O_2 to water and 6,6′-dihydroxy-3,3′-biphenyldiacetic acid. This product is fluorescent with a peak excitation of 320 nm and emission of 400 nm. Using this method, the H_2O_2 concentration is proportional to fluorescence intensity. Lee and Tang (1990) developed a nonenzymatic method to measure H_2O_2 in aqueous atmospheric samples. Their analytic scheme is based on the Fenton reaction, in which each ferrous ion reacts with H_2O_2 to yield an hydroxyl radical. The hydroxyl radical is scavenged by benzoic acid to form isomeric hydroxybenzoic acid, which exhibits strong fluorescence. The method of tunable diode laser absorption spectroscopy (TDLAS) developed by Schiff and associates (1983) measures H_2O_2 directly in the vapor phase. The basic operational principle of TDLAS is measurement of vibrational absorption from a single rotational-vibrational line in the mid-infrared spectrum of a molecule. Slemr and coworkers (1986) used TDLAS to determine the concentration of vapor-phase H_2O_2 in ambient air. The highest 1-hour average was 2.1 ppb in Ontario, Canada. Mackay and colleagues (1990) used TDLAS to measure H_2O_2 concentrations ranging from 0.25 to 1.1 ppb in Glendora, California.

In the Section 2 studies, an enzymatic method similar to that of Lazrus and colleagues (1986) was used to quantify total H_2O_2 concentration by fluorescence after aqueous stripping of H_2O_2. A real-time H_2O_2 monitor was constructed for this analysis. The peroxidase concentration, pH range, and sampling flow rate were optimized and the fluorometric detector was interfaced with a computer for data

acquisition. This real-time instrument was used to monitor exposure conditions during our animal experiments.

METHODS

Collection Devices

Two types of devices, both designed to strip H_2O_2 from air, were developed and tested. These were (1) a diffusion scrubber (DS) and (2) a collection coil. Based on the work described here, the collection coil was selected for use with the real-time H_2O_2 analyzer.

The DS was constructed in the laboratory according to the design of Dasgupta and associates (1998) (Figure 10A). The DS consisted of a 60-cm porous polypropylene membrane tube (model X-20: 400 µm internal diameter, 25 µm wall, 40% surface porosity, 0.02 µm mean pore size, Celgard, Charlotte NC) placed in the sample vapor stream, which was controlled at 0.5 L/min. The end of the membrane was inserted into 500-µm polytetrafluoroethylene (PTFE) tubing (Fisher Scientific, Pittsburgh PA) and crimped with a copper wire, which was covered with PTFE tape. The membrane assembly was placed in a polypropylene tee (Cole-Parmer, Vernon Hills IL) with the help of a space-fitting PTFE tube (Fisher Scientific). The membrane was circumscribed by 5-mm inner diameter PTFE tubing, which was maintained in a linear shape by an outer glass tube (9 mm, Friedrich & Dimmock, Millville NJ). The scrubbing solution was pumped through the membrane tube at 100 µL/min. The H_2O_2 diffused to the membrane where it was absorbed by the scrubbing solution for subsequent analysis in the analytic system. Deposition of particles to the surfaces in the DS was expected to be very low due to the laminar vapor flow in the vertically mounted DS and the much lower diffusion coefficient for particles.

H_2O_2 was scrubbed using a collection coil (Figure 10B) consisting of a horizontal 30-turn glass coil (Skalar, Norcross GA) with an inner diameter of 2 mm. The scrubbing solution was pumped to the collection coil at a flow rate of 100 µL/min. Ambient air was pulled through the device at 0.5 L/min, creating turbulent flow with a high surface area for diffusion of water-soluble vapors like H_2O_2 and for impaction of particles. Air and scrubbing solution were pumped from the collection coil into a vertical separator tube (Skalar). The scrubbed air was pumped from the bottom of the separator, and the scrubbing solution flowed into the analytic system (Figure 11).

Detection Units

Fluorescence intensity was monitored at an emission wavelength (λ_{em}) of 410 nm. Two types of fluorescence

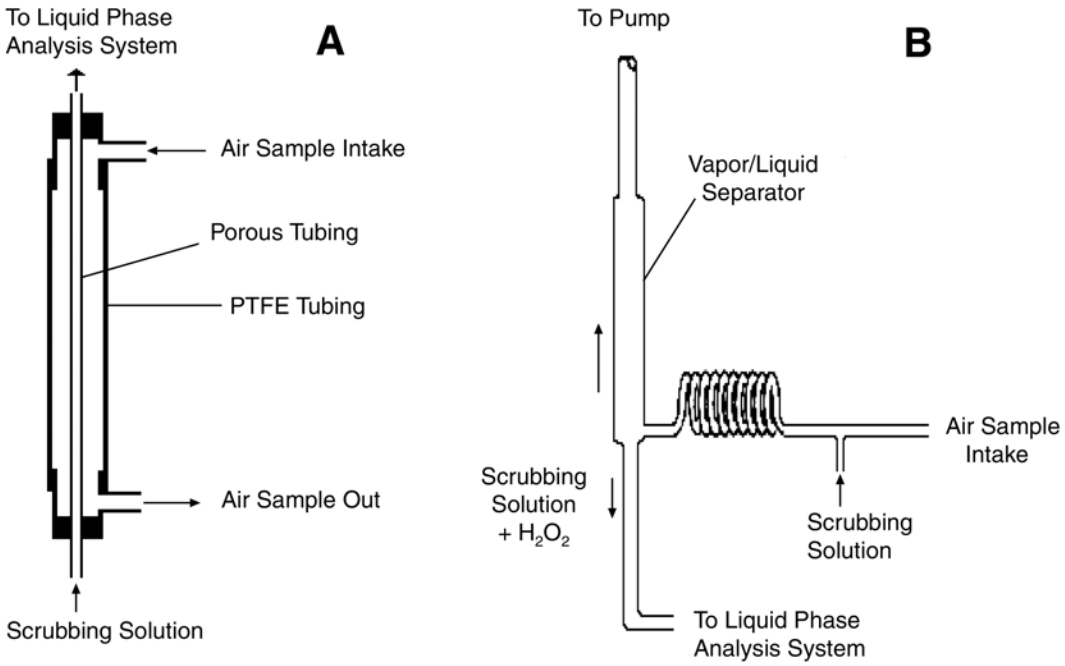

Figure 10. The diffusion scrubber (*A*) and collection coil (*B*) with separator.

detectors were used: (1) For optimization of the operating parameters, we used a compact fluorescence detector (model 474, Waters Corporation, Milford MA) with a single monochromator for excitation (λ_{ex} = 320 nm) and an adjustable emission wavelength. (2) For monitoring animal exposures, we used a portable fiberoptic spectrophotometer (Ocean Optics, Dunedin FL), consisting a deuterium light source (D-1000) with an attached cuvette holder, a detection unit (S-2000), a 2-m fiber (600 µm), and an installed 375-nm cutoff filter for emitted light. A 100-µL quartz flow-through cell (Hellma Optik, Jena, Germany) was placed in the cuvette holder. The detector was interfaced to a laptop computer and controlled by Ocean Optics proprietary software (Ooibase).

Reagents

All reagents, standards, and the scrubbing solution were prepared from high purity deionized water from a ultrapurification system (resistivity > 18 MΩ/cm, Millipore). Horseradish peroxidase (HRP), type II and p-hydroxyphenylacetic acid (PHPA), purchased from Sigma Chemical Company (St Louis MO) were the highest purity grade. The remaining reagents [KH_2PO_4, NaOH, Na_4-ethylenediaminetetraacetic acid (EDTA), 30% H_2O_2] were reagent grade materials from Fisher Scientific. Aqueous H_2O_2 standard solutions were prepared by serial dilution of a stock H_2O_2 standard solution. The stock H_2O_2 standard solution (1%) was prepared by dilution of 30% H_2O_2. The working H_2O_2 standard solutions and the PHPA reagent were prepared daily.

Analytic Measurements for Testing and Optimization

Air measurements were performed consecutively with the two collection devices. These were connected to the outlet of the H_2O_2 generation system with a 1/4-inch outer diameter PTFE tube (Fisher Scientific). All tubing (1/4-inch outer diameter for vapor system and 1/16-inch outer diameter for liquid phase system), connections, and valves were made of PTFE, which minimized the formation of H_2O_2 artifacts. The scrubbing solution from the two collection devices was introduced to the analytic system at 100 µL/min via a switching valve (Figure 11). The valve was used to select between the scrubbing solution flow from the collection coil and from the denuder. The optical detection system was based on the enzyme-catalyzed reaction of peroxides with PHPA, which forms a fluorescent dimer (Figure 12). The buffered PHPA (0.8 g/L PHPA with 0.6 g/L Na_4-EDTA in 0.01 M potassium phosphate buffer, pH 5.8)

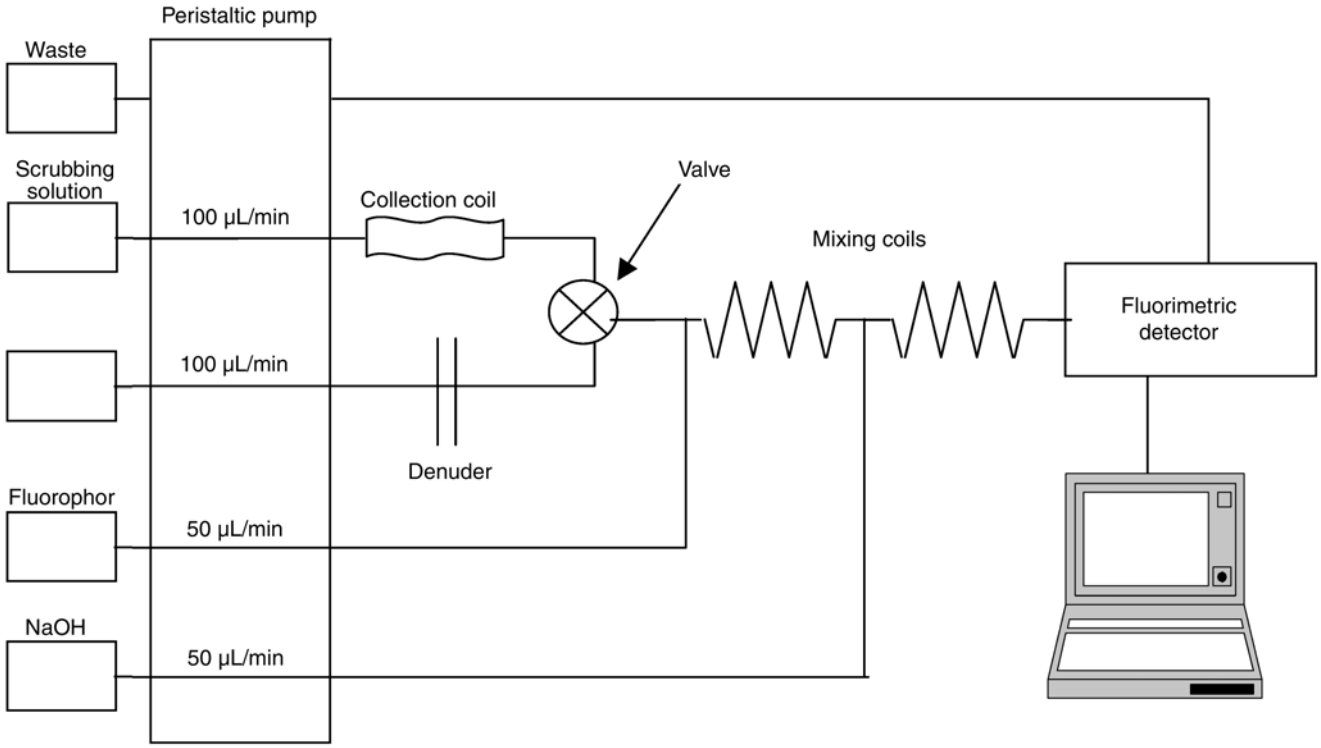

Figure 11. Experimental setup for aqueous-phase analytic system.

and 30 mg/L of HRP were mixed and then added to the stream of the scrubbing solution from the collection devices at 50 µL/min. Subsequently, an NaOH solution (0.05 M) was introduced via a second tee at 50 µL/min to raise the pH above 10. The mixed streams flowed immediately from both tees into knitted reaction coils. A 12-channel peristaltic pump (Skalar) was used to control fluid flow, with flow rates calibrated in situ.

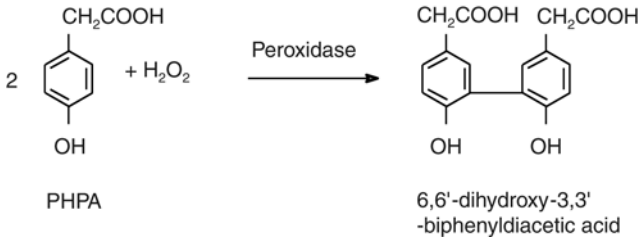

Figure 12. Formation of fluorescent dimer from peroxidase-catalyzed reaction of H_2O_2 with PHPA.

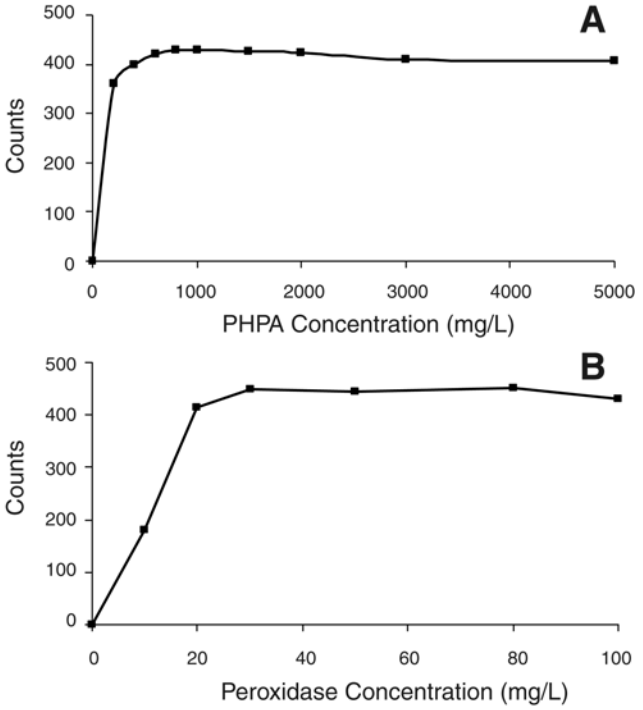

Figure 13. PHPA and peroxidase concentrations as related to intensity of fluorescence signal. ***A***. Fluorescence reagent contained 30 mg/L peroxidase and the indicated concentration of PHPA in a 0.01 M phosphate buffer. ***B***. Fluorescence reagent contained 800 mg/L PHPA and the indicated concentration of peroxidase in a 0.01 M phosphate buffer. The experimental apparatus is illustrated in Figure 11. H_2O_2 concentration was 1 µM, and the λ_{exc} and λ_{em} were 320 and 410 nm, respectively. For flow rates and other conditions, see the Methods section.

RESULTS AND DISCUSSION

Analytic Method

We investigated the relation between signal intensity and concentration of PHPA and peroxidase solutions as well as the pH of the fluorescence solution containing both PHPA and peroxide. We also examined the effect of changing the emission (λ_{em}) and excitation (λ_{exc}) wavelength of the detector on the signal. The fluorescence detector was used for these studies. The effects of different PHPA and peroxidase concentrations on intensity of the fluorescence signal are shown in Figure 13. The fluorescence signal increased with increasing PHPA and peroxidase concentrations and reached a maximum at concentrations of 800 and 30 mg/L, respectively. These concentrations were selected for subsequent experiments. At higher concentrations, the signal sensitivity leveled off.

The fluorescence signal was also measured as a function of the pH. The pH of the solution flowing into the detector was adjusted between 6 and 14 by adding 0.0 to 0.1 M NaOH. The signal showed an increase with increasing pH up to pH 12; at greater pH the sensitivity decreased slightly (Figure 14). The optimal pH of 12 was obtained by adding 0.05 M NaOH. In the final step, we examined the effect of excitation and emission wavelength on signal intensity. The results are shown in Figure 15, where the fluorescence signal is shown as a function of excitation wavelength for a fixed emission wavelength and as a function of emission wavelength for a fixed excitation wavelength. The best results were obtained at excitation and emission wavelengths of 320 nm and 410 nm, respectively.

Detection System

To adapt the instrument for field measurements, a portable fiberoptic spectrofluorometer and laptop computer

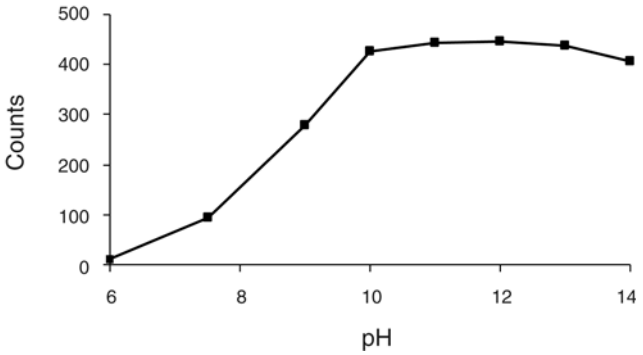

Figure 14. Intensity of fluorescence signal as function of pH. Fluorescence reagent contained 30 mg/L peroxidase and 800 mg/L PHPA in a 0.01 M phosphate buffer. The experimental apparatus is illustrated in Figure 11. H_2O_2 concentration was 1 µM, and the λ_{exc} and λ_{em} were 320 and 410 nm, respectively. For flow rates and other conditions, see the Methods section.

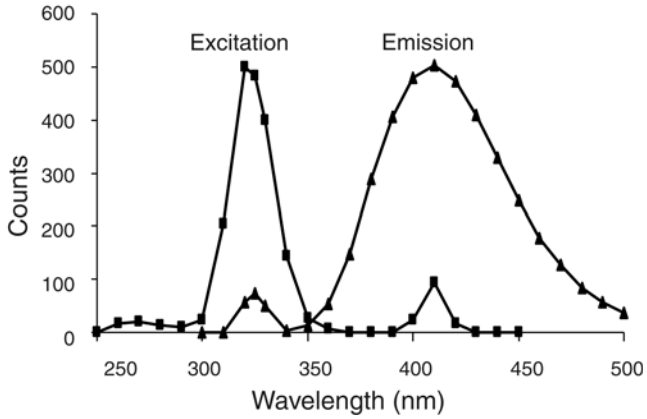

Figure 15. Relation of excitation (■) and emission (▲) wavelength of fluorescence detector to intensity of fluorescence signal. Fluorescence reagent contained 30 mg/L peroxidase and 800 mg/L PHPA in a 0.01 M phosphate buffer. The experimental apparatus is illustrated in Figure 11. H_2O_2 concentration was 1 µM. For flow rates and other conditions, see the Methods section.

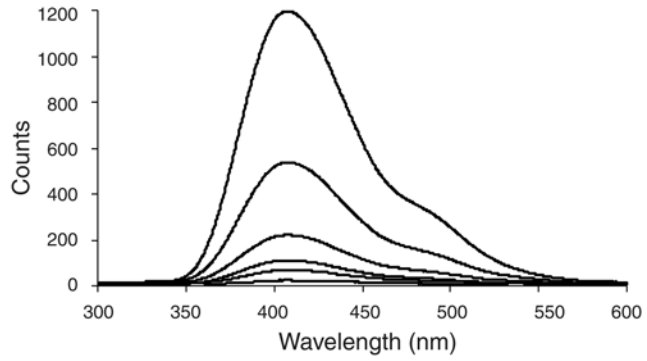

Figure 16. Scans of aqueous H_2O_2 solutions (0.25, 0.5, 1, 2, 5 and 10 µM) recorded with the fiberoptic spectrometer. The experimental apparatus is illustrated in Figure 11. For reagent compositions and flow rates, see the Methods section.

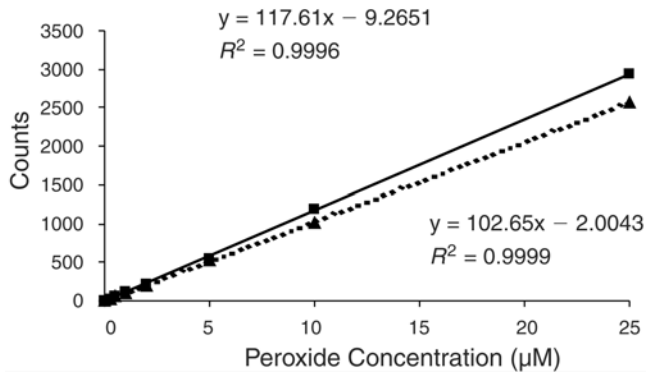

Figure 17. Calibration graphs for aqueous H_2O_2 solutions recorded with fluorescence detector (▲) and fiberoptic spectrometer (■) at an integration time of 20 seconds. The experimental apparatus is illustrated in Figure 11. For reagent compositions, fluorometer settings and flow rates, see the Methods section.

were used. The fiberoptic device was lighter and more compact than the fluorescence detector. To compare the sensitivity and reproducibility of both detection devices, we constructed calibration curves using 7 aqueous H_2O_2 standards (0.25, 0.5, 1, 2, 5, 10 and 25 µM). For the fluorescence detector, single excitation and emission wavelengths were chosen (320 nm and 410 nm, respectively) with the counts recorded every 20 seconds. The fiberoptic spectrometer software permitted scanning and integration across wavelengths (380–800 nm). The optimum integration time was found to be 20 seconds. Figure 16 shows the recorded scans for the 7 aqueous H_2O_2 standards using the fiberoptic spectrometer. Under optimum conditions, the calibration graphs were linear (correlation coefficients better than 0.99) in the range tested with both detectors (Figure 17). A shorter integration time could extend the linear range of the fiberoptic spectrometer. The limits of detection of aqueous H_2O_2 (defined as three times the standard deviation of 10 repeated scans [readings] of 0.25 µM of aqueous H_2O_2) with the fiberoptic spectrometer and the fluorescence detector, were 10 nM and 15 nM, respectively. These findings indicate that the fiberoptic spectrometer was more sensitive than the fluorescence detector. Therefore, the fiberoptic spectrophotometer was used in all animal studies.

Collection Efficiencies

To determine the efficiency of the collection coil for total (vapor plus particle phase) H_2O_2, two independent coils were used in series and the breakthrough of H_2O_2 vapor from the first to the second device was measured. We used the method described by Dasgupta and associates (1988) to calculate the collection efficiencies. The efficiency of the collection coil was greater than 99% (ie, ~100%). This is consistent with previous studies (Kleindienst et al 1988).

To determine the collection efficiency of the DS, the H_2O_2 steady state signals from the DS and from the collection coil were compared when both were sampling the same air. Vapor flow rates and the scrubbing solution flow rates into the collection coil and into the DS were the same. For the first measurements, a 30-cm DS was used and the H_2O_2 vapor was pumped at a flow rate of 2 L/min through the device. The collection efficiency for this DS under the described conditions was found to be 27% ± 3% (N = 5) for a H_2O_2 concentration of 1 ppbv. This rate is in good agreement with previous studies (Dasgupta et al 1990) with a comparable denuder and similar conditions. To improve the collection efficiency, we investigated the effect of changing the sampling rate and the denuder length. The Gormley-Kennedy equation predicts collection efficiency for conventional diffusion denuders as a

function of denuder length and sampling rate. According to this equation, the collection efficiency should increase with decreasing flow rates and increasing denuder length. In the first experiment, 1-ppbv H_2O_2 vapor was pulled through the 30-cm denuder and collection coil in parallel at different flow rates (0.5, 1, 1.5 and 2 L/min), and the H_2O_2 concentration was measured. Figure 18 shows the collection efficiencies plotted against the vapor flow rate for the 30 cm long denuder and the collection coil. The denuder collection efficiency decreased with increasing flow rates, whereas the collection coil efficiency was independent of flow rate.

In the next step, the collection efficiency was determined as a function of DS length at a constant sampling rate of 0.5 L/min. For this experiment, we constructed scrubbers with 5 different lengths (20, 30, 40, 50 and 60 cm). The collection efficiency increased with the length of the denuder scrubber; the collection efficiency of the longest denuder tested (60 cm) was 95% ± 2% (N = 5) (Figure 19). Based on these results, we recommend a 60-cm denuder and a vapor flow rate of 0.5 L/min for future studies with the DS. A signal-to-noise ratio of 3 was achieved at approximately 50 pptv when either the collection coil or the DS was used as the collection device.

Application to $(NH_4)_2SO_4$ Exposure System

As a result of the experiments described here, the real-time system for H_2O_2 analysis used to measure animal exposures can be described as follows. H_2O_2 was scrubbed from air (0.5 L/min) with a 30-turn glass collection coil containing scrubbing solution at a flow rate of 100 µL/min. PHPA and peroxidase concentrations were 800 and 30 mg/L, respectively. The H_2O_2 concentration was proportional to the fluorescence measured with the fiberoptic spectrophotometer (Ocean Optics) using a 20-second scan time. The instrument was calibrated during each exposure (real-time) with 5 aqueous H_2O_2 standard solutions (0.25–8.2 µM) prepared from a H_2O_2 stock solution (3%) standardized against a potassium permanganate primary standard solution. The coefficient of determination (R^2) for the calibration curve was typically 99%. The detection limit of the spectrophotometer was 10 nM of H_2O_2 with a precision within 2% by measuring a 0.25-µM standard H_2O_2 solution (n = 10). The stripping coil was 99.95% efficient at collecting H_2O_2, based on comparisons of upstream and downstream measurements.

The real-time peroxide analyzer was used to monitor animal exposures by placing a probe in a nose-only exposure cone. During system testing, we also collected time-integrated samples: all exposure ports but one were sealed; H_2O_2 vapor was generated as described above and pushed through the remaining exposure port into two bubblers placed in series, each containing 100 mL of deionized distilled low-endotoxin water. Detection of the fluorescent dimer signal was linearly proportional to the H_2O_2 concentration in the exposure chamber. The H_2O_2 concentration in the second bubbler was below detection limits for all samples, suggesting that the collection efficiency of the first bubbler was essentially 100%. Good agreement was found between the real-time and integrated methods. The integrated method measured a vapor-phase H_2O_2 concentration of 18 ± 5 ppb (n = 3), and the real-time instrument measured 22 ± 0.5 ppb (n = 4) when the bubbler solution strength was held constant.

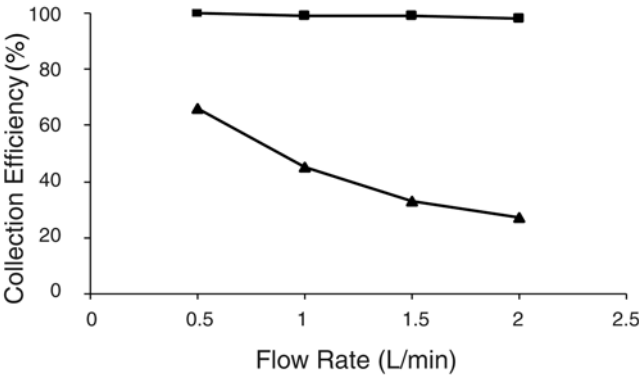

Figure 18. Collection efficiency of collection coil (■) and diffusion scrubber (▲, 30 cm scrubber) as function of H_2O_2 vapor flow rate. The H_2O_2 vapor concentration was 1 ppbv. The experimental apparatus is illustrated in Figure 11. For reagent compositions, fluorometer settings and flow rates, see the Methods section.

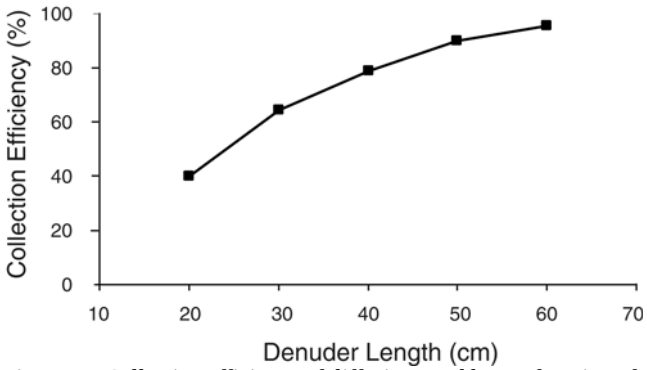

Figure 19. Collection efficiency of diffusion scrubber as function of scrubber length at H_2O_2 vapor flow rate of 0.5 L/min. The H_2O_2 vapor concentration was 1 ppbv. The experimental apparatus is illustrated in Figure 11. For reagent compositions, fluorometer settings and flow rates, see the Methods section.

SECTION 3. ACUTE EFFECTS OF INHALED $(NH_4)_2SO_4$ and H_2O_2 ON LUNG TISSUES

INTRODUCTION

The precise mechanism underlying the toxicity of inhaled PM is unknown. We hypothesize that particle-associated peroxides and alveolar macrophages are important in the pathogenic process. Preliminary support for a role of macrophages in fine PM-induced toxicity comes from reports that various types of particles, including carbon black and concentrated ambient PM_{10} (particles with aerodynamic diameters less than 10 μm), exert effects on these cells (eg, altered phagocytosis and increased oxidant production [Goldsmith et al 1998], as well as increased production of cytokines such as TNF-α [Becker et al 1996; Dong et al 1996; Chin et al 1998]). The studies described in this section of this Investigators' Report were designed to analyze the role of H_2O_2 in fine PM-induced macrophage activation and tissue injury, using $(NH_4)_2SO_4$ as a model particle. An overview of the experimental approach is given in the Specific Aims section and Table 1.

METHODS

Animals and Exposures

Female, specific pathogen-free, Sprague Dawley rats (150–175 g) were purchased from Taconic Farms (Germantown NY). The animals were housed in microisolator cages and received sterile food and pyrogen-free water ad libitum. All animal research protocols were approved by Rutgers University Animal Care and Facilities Committee according to guidelines established in the National Institutes of Health *Guide for the Care and Use of Laboratory Animals*.

Rats were exposed to $(NH_4)_2SO_4$ (430 or 215 μg/m^3), vapor-phase H_2O_2 (10, 20, or 100 ppb), $(NH_4)_2SO_4 + H_2O_2$, or particle-free air at 85% relative humidity for 2 hours. Additional rats were exposed to room air. Based on our initial characterization studies (see Section 1), we determined that the chamber should be conditioned for 60 minutes prior to animal exposures. Particle size and number, and the concentrations of particles and H_2O_2 were measured from empty ports at the ends of the chamber during each experiment. We found that concentrations of particles and H_2O_2 in the nose cones were approximately 30% less when the animals were present compared with when they were not [293.3 ± 2.8 μg/m^3 $(NH_4)_2SO_4$ and 6.8 ± 0.2 ppb, 14.1 ± 0.6 ppb, or 72 ± 2 ppb H_2O_2]. In some pilot experiments, the animals were exposed to particle-free air for 1 hour on each of the 2 days prior to test atmosphere exposure. The intent was to acclimate them to the exposure system and to isolate any chamber-related effect. No effect was found and the particle-free air was not continued. This period of acclimation did not affect any measured endpoint. In two pilot experiments, rats were exposed cumene hydroperoxide particles (102 ± 23 μg/m^3, 106 ± 21 μg/m^3) or a filtered solvent control at 45% relative humidity for 2 hours.

BAL and Macrophage Isolation

Rats were anesthetized with sodium pentobarbital (125 mg/kg, intraperitoneally). The lungs were perfused in situ via the portal vein with 50 mL of warm (37°C) Ca^{++}/Mg^{++}-free Hank balanced salt solution (HBSS, pH 7.4) (Sigma) containing ethylene diamine tetraacetic acid (0.5 mM) followed by 50 mL of HBSS at 16 mL/min. The trachea was cannulated, and the lung excised en bloc and lavaged with 50 mL (5 × 10 mL) of Ca^{++}/Mg^{++}-free HBSS (pH 7.4). The first 10 mL of BAL fluid was processed separately for analysis of protein and LDH content. BAL fluid protein content was measured spectrophotometrically using a Biorad kit (Hercules CA). LDH was quantified spectrophotometrically with a kit from Sigma. After centrifugation (300*g*, 10 minutes, 4°C), cells collected from the first lavage were combined with the remaining BAL fluid and washed three times with HBSS containing 2% fetal bovine serum (FBS). BAL cells were counted on a hemocytometer. Viability, as determined by trypan blue exclusion, was found to be > 85% for all experiments. For cell differentials, slides were prepared using a Cytospin 2 (Shandon, Cheshire, England) and stained with Giemsa (Fisher Scientific, Springfield NJ). Alveolar macrophages were 95% to 99% pure as determined morphologically and by peroxidase staining. Macrophages were isolated and tested for activation as described later in this section. For histological evaluations, lung was isolated after perfusion. Lung and trachea were removed en bloc and fixed by instillation with 10% phosphate-buffered formalin. Paraffin-embedded histologic sections (6 μm) were prepared from the fixed tissue. Tissue sections were examined for TNF-α, reactive oxygen intermediates, and reactive nitrogen intermediates as described later in the Methods for Section 3.

Electron Microscopy

Lungs from a separate group of animals were perfused with 50 mL HBSS and then inflated in situ via the trachea with phosphate-buffered saline (PBS) containing 4% paraformaldehyde and 1% glutaraldehyde. After 1 hour, the lungs were excised en bloc and placed in PBS containing 4% paraformaldehyde and 1% glutaraldehyde for 24 hours. Lungs were then dissected into sections that included small bronchi, bronchioles, alveolar ducts and

the surrounding alveoli, washed with sodium cacodylate buffer, and treated with 1% osmium tetraoxide for 1 hour followed by ethanol dehydration in graded steps. The tissues were then exposed to propylene oxide and embedded in embed 812 (Electron Microscopy Services, Ft Washington PA). Ultrathin sections (80–90 nm) were stained with uranyl acetate and lead citrate and examined with a transmission electron microscope (model JEM 100CX, JEOL, Tokyo, Japan).

Immunohistochemistry for TNF-α and Nitrotyrosine

Slides were incubated with 10% nonimmune rabbit or goat serum for 20 minutes followed by incubation overnight with a polyclonal goat antimouse TNF-α antibody (1:250) (R&D Systems, Minneapolis MN), polyclonal rabbit antinitrotyrosine antibody (1:2000) (Upstate Biotechnology, Lake Placid NY), or the appropriate dilution of pooled normal goat or rabbit sera. In some experiments the antinitrotyrosine antibody was incubated with 1 mM 3-nitrotyrosine for 10 minutes prior to immunostaining. A Vectastain Elite kit (Vector Laboratories) was utilized to show antibody binding.

Measurement of Superoxide Anion Release

Macrophages (1.5×10^5 cells) were incubated at 37°C in balanced salt solution (128 mM NaCl, 12 mM KCl, 1 mM $CaCl_2 \bullet 2H_2O$, 2 mM $MgCl_2$, 2 mM glucose, 3.43 mM anhydrous Na_2HPO_4, 0.57 mM anhydrous NaH_2PO_4) containing 44 μM ferricytochrome C, with or without 1 mM superoxide dismutase (Sigma) and/or 170 nM 12-O-tetradecanolyphorbol-13-acetate (TPA) (LC Laboratories, Woburn MA). Absorbance was determined spectrophotometrically at 550 nm 45 minutes later. The amount of superoxide anion released was calculated using a baseline value (E = 21.1 nM/cm at 550 nm) obtained from samples containing superoxide dismutase (Pilaro and Laskin 1986).

Measurement of Nitric Oxide and Peroxynitrite Production

Nitric oxide production by the cells was quantified by nitrite accumulation in the culture medium using the Griess reaction with sodium nitrite as the standard (Green et al 1982). Cells in 200 μL of phenol red-free Dulbecco modified Eagle medium (DMEM) (Sigma) containing 10% FBS, 2 mM glutamine, penicillin (100 IU)-streptomycin (100 μg), and 0.05 IU/mL porcine pancreas insulin (complete DMEM) were inoculated into 96-well dishes (2×10^5 cells/well). After 2 hours incubation, the cells were fed with media in the presence and absence of 1 to 100 U/mL IFN-γ (GIBCO, Grand Island NY) and/or 1 to 100 ng/mL LPS (Escherichia coli, serotype 0128:B12; Sigma). Culture supernatants were collected 48 hours later and analyzed for nitrite content.

Peroxynitrite production by alveolar macrophages was quantified using dihydrorhodamine 123 (Wizemann et al 1994; Ischiropoulos et al 1999). Cells were cultured in 8-well slide chambers (1.5×10^5/well) with LPS (100 ng/mL) and IFN-γ (100 U/mL) or medium control for 24 hours. TPA (170 nM) was added to the wells containing the cells 30 minutes prior to analysis. Supernatants were then removed, the cells washed with PBS and incubated for 10 minutes at room temperature with dihydrorhodamine 123 (0.5 mg/mL). The cells were then washed with PBS and visualized on a fluorescence microscope (Insight Plus, Meridian, Okemos MI).

Western Blot Analysis

Cells were incubated overnight in 24-well dishes (5×10^5 cells/well) in complete DMEM at 37°C. The cells were then washed twice and fed with DMEM containing LPS and IFN-γ or medium control. After 24 hours incubation, the cells were washed with PBS and lysed in buffer containing 10 mM Tris-HCl and 1% sodium dodecyl sulfate (SDS), pH 7.4. Protein concentrations were determined using the DC Protein Assay kit (Biorad, Hercules CA). Five μg of cellular proteins were fractionated on 7.5% SDS polyacrylamide gels and transferred onto nitrocellulose membranes. The membranes were incubated with monoclonal anti-NOS II antibody (clone 54; Transduction Laboratories, Lexington KY), goat polyclonal anticyclooxygenase (COX)-2 antibody (Santa Cruz Biotechnology, Santa Cruz CA), or with rabbit polyclonal anti-HO-1 antibody, anti–heat shock protein (HSP) 70 antibody, or anti-HSP60 antibody (Stressgen, Victoria, BC, Canada), followed by incubation with an HRP-labeled secondary antibody. Binding was visualized by autoradiography with enhanced chemiluminescence Western blotting reagents (Amersham Life Science, Arlington Heights IL).

Statistics

Statistical methods used to analyze our results included student *t* tests, and one-way and multifactorial analysis of variance (ANOVA) using SPSS (version 9.0, SPSS Inc, Chicago IL). Significant results ($P \leq 0.05$) derived from one-way ANOVA were further evaluated by multiple group comparisons procedures, which were performed in collaboration with the Office of Statistical Consulting at Rutgers University. In the majority of the studies, the animals were exposed to one of 8 test atmospheres [$(NH_4)_2SO_4$ (430 μg/m^3), vapor phase H_2O_2 (10, 20, or 100 ppb), $(NH_4)_2SO_4 + H_2O_2$ (10, 20, or 100 ppb), or particle-free air] or to room air. Data for multiple endpoints were collected at 0 hours and 24 hours after exposure. An individual experiment consisted of exposing

2 to 4 animals at a time to room air or to one of the test atmospheres on consecutive days, using animals obtained from the supplier at the same time for each group. Each animal was exposed once and then killed immediately or 24 hours after exposure. While it would have been ideal to expose animals to room air and test atmospheres on the same day, this was not practical in terms of our equipment or personnel. Efforts were made to assay multiple endpoints for each animal to minimize the number of animals used; however, assays were limited by the number of cells recovered. In a typical experiment, measurements were simultaneously made for BAL fluid cell number and viability, BAL fluid protein and LDH content, serum LDH, and alveolar macrophage production of superoxide anion and nitric oxide.

All experiments were repeated at least 3 times, and $P \leq 0.05$ was considered statistically significant. Our analysis of each measured endpoint addressed comparisons of means for 4 conditions: (1) room air versus particle-free air at 0 hours and 24 hours; (2) particle-free air at 0 hours versus the other seven test atmospheres at 0 hours; (3) particle-free air at 24 hours versus the other seven test atmospheres at 24 hours; and results for each atmosphere at 0 hours and 24 hours. Two types of simultaneous testing procedures were performed. One applies to the first three conditions, which involved many comparisons with the same standard (or control). For these procedures, the Dunnett *t* test, implemented in SAS (version 8.1, SAS Institute, Cary NC), was used. SAS 8.1 allows for different sample sizes of the various exposure groups being compared with the control; this capability was essential for these data sets.

The fourth condition involved a different sort of simultaneous testing: 8 independent two-sample *t* tests were required. In this case, the significance level at which the individual *t* tests were carried out was adjusted so that the overall procedure was significant at $P \leq 0.05$. The adjustment was done in two equivalent ways:

1. Declare any of the 8 individual differences significant if the corresponding (one-sided) *t* statistic exceeds the corresponding 0.64% critical value for the *t* distribution. The 0.64% (or 0.0064) arises from the computation:

$$1 - 0.0064 = (1 - 0.05)^{1/8} \quad (15)$$

2. Equivalently, an individual difference is declared as significant if its adjusted *P* value is less than 0.05, where

$$1 - \text{adjusted } P \text{ value} = (1 - \text{ordinary } P \text{ value})^{8}$$

The preceding applied to the tests performed on (any) one of the variables of interest. No attempt was made to allow for the fact that multiple tests were performed on a total of 10 variable endpoints. The theoretical basis for the latter type of adjustment across variables is not well understood.

RESULTS

Pulmonary Effects of Inhaled $(NH_4)_2SO_4$ and H_2O_2

Inflammation, BAL Protein and LDH Content Animals that inhaled H_2O_2, alone or in combination with $(NH_4)_2SO_4$ (430 μg/m^3), showed no major differences in BAL fluid cell number or viability (Table 4), but animals that inhaled $(NH_4)_2SO_4$ alone showed a lower cell number than the room air controls immediately after exposure. This difference was not significant when rats were exposed to a lower dose of $(NH_4)_2SO_4$ (215 μg/m^3) (not shown). Differential staining of BAL cells revealed that the majority (95%) were macrophages and the remainder were multinucleated cells or small mononuclear cells. The composition of the cells recovered in BAL fluid was unaltered by the exposures.

We also evaluated BAL fluid protein and LDH content, which are markers of alveolar epithelial injury (Kleeberger and Hudak 1992). BAL fluid from control animals (room air) contained low levels of protein (Table 4). No significant changes were observed immediately or 24 hours after exposure of rats to $(NH_4)_2SO_4$ and/or H_2O_2. Similarly, no changes were observed in LDH levels in BAL fluid with respect to the exposure conditions or postexposure times. However, increases in serum LDH levels were observed both immediately (trend) and 24 hours after exposure to 20 ppb H_2O_2 (Table 4).

To determine whether inhalation of $(NH_4)_2SO_4$ + H_2O_2 caused structural alterations in the lung, we analyzed histological sections microscopically. No significant changes in gross morphology were detected in lung sections from rats exposed to air, $(NH_4)_2SO_4$ (430 μg/m^3), H_2O_2 (10 or 20 ppb) or $(NH_4)_2SO_4$ + H_2O_2 by light microscopy (not shown). However, electron microscopy revealed an increase in the number of neutrophils in the capillary spaces adjacent to terminal respiratory bronchioles and in alveolar ducts in lungs from rats after inhalation of $(NH_4)_2SO_4$ + 20 ppb H_2O_2 or 20 ppb H_2O_2 alone (Figure 20). Moreover, there was evidence of increased adherence of the neutrophils to the vascular endothelium (Figure 21). These effects were more pronounced in lungs from animals exposed to $(NH_4)_2SO_4$ + 20 ppb H_2O_2 rather than 20 ppb H_2O_2 alone. These changes were not evident in lung sections from rats exposed to $(NH_4)_2SO_4$ alone or from both air controls. No

Table 4. Effects of $(NH_4)_2SO_4$ and H_2O_2 on Lung Lavage Cells, Protein, and LDH[a]

Atmosphere	*N*	Total Cells[b] ($\times 10^7$)	Viable Cells[b] (%)	BAL Protein[b] (mg/mL)	BAL LDH[b] (nmol/min/mL)	Serum LDH[b] (nmol/min/mL)
Room air	21	1.2 ± 0.1	87.4 ± 0.8	0.10 ± 0.01	74.4 ± 5.3	321.6 ± 26.4
0 Hours After Exposure						
Particle-free air	11	1.1 ± 0.1	87.2 ± 1.5	0.11 ± 0.02	80.0 ± 9.2	368.8 ± 52.9
$(NH_4)_2SO_4$ (430 µg/m^3)	12	**0.8 ± 0.1**[c]	87.1 ± 1.7	0.13 ± 0.01	78.8 ± 4.8	338.8 ± 25.9
10 ppb H_2O_2	6	1.1 ± 0.1	91.5 ± 1.7	0.12 ± 0.02	87.8 ± 6.3	526.8 ± 124.9
20 ppb H_2O_2	9	1.4 ± 0.1	91.8 ± 1.1	0.09 ± 0.01	77.3 ± 4.3	506.7 ± 129.6
100 ppb H_2O_2	4	1.1 ± 0.1	89.8 ± 1.8	0.09 ± 0.02	70.0 ± 9.9	320.0 ± 120.0
$(NH_4)_2SO_4$ + 10 ppb H_2O_2	10	1.1 ± 0.1	89.0 ± 1.6	0.12 ± 0.01	68.7 ± 2.7	287.7 ± 14.4
$(NH_4)_2SO_4$ + 20 ppb H_2O_2	6	1.0 ± 0.1	88.2 ± 1.7	0.09 ± 0.01	86.0 ± 7.8	297.2 ± 39.7
$(NH_4)_2SO_4$ + 100 ppb H_2O_2	7	1.0 ± 0.1	87.2 ± 2.9	0.10 ± 0.01	NM	NM
24 Hours After Exposure						
Particle-free air	12	1.0 ± 0.1	83.4 ± 2.4	0.15 ± 0.04	71.9 ± 3.4	321.6 ± 26.4
$(NH_4)_2SO_4$ (430 µg/m^3)	16	0.8 ± 0.1	**92.2 ± 1.2**[c]	0.12 ± 0.01	68.4 ± 3.5	423.0 ± 57.7
10 ppb H_2O_2	18	0.8 ± 0.1	89.3 ± 1.0	0.12 ± 0.01	76.6 ± 9.9	361.5 ± 55.0
20 ppb H_2O_2	6	0.9 ± 0.1	82.0 ± 1.5	0.09 ± 0.01	86.7 ± 4.2	**943.3 ± 120.3**[c]
100 ppb H_2O_2	4	1.1 ± 0.1	88.5 ± 1.0	0.09 ± 0.01	NM	NM
$(NH_4)_2SO_4$ + 10 ppb H_2O_2	18	1.0 ± 0.1	85.4 ± 1.8	0.11 ± 0.01	76.3 ± 4.6	496.0 ± 84.6
$(NH_4)_2SO_4$ + 20 ppb H_2O_2	4	1.4 ± 0.1	92.1 ± 1.0	0.13 ± 0.01	70.9 ± 4.4	396.5 ± 42.1
$(NH_4)_2SO_4$ + 100 ppb H_2O_2	6	1.0 ± 0.1	87.2 ± 2.9	0.08 ± 0.01	NM	NM

[a] BAL fluid was collected from rats at 0 or 24 hours after exposure to room air, particle-free air, $(NH_4)_2SO_4$, H_2O_2, or $(NH_4)_2SO_4$ + H_2O_2.

[b] Each value represents the mean ± SE of the number (*N*) of experiments indicated. Means from animals exposed to particle-free air were not significantly different from means from animals exposed to room air.

[c] Statistical comparison by ANOVA of data from animals exposed to room air versus the experimental atmospheres, followed by multiple comparison tests, were significant at $P < 0.05$.

NM = not measured.

changes in the number or morphology of alveolar macrophages were observed in the tissue.

TNF-α Expression Low level staining of TNF-α was observed in lung sections from air-exposed rats (Figure 22A) when compared to sections stained with pooled normal goat serum (Figure 22G,H). This was most prominent in the epithelium. Although exposure of rats to $(NH_4)_2SO_4$ (Figure 22B) or to 10 ppb H_2O_2 alone (Figure 22C) or in combination had no effect on TNF-α expression in lung sections immediately after exposure, a small increase in staining was noted in alveolar macrophages immediately after rats were exposed to 20 ppb H_2O_2 (not shown). In contrast, a marked increase in TNF-α expression in lung macrophages and epithelial cells was observed after rats were exposed to the combination of $(NH_4)_2SO_4$ + 20 ppb H_2O_2. This was apparent immediately after exposure (not shown) and became more pronounced after 24 hours

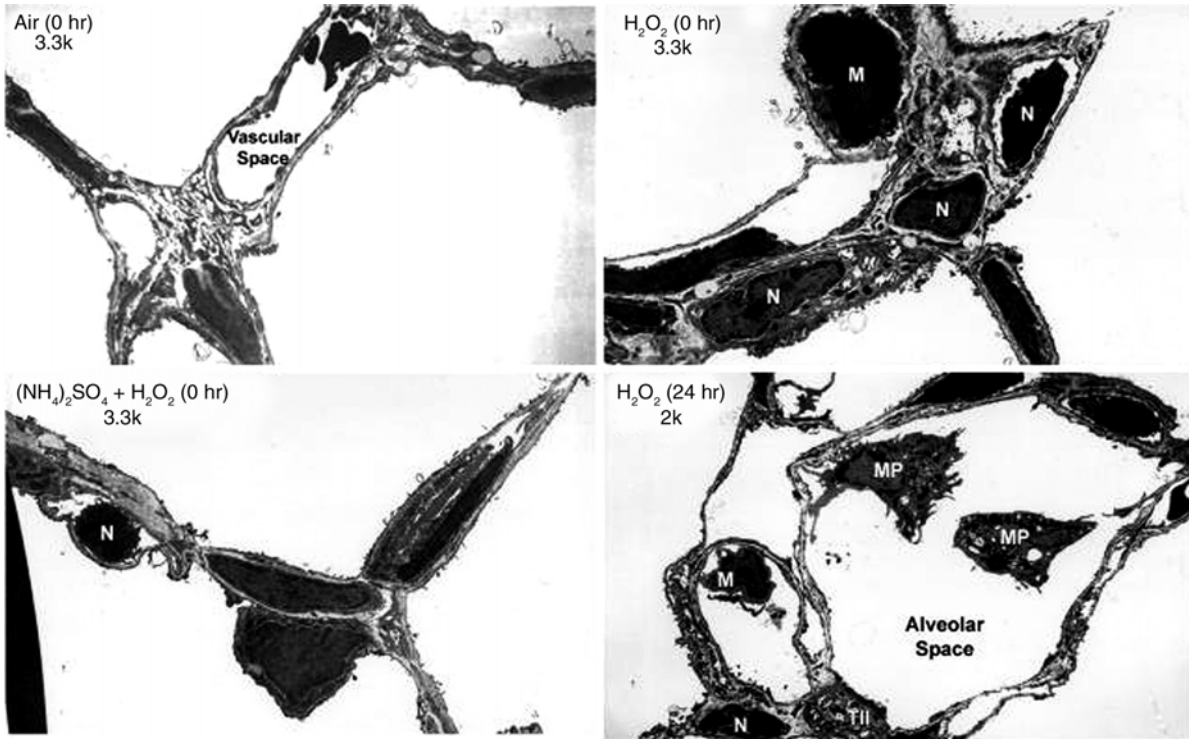

Figure 20. Electron micrographs showing neutrophil influx into rat lung. Influx is evident immediately after inhalation of 20 ppb H_2O_2 or $(NH_4)_2SO_4$ + 20 ppb H_2O_2, but not after inhalation of particle-free air. Neutrophil influx was more pronounced 24 hours after inhalation of H_2O_2 than immediately after exposure. N = neutrophil. MP = macrophage. M = monocyte. TII = Type II cell. Original magnification indicated in each panel.

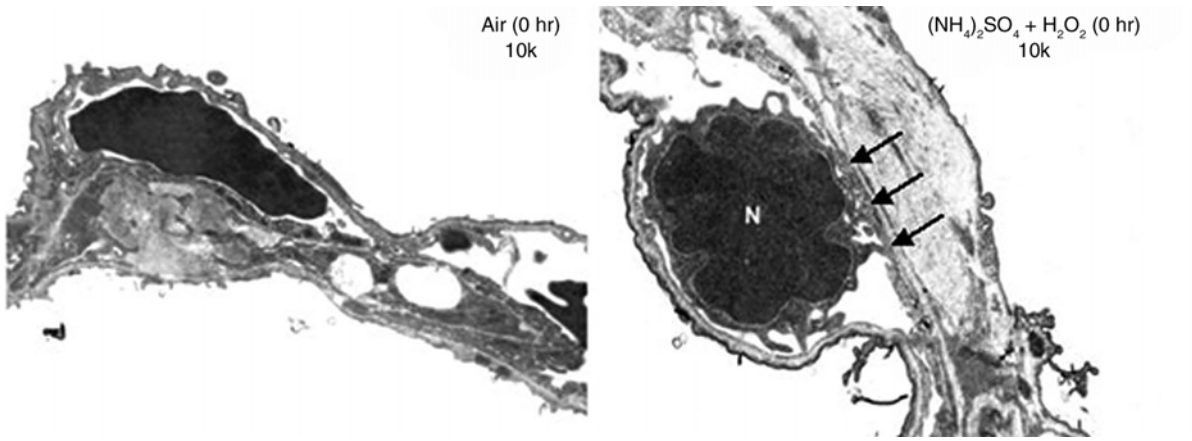

Figure 21. Electron micrographs showing neutrophil adherence. Increased adherence of neutrophils to the endothelium (indicated by arrows) is evident immediately after inhalation of $(NH_4)_2SO_4$ + 20 ppb H_2O_2 but not after inhalation of particle-free air. Original magnification indicated in each panel. N = neutrophil.

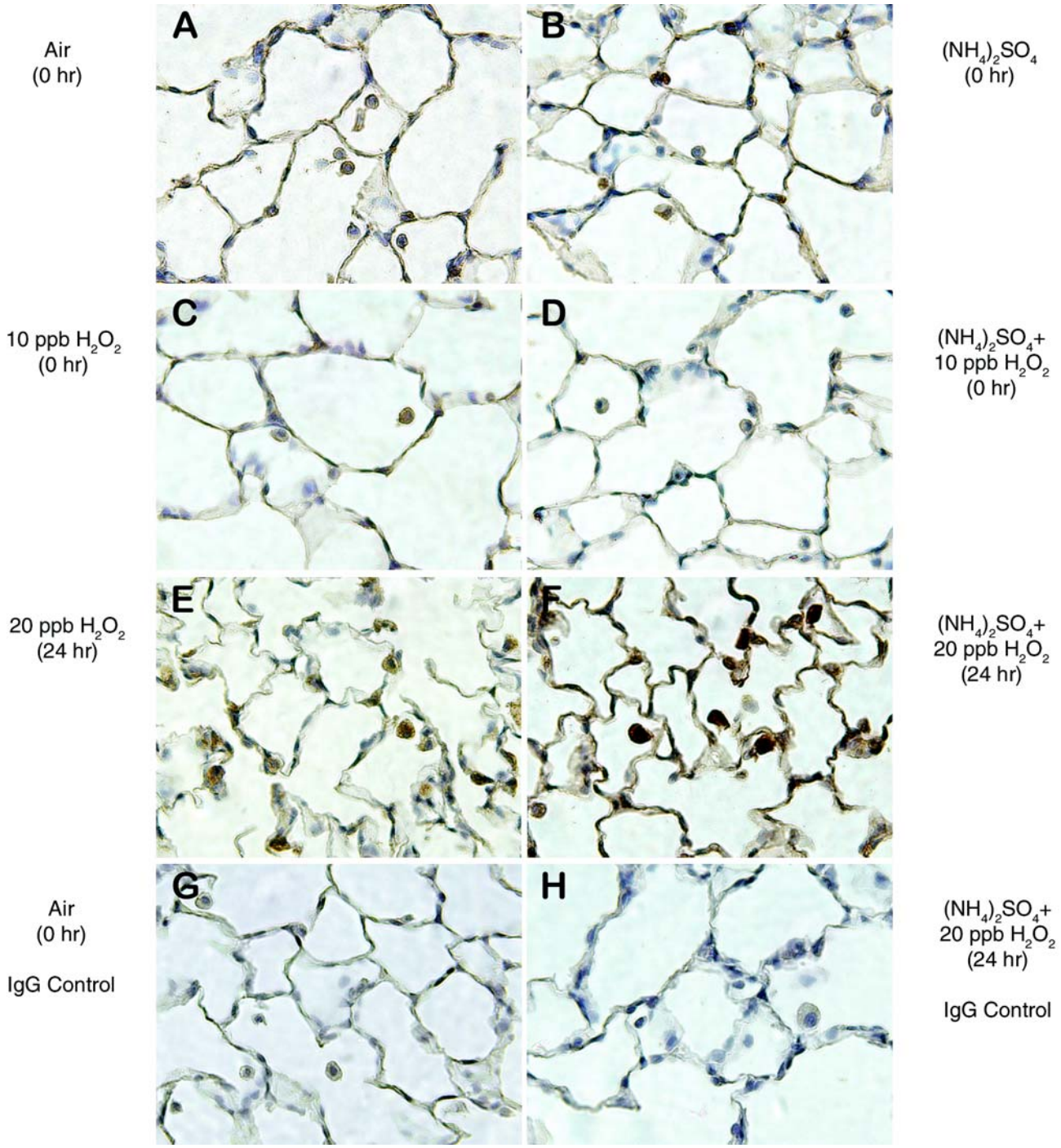

Figure 22. TNF-α immunostaining in lung epithelial tissue. Rats were exposed to air *(**A** and **G**)*, $(NH_4)_2SO_4$ *(**B**)*, 10 ppb H_2O_2 *(**C**)*, $(NH_4)_2SO_4$ + 10 ppb H_2O_2 *(**D**)*, 20 ppb H_2O_2 *(**E**)*, or $(NH_4)_2SO_4$ + 20 ppb H_2O_2 *(**F** and **H**)*. Sections were stained with anti–TNF-α antibody *(**A–F**)* or IgG control *(**G** and **H**)*. Original magnification, 400×.

Table 5. Quantitation of Alveolar Macrophages Staining Positive for TNF-α[a]

Atmosphere	Positive Cell Count
Room air	14 ± 3
$(NH_4)_2SO_4$	7 ± 3
10 ppb H_2O_2	10 ± 2
20 ppb H_2O_2	**27 ± 5**[b]
$(NH_4)_2SO_4$ + 10 ppb H_2O_2	10 ± 3
$(NH_4)_2SO_4$ + 20 ppb H_2O_2	**64 ± 14**[b]

[a] Histologic lung sections were prepared 24 hours after exposure of rats to the test atmosphere. Positively stained alveolar macrophages were quantified by light microscopy (400×). Data represent the average number of cells ± SEM (n = 3 animals) in 30 random fields.

[b] Statistical comparison by ANOVA of data from animals exposed to room air versus the experimental atmospheres, followed by multiple comparison tests, were significant at $P < 0.05$.

(Figure 22F). TNF-α staining was also noted in lung sections 24 hours after exposure of the animals to 20 ppb H_2O_2 alone (Figure 22E). This was confirmed by quantifying the number of macrophages staining positive for TNF-α. Thus, greater numbers of positively stained macrophages were observed in sections obtained 24 hours after exposure to 20 ppb H_2O_2 or $(NH_4)_2SO_4$ + 20 ppb H_2O_2 (Table 5). However, these effects were not seen at 24 hours after exposure of rats to 10 ppb H_2O_2 or $(NH_4)_2SO_4$ + 10 ppb H_2O_2.

Production of Reactive Oxygen and Nitrogen Intermediates by Alveolar Macrophages In the absence of stimulation, alveolar macrophages produced relatively low levels of superoxide anion. TPA, which is known to induce a respiratory burst in phagocytic cells (Pendino et al 1993; Laskin et al 1994; Prokhorova et al 1994), was used to stimulate alveolar macrophage production of superoxide anion. Exposure of rats to $(NH_4)_2SO_4$ + 20 ppb H_2O_2 resulted in significantly greater TPA-stimulated superoxide anion production by alveolar macrophages isolated immediately after exposure compared to macrophages from air-exposed rats (Figure 23). This effect was transient; by 24 hours after exposure, levels of superoxide anion were at or below control levels. Superoxide anion production by cells from rats exposed to $(NH_4)_2SO_4$ + 100 ppb H_2O_2 were also below control levels at this time. At 24 hours after exposure, superoxide anion production by cells from rats exposed to $(NH_4)_2SO_4$ alone was also decreased (Figure 23). In contrast, inhalation of 20 ppb H_2O_2 alone resulted in significantly increased superoxide anion production by the cells, a response that was only observed after 24 hours.

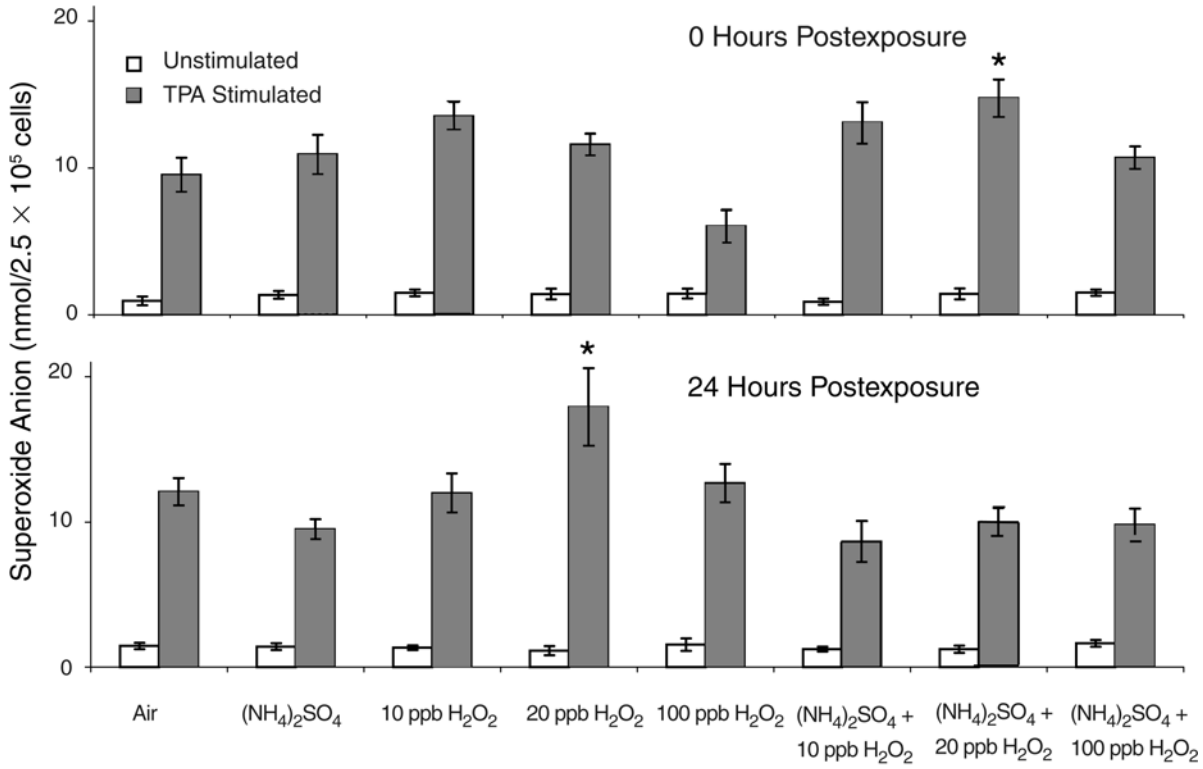

Figure 23. Superoxide production by alveolar macrophages collected at 0 or 24 hours after rats inhaled air, $(NH_4)_2SO_4$, H_2O_2 or $(NH_4)_2SO_4$ + H_2O_2. Cells were incubated with medium (□) or TPA (■) prior to measurement of superoxide anion production. Data are means ± SEM from 6 to 12 experiments. Comparison of exposure to air versus experimental atmospheres by ANOVA followed by multiple comparison tests, $P < 0.05$.

Unstimulated cells from control and exposed rats released negligible quantities of nitric oxide. Previously we have shown that alveolar macrophages generate nitric oxide after stimulation with LPS and/or IFN-γ in a dose-dependent and time-dependent fashion (Pendino et al 1993; Prokhorova et al 1994). The effect of stimulation with LPS + IFN-γ was also additive (Table 6). Exposure of rats to $(NH_4)_2SO_4$ + 10 or 100 ppb H_2O_2 resulted in a significantly lower LPS + IFN-γ–induced nitric oxide production by macrophages isolated 24 hours after exposure (Table 7) when compared with cells from air-exposed rats. Lower production was also evident in stimulated cells isolated 24 hours after rats inhaled 10 or 100 ppb H_2O_2 alone and in cells isolated 0 and 24 hours after exposure to 20 ppb H_2O_2 alone. Exposure of rats to $(NH_4)_2SO_4$ alone resulted in lower nitric oxide production by LPS-stimulated macrophages.

Alveolar macrophages are known to generate nitric oxide via the enzyme NOS II. As expected, unstimulated alveolar macrophages from animals exposed to air or $(NH_4)_2SO_4$ + 20 ppb H_2O_2 did not express NOS II protein as determined by Western blotting (Figure 24A). Despite changes in nitric oxide production, exposure of rats to $(NH_4)_2SO_4 + H_2O_2$ had no effect on expression of this protein after treatment of the cells in vitro with LPS and IFN-γ (Figure 24B).

Superoxide anion and nitric oxide are known to react rapidly to form peroxynitrite (Ischiropoulos et al 1992). In our study, production of nitric oxide by macrophages from rats exposed to $(NH_4)_2SO_4 + H_2O_2$ was reduced when compared to cells from air-exposed rats. Thus we speculated that these effects may have been due to the rapid formation of peroxynitrite, which might have depleted the supplies of nitric oxide. To investigate this possibility, we used dihydrorhodamine 123 (Ischiropoulos et al 1999), in conjunction with fluorescence image analysis, to quantify peroxynitrite formation. Unstimulated alveolar macrophages from air-exposed rats generated small quantities of peroxynitrite (Figure 25). Exposure of the cells to LPS and IFN-γ alone or in combination induced formation of peroxynitrite, with LPS and LPS + IFN-γ, causing the greatest effect (Figure 25). Stimulated alveolar macrophages from rats exposed to $(NH_4)_2SO_4$ + 10 ppb H_2O_2 synthesized less peroxynitrite than cells from air-exposed rats (Figure 26).

Histologic sections of lung tissue were examined for the presence of nitrotyrosine residues, which are formed by peroxynitrite-mediated nitration of tyrosine (Ischiropoulos et al 1992) and have been used as markers of peroxynitrite-induced tissue injury (Robbins et at 2000). The most pronounced nitrotyrosine staining was noted in tissue taken from rats 24 hours after exposure to $(NH_4)_2SO_4$ + 10 ppb H_2O_2, relative to tissue taken from rats exposed to air (Figure 27). Similar pronounced staining was observed in lung tissue from rats exposed to $(NH_4)_2SO_4$ + 20 ppb H_2O_2 (not shown). This was confirmed by quantifying the number of macrophages staining positive for nitrotyrosine. Thus, greater numbers of positively stained macrophages were observed in sections from rats exposed to $(NH_4)_2SO_4$ + 10 or 20 ppb H_2O_2 or to $(NH_4)_2SO_4$ alone (Table 8). The specificity of the antinitrotyrosine antibody was verified by preincubating it overnight with 3-nitrotyrosine, which indeed prevented antibody binding (not shown).

Expression of HSPs and COX-2 HO-1, also known as *HSP32*, was strongly expressed in unstimulated alveolar macrophages from air-exposed rats (Figure 28A). After inhalation of $(NH_4)_2SO_4$ + 20 ppb H_2O_2, HO-1 expression by alveolar macrophages was observed to be lower at

Table 6. Nitric Oxide Production by Alveolar Macrophages[a]

	LPS Treatment[b] (mean ± SE)			
IFN-γ (U/mL)	0	1	10	100
0	0.3 ± 0.0	0.3 ± 0.1	5.8 ± 1.2	11.0 ± 0.6
1	0.6 ± 0.10	NM[c]	NM	NM
10	2.4 ± 0.4	NM	7.7 ± 1.1	15.2 ± 0.5
100	4.7 ± 0.5	NM	10.1 ± 0.8	15.0 ± 0.6

[a] Macrophages were collected 24 hours after rats were exposed to particle-free air. Cells were treated with LPS (1–100 ng/mL) and/or IFN-γ (1–100 U/mL). Nitrite release (nmol/2 × 10^5 cells), a measure of nitric oxide production, was quantified 48 hours later.

[b] Values are means ± SEM of 12–20 experiments.

[c] NM = not measured.

Table 7. Nitric Oxide Production in Alveolar Macophages Collected After Inhalation of $(NH_4)_2SO_4$ and H_2O_2[a]

Atmosphere	*N*	Media[b]	LPS[b]	IFN-γ[b]	LPS + IFN-γ[b]
Room air	9	1.3 ± 0.8	9.6 ± 1.2	4.5 ± 1.2	13.5 ± 1.1
0 Hours After Exposure					
Particle-free air	5	0.3 ± 0.0	7.3 ± 0.5	1.8 ± 0.6	12.1 ± 0.8
$(NH_4)_2SO_4$	7	0.4 ± 0.0	9.2 ± 0.5	2.6 ± 0.5	14.3 ± 0.3
10 ppb H_2O_2	6	0.3 ± 0.0	7.5 ± 0.7	0.6 ± 0.1	11.7 ± 0.5
20 ppb H_2O_2	6	0.2 ± 0.1	5.8 ± 0.9	0.9 ± 0.1	**9.2 ± 0.3**[c]
100 ppb H_2O_2	4	0.3 ± 0.0	8.6 ± 0.6	0.5 ± 0.2	12.4 ± 0.4
$(NH_4)_2SO_4$ + 10 ppb H_2O_2	5	0.4 ± 0.1	5.8 ± 0.7	1.4 ± 0.5	8.9 ± 1.3
$(NH_4)_2SO_4$ + 20 ppb H_2O_2	6	0.3 ± 0.1	7.7 ± 0.7	1.2 ± 0.2	13.6 ± 0.6
$(NH_4)_2SO_4$ + 100 ppb H_2O_2	5	0.2 ± 0.0	8.3 ± 1.2	0.4 ± 0.1	10.1 ± 1.4
24 Hours After Exposure					
Particle-free air	16	0.3 ± 0.0	11.0 ± 0.6	2.4 ± 0.4	15.2 ± 0.5
$(NH_4)_2SO_4$	21	0.4 ± 0.0	**8.4 ± 0.8**[c]	2.5 ± 0.4	12.7 ± 0.7
10 ppb H_2O_2	13	0.4 ± 0.1	8.9 ± 0.6	1.0 ± 0.2	**11.4 ± 0.6**[c]
20 ppb H_2O_2	13	0.6 ± 0.2	8.8 ± 0.7	2.4 ± 0.6	**12.1 ± 1.0**[c]
100 ppb H_2O_2	4	0.4 ± 0.0	**6.5 ± 0.7**[c]	0.7 ± 0.2	**8.9 ± 1.3**[c]
$(NH_4)_2SO_4$ + 10 ppb H_2O_2	10	0.3 ± 0.0	**4.1 ± 0.9**[c]	0.6 ± 0.1	**7.2 ± 1.6**[c]
$(NH_4)_2SO_4$ + 20 ppb H_2O_2	8	**0.8 ± 0.3**[c]	9.4 ± 0.8	3.3 ± 1.1	13.0 ± 0.6
$(NH_4)_2SO_4$ + 100 ppb H_2O_2	4	0.4 ± 0.1	8.3 ± 0.7	0.7 ± 0.3	**8.5 ± 1.7**[c]

[a] Macrophages were collected at 24 hours after exposure to room air, particle-free air, $(NH_4)_2SO_4$, H_2O_2, or $(NH_4)_2SO_4$ + H_2O_2. Cells were treated with media, LPS (100 ng/mL), IFN-γ (10 U/mL), or LPS (100 ng/mL) + IFN-γ (10 U/mL). Nitrite release (nmol/2 × 10^5 cells), a measure of nitric oxide production, was quantified 48 hours after cells were treated.

[b] Values represent the mean ± SEM of the number (*N*) of experiments. Means from room air-exposed animals were not significantly different from animals exposed to room air.

[c] Statistical comparison by ANOVA of data from animals exposed to room air versus the experimental atmospheres, followed by multiple comparison tests, were significant at $P < 0.05$.

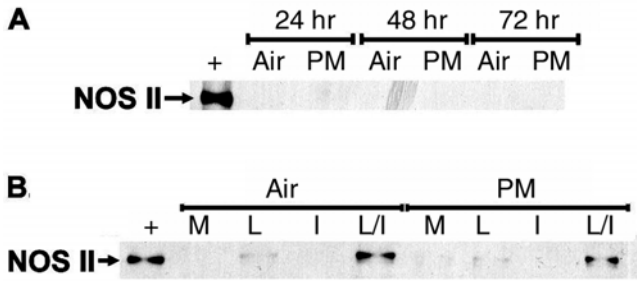

Figure 24. Western blot analysis of NOS II expression by alveolar macrophages. ***A.*** Cells were collected 24, 48, or 72 hours after exposure of rats to air or $(NH_4)_2SO_4$ + 20 ppb H_2O_2 (PM). ***B.*** Cells, collected immediately after exposure of rats to air or $(NH_4)_2SO_4$ + 20 ppb H_2O_2 (PM), were cultured for 24 hours with medium (M) or with 100 ng/mL LPS (L), 10 U/mL IFN-γ (I), or LPS + IFN-γ (L/I). The positive control (+) for the 130-kd NOS II protein is also shown.

Table 8. Quantitation of Alveolar Macrophages Staining Positive for Nitrotyrosine[a]

Atmosphere	Positive Cell Count
Room air	14 ± 2
$(NH_4)_2SO_4$	**23 ± 4**[b]
10 ppb H_2O_2	18 ± 3
20 ppb H_2O_2	NM[c]
$(NH_4)_2SO_4$ + 10 ppb H_2O_2	**26 ± 6**[b]
$(NH_4)_2SO_4$ + 20 ppb H_2O_2	**24 ± 9**[b]

[a] Histologic lung sections were prepared 24 hours after exposure of rats to the test atmosphere. Positively stained alveolar macrophages were quantified by light microscopy (400×). Data represent the average number of cells ± SEM ($n = 3$ animals) in 10 random fields.

[b] Statistical comparison by ANOVA of data from animals exposed to room air versus the experimental atmospheres, followed by multiple comparison tests, were significant at $P < 0.05$.

NM = not measured.

24 hours after exposure, and the lower value persisted for 72 hours (Figure 28). Similar results were observed with HSP60 (Figure 28A). In contrast, HSP70 was not detectable in unstimulated alveolar macrophages collected from rats exposed to air or $(NH_4)_2SO_4$ + 20 ppb H_2O_2. In additional experiments, we evaluated HO-1 expression in alveolar macrophages cultured with LPS and IFN-γ. In unstimulated alveolar macrophages taken from air-exposed rats and cultured for 24 hours, HO-1 was expressed at low levels (Figure 28B). LPS and IFN-γ had no major effect on HO-1 protein expression. In contrast, alveolar macrophages from rats exposed to $(NH_4)_2SO_4$ + 20 ppb H_2O_2 expressed significantly greater levels of HO-1 in both unstimulated cells and in cells cultured with LPS and/or IFN-γ. HO-1 protein was not detected in lung tissue or in whole-lung homogenates from animals exposed to air (Figure 28B) or $(NH_4)_2SO_4$ + 20 ppb H_2O_2 (Figure 29).

COX, also known as *prostaglandin H synthase*, catalyzes the synthesis of prostaglandin H_2 from arachidonate. This enzyme is a key regulator of prostanoid synthesis (Smith et al 1996; Williams et al 1999). Two isoforms of COX have been identified: COX-1, which is constitutively expressed and COX-2, which is inducible and has been implicated in the inflammatory response (Feng et al 1995; Smith et al 1996; Williams et al 1999). We found that COX-2 was undetectable in freshly isolated and cultured alveolar macrophages from animals exposed to air or $(NH_4)_2SO_4$ + 20 ppb H_2O_2 (data not shown). Although COX-2 protein was detected in whole-lung homogenates, no significant differences were observed between samples from animals exposed to air or $(NH_4)_2SO_4$ + 20 ppb H_2O_2 (Figure 29).

Gadolinium Chloride Effects on Alveolar Macrophages

Gadolinium chloride ($GdCl_3$) is a rare earth metal known to inhibit macrophage function (Shibayama et at 1991). This metal has been reported to abrogate ozone-induced pulmonary injury (Pendino et al 1995), suggesting that the toxicity of ozone is mediated, in part, by macrophages. In pilot studies, we gave rats intravenous $GdCl_3$ (5 mg/kg) 24 hours before inhalation of $(NH_4)_2SO_4$ + H_2O_2. Unfortunately, the results of these studies were difficult to interpret because of animal variability. After the exposures, BAL fluid protein levels fluctuated from 0.1 mg/mL to 9.0 mg/mL. Histological

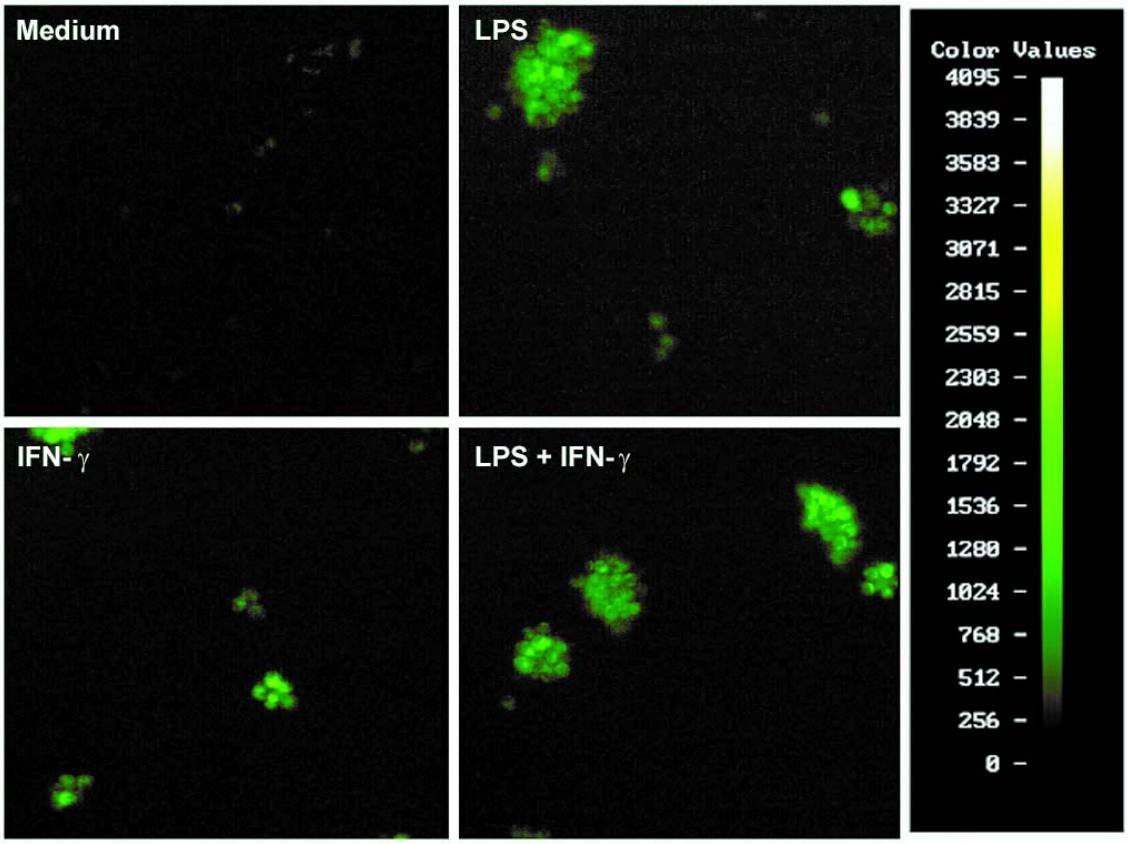

Figure 25. Micrographs of peroxynitrite formation by alveolar macrophages isolated from air-exposed rats. Cells were cultured for 24 hours with medium control, LPS (100 ng/mL), IFN-γ (100 U/mL), or LPS + IFN-γ followed by TPA (170 nM) for 30 minutes. The color bar represents relative fluorescence on a four-decade log scale. Original magnification, 20×.

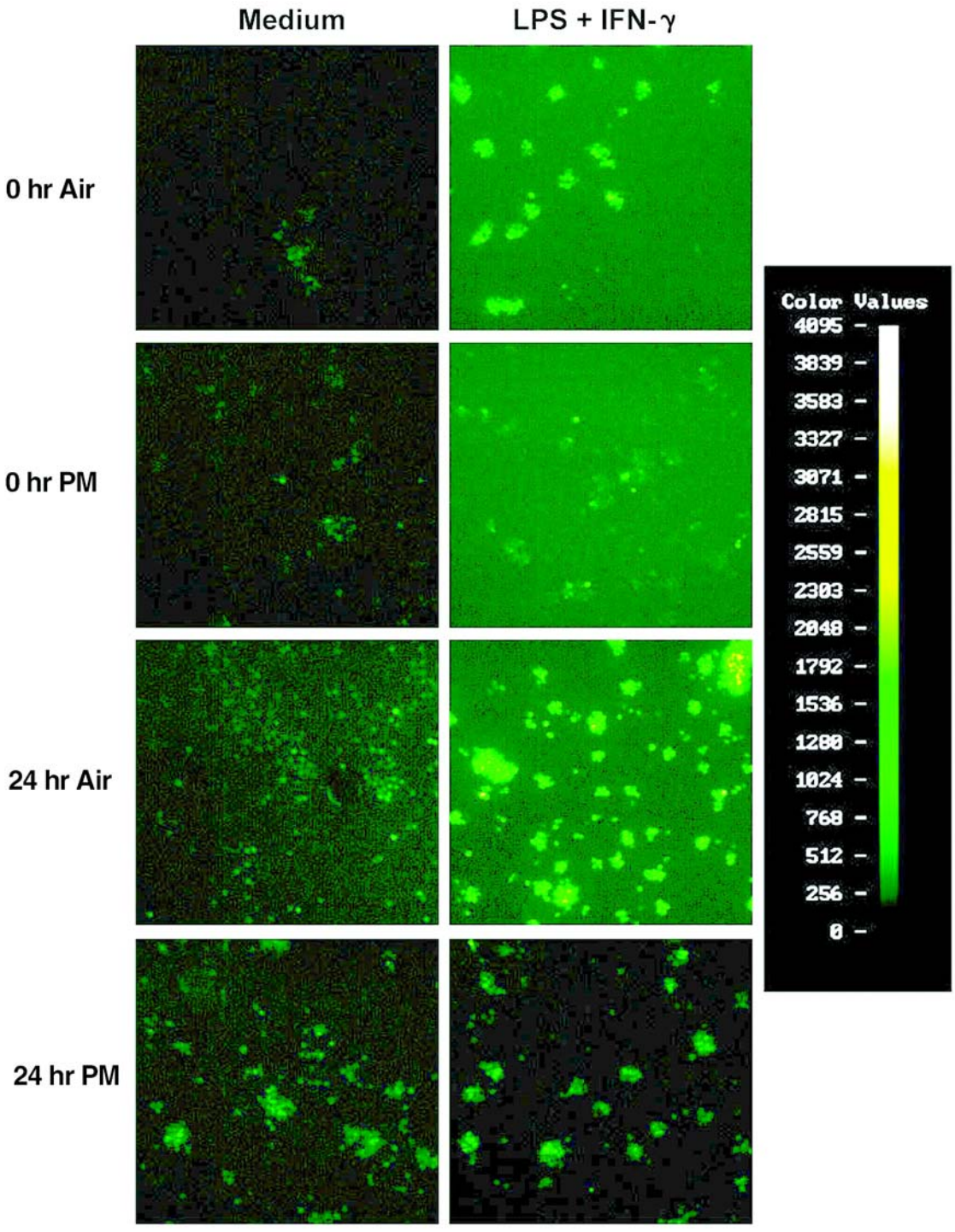

Figure 26. Micrographs showing peroxynitrite formation by macrophages. Alveolar macrophages were isolated 0 hours or 24 hours after exposure of rats to air or $(NH_4)_2SO_4$ + 10 ppb H_2O_2 (PM). Cells were cultured with medium or LPS (100 ng/mL) + IFN-γ (100 U/mL) followed by TPA (170 nM). The color bar represents relative fluorescence on a four-decade log scale. Original magnification, 20×.

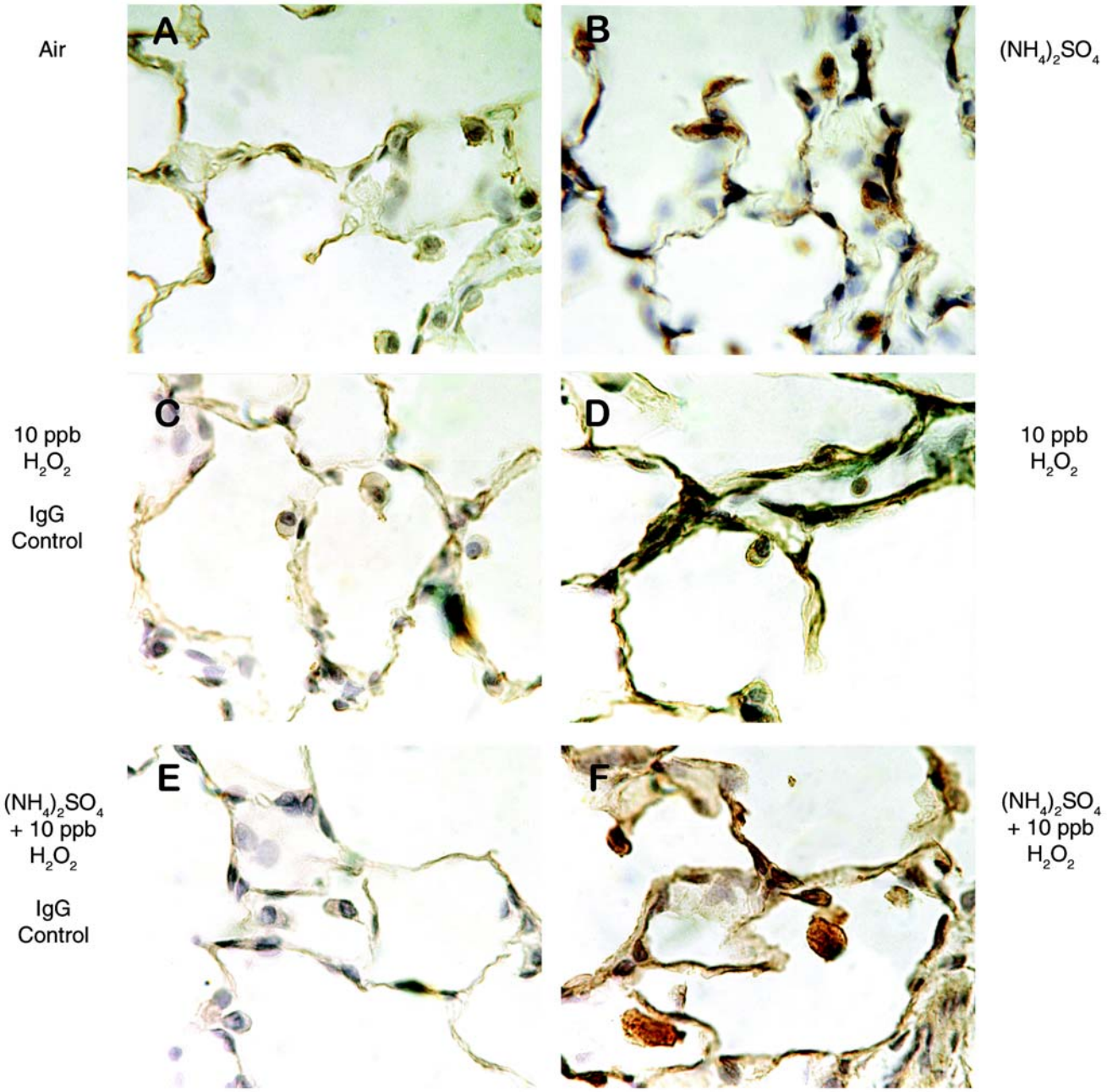

Figure 27. Nitrotyrosine immunostaining of lung tissue. Rats were exposed to air ***(A)***, $(NH_4)_2SO_4$ ***(B)***, 10 ppb H_2O_2 ***(C*** and ***D)***, or $(NH_4)_2SO_4$ + 10 ppb H_2O_2 ***(E*** and ***F)***. Sections were prepared 24 hours after exposure and stained with anti-nitrotyrosine antibody ***(A***, ***B***, ***D***, and ***F)*** or IgG control ***(C*** and ***E)***. Original magnification, 400×.

examination of lung sections from gadolinium-treated animals revealed large numbers of inflammatory cells in some of the samples. This finding suggested that this group of animals may have been exposed to an infectious agent. Therefore, data from these experiments are not included in this report.

Pulmonary Effects of Inhaled Cumene Hydroperoxide

Tobias and Ziemann (2000) recently reported results of smog chamber studies in which the particle-phase products of 1-tetradecene and ozone, in the presence of excess alcohols and carboxylic acids, were identified by semicontinuous collection and analysis in a thermal desorption, particle-beam mass spectrometer. The aerosol products were almost exclusively α-alkoxytridecyl and α-acyloxytridecyl hydroperoxides, which are entirely in the particle phase at atmospheric temperature and pressure. These results suggest that these and other alkene-ozone reactions will yield low-volatility organic hydroperoxides that may condense on preexisting particles or form new particles. These organic hydroperoxides comprise additional strong oxidants that could also contribute to PM-induced injury. We conducted preliminary studies to evaluate the effects of exposure to organic hydroperoxide on alveolar macrophage function. We used cumene hydroperoxide, a commercially available organic peroxide with a similar chemical structure. Because these compounds are found entirely in the particle phase, the exposures were conducted with particles composed entirely of cumene hydroperoxide (no sulfate).

Inflammation and BAL Protein Content The exposure of rats to cumene hydroperoxide particles had no significant effects on BAL cell number (Table 9). BAL fluid from control animals exposed to room air or solvent contained low levels of protein. No significant changes were observed

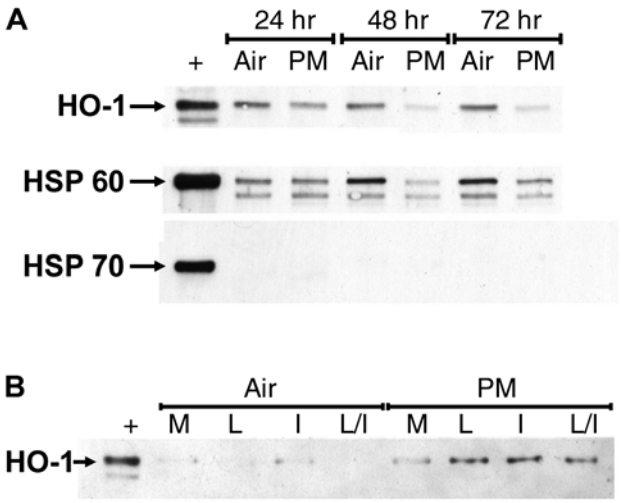

Figure 28. Western blot analysis of HSP expression by alveolar macrophages. ***A***. Cells were collected 24, 48, or 72 hours after exposure of rats to air or $(NH_4)_2SO_4$ + 20 ppb H_2O_2 (PM). ***B***. Cells, collected immediately after exposure of rats to air or $(NH_4)_2SO_4$ + 20 ppb H_2O_2 (PM), were cultured for 24 hours with medium (M), 100 ng/mL LPS (L), 10 U/mL IFN-γ (I), or LPS + IFN-γ (L/I). The positive controls (+) for the 32 kd HO-1, 60 kd HSP60, or 70 kd HSP70 protein are also shown.

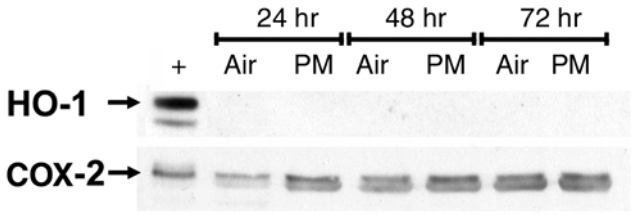

Figure 29. Western blot analysis of HO-1 and COX-2 expression of whole-lung homogenates. Lung tissue was collected 24, 48, or 72 hours after exposure of rats to air or $(NH_4)_2SO_4$ + 20 ppb H_2O_2 (PM). The positive controls (+) for the 32 kd HO-1 or 72 kd COX-2 protein are shown.

Table 9. Lung Lavage Cell and Protein Levels After Inhalation of Cumene Hydroperoxide[a]

Atmosphere	*N*	Total Cells ($\times 10^7$)	Viable Cells (%)	BAL Protein (mg/mL)
Room air	21	1.2 ± 0.1	87.4 ± 0.8	0.10 ± 0.01
0 Hours After Exposure				
Solvent control	3	1.1 ± 0.1	82.9 ± 3.7	0.11 ± 0.01
Cumene hydroperoxide	3	1.4 ± 0.3	87.4 ± 2.0	0.11 ± 0.02
24 Hours After Exposure				
Solvent control	3	1.3 ± 0.2	88.6 ± 0.6	0.07 ± 0.06
Cumene hydroperoxide	3	1.3 ± 0.2	87.3 ± 2.9	0.09 ± 0.07

[a] BAL fluid was collected 0 hours or 24 hours after exposure to solvent control, cumene hydroperoxide, or room air. Each value represents the mean ± SEM of the number (*N*) of experiments. Means from air-exposed animals were not significantly different from unexposed animals.

[b] Statistical comparison by ANOVA of data from animals exposed to room air versus the experimental atmospheres, followed by multiple comparison tests, were significant at $P < 0.05$.

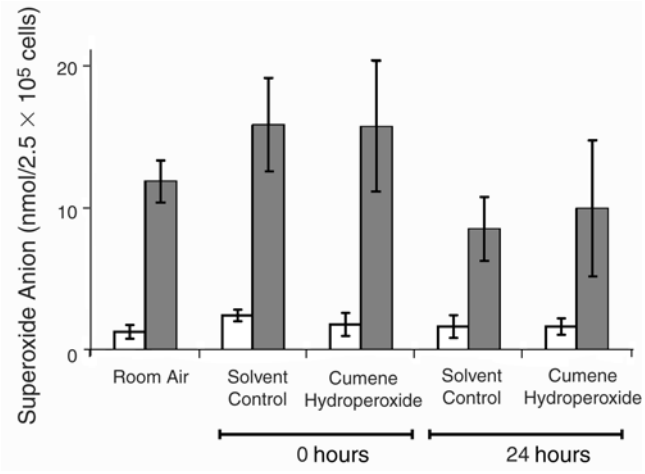

Figure 30. Superoxide production by alveolar macrophages from rats exposed to cumene hydroperoxide. Cells collected 0 hours or 24 hours after exposure of rats to the test atmosphere were incubated with medium (□) or TPA (■) prior to measurement of superoxide anion production. Data are mean ± SEM of 3 experiments. Statistical comparisons (ANOVA followed by multiple comparisons testing) of particle-free air exposed animals to room-air animals, or air-exposed animals to animals exposed to experimental atmospheres showed no differences among means ($P < 0.05$).

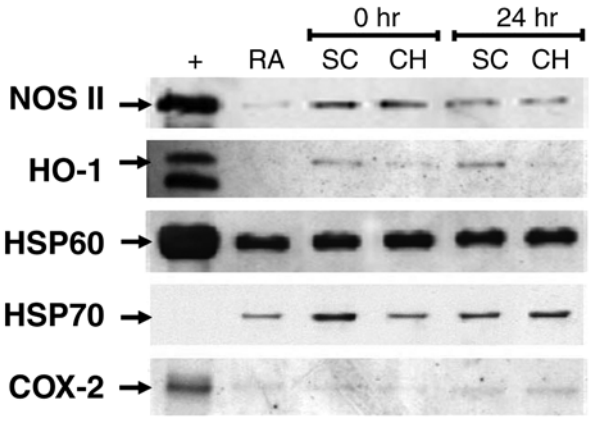

Figure 31. Western blot analysis of NOS II, HSP and COX-2 expression by alveolar macrophages. Cells were collected 0 hours and 24 hours after exposure of rats to solvent control (SC), cumene hydroperoxide (CH), or room air (RA). The positive controls (+) for the 130 kd NOS II, 32 kd HO-1, 60 kd HSP60, 70 kd HSP70, or 72 kd COX-2 protein are also shown.

immediately or 24 hours after exposure to cumene hydroperoxide particles.

Production of Reactive Oxygen and Nitrogen Intermediates Unstimulated alveolar macrophages from room air, solvent control, or cumene hydroperoxide–exposed rats produced relatively low levels of superoxide anion (Figure 30). TPA-stimulated alveolar macrophages from rats exposed to solvent control or cumene hydroperoxide showed a measurable but not significantly greater in production of superoxide anion when compared with unexposed animals. These effects were transient; by 24 hours after exposure, levels of superoxide anion were below control levels.

In contrast, exposing rats to cumene hydroperoxide particles did not affect LPS, IFN-γ, or LPS + IFN-γ stimulated nitric oxide production when compared to animals exposed to room air (Table 10). Interestingly, cells isolated 24 hours after exposure to the solvent control produced significantly more nitric oxide when unstimulated and in response to IFN-γ stimulation. NOS II protein expression was greater in unstimulated cells isolated immediately and 24 hours after exposure of rats to solvent control or cumene hydroperoxide compared to cells isolated from rats exposed to room air (Figure 31).

Table 10. Nitric Oxide Production by Alveolar Macrophages After Inhalation of Cumene Hydroperoxide[a]

Atmosphere	*N*	Media	LPS	IFN	LPS + IFN
Room air	9	1.3 ± 0.8	9.6 ± 1.2	4.5 ± 1.2	13.5 ± 1.1
0 Hours After Exposure					
Solvent control	3	0.2 ± 0.0	9.3 ± 0.6	2.7 ± 0.4	14.2 ± 0.8
Cumene hydroperoxide	3	0.3 ± 0.0	7.6 ± 1.4	4.4 ± 0.5	14.1 ± 3.0
24 Hours After Exposure					
Solvent control	3	**5.7 ± 1.5**[b]	8.1 ± 1.5	**11.1 ± 1.3**[b]	13.0 ± 0.8
Cumene hydroperoxide	3	0.3 ± 0.0	6.7 ± 2.1	0.7 ± 0.1	12.3 ± 0.7

[a] Alveolar macrophages were collected 0 hours or 24 hours after exposure of rats to cumene hydroperoxide, solvent control, or room air, and treated with LPS (100 ng/mL), IFN-γ (10 U/mL) or LPS (100 ng/mL) + IFN-γ (10 U/mL). Nitrite release (nmol/2 × 10^5 cells), a measure of nitric oxide production, was quantified 48 hours later. Values are the mean ± SEM of the number of experiments indicated.

[b] Statistical comparison by ANOVA of data from animals exposed to room air versus solvent control or cumene hydroperoxide followed by multiple comparison tests were significant at $P < 0.05$.

Expression of HSPs and COX-2 HO-1 protein was detectable in freshly isolated alveolar macrophages from rats exposed to solvent control (Figure 31). In cells from rats exposed to cumene hydroperoxide particles, HO-1 protein expression was detectable but lower. Both HSP60 and HSP70 were detectable in alveolar macrophages from rats exposed to room air, solvent control, or cumene hydroperoxide particles. Levels of expression were not affected by the exposures (Figure 31). COX-2 protein expression was detected at a low level in freshly isolated alveolar macrophages. No significant differences in COX-2 expression were observed between cells obtained from rats exposed to room air or cumene hydroperoxide (Figure 31).

DISCUSSION

These studies were designed to analyze the role of peroxides and alveolar macrophages in fine PM-induced lung toxicity. We hypothesized that fine PM transports peroxides into the lower lung, leading to tissue injury and to accumulation and activation of macrophages in these regions. To test this hypothesis, we analyzed the effects of inhaled $(NH_4)_2SO_4$ + H_2O_2 on lung structure, protein leakage, and macrophage functioning. A summary of the results is presented in Table 11. We found that exposure of rats to $(NH_4)_2SO_4$ + H_2O_2 resulted in increased neutrophil influx and adherence to the vascular endothelium. Moreover, alveolar macrophage production of cytotoxic mediators was altered. Although exposure to $(NH_4)_2SO_4$ or H_2O_2 alone also exerted some biological activity, the response to the combination of these atmospheres was, for the most part, greater. These findings support our hypothesis and suggest that H_2O_2 may be a contributing factor in the response to inhaled PM.

Transmission electron microscopy revealed an influx of neutrophils into the pulmonary airways after exposure of rats to $(NH_4)_2SO_4$ + 20 ppb H_2O_2. The majority of these cells showed adherence to the vascular endothelium. Neutrophil influx and adherence is the first step in the inflammatory response to tissue injury. These findings suggest that some degree of tissue injury has occurred. However, this response was relatively modest: since it was not readily detectable in histological sections and no changes in BAL fluid protein or LDH content were observed.

Table 11. Comparison of Pulmonary Response to Inhaled PM[a]

	$(NH_4)_2SO_4$ Alone	H_2O_2 Alone			$(NH_4)_2SO_4$ + H_2O_2			Cumene Hydroperoxide
		10 ppb	20 ppb	100 ppb	10 ppb	20 ppb	100 ppb	
Cell number	0 h⇩	⇔	⇔	⇔	⇔	⇔	⇔	⇔
Cell viability	24 h⇧	⇔	⇔	⇔	⇔	⇔	⇔	⇔
BAL fluid protein	⇔	⇔	⇔	⇔	⇔	⇔	⇔	NM
BAL fluid LDH	⇔	⇔	⇔	⇔	⇔	⇔	⇔	NM
Serum LDH	⇔	⇔	24 h⇧	⇔	⇔	⇔	⇔	NM
Neutrophil influx and adherence	⇔	NM	0,24 h⇧	NM	NM	0,24 h⇧	NM	NM
TNF-α expression	⇔	⇔	0,24 h⇧	NM	⇔	0,24 h⇧	NM	NM
Reactive oxygen intermediates (superoxide anion)	⇔	⇔	24 h⇧	⇔	⇔	0 h⇧	⇔	⇔
Reactive nitrogen intermediates								
Nitric oxide production	⇔	24 h⇩	0,24 h⇩	24 h⇩	24 h⇩	⇔	24 h⇩	⇔
NOS II protein expression	NM	NM	NM	NM	NM	⇔	NM	⇔
Peroxynitrite formation	NM	NM	NM	NM	0,24 h⇩	NM	NM	NM
Nitrotyrosine residues	24 h⇧	⇔	NM	NM	24 h⇧	24 h⇧	NM	NM
HSP expression	NM	NM	NM	NM	NM	⇩/⇧[b]	NM	⇩[c]
COX-2 expression	NM	NM	NM	NM	NM	⇔	NM	⇔

[a] NM = not measured; ⇔ = not significant; ⇧= significant increase; ⇩= significant decrease at the indicated time (0 or 24 hr after exposure) and compared with cells from rats exposed to particle-free air.

[b] Unstimulated cells showed decreased HSP (HO-1, HSP60, HSP70) expression (see Figure 29A); cells stimulated with LPS + IFN-γ showed increased HO-1 expression (HSP60 and HSP70 not measured) (see Figure 29B).

[c] HO-1 expression was decreased; HSP60 and HSP70 were not measured.

Neutrophil adherence has been reported to stimulate the release of TNF-α from tissue macrophages (Sredni-Kenigsbuch et al 2000). TNF-α is a proinflammatory, early response cytokine known to activate neutrophils and macrophages (Brouckaert and Fiers 1996). It is unique among cytokines because it can also directly induce cytotoxicity (Bohlinger et al 1995; Wang et al 1995). We found that exposure of rats to $(NH_4)_2SO_4$ + 20 ppb H_2O_2 resulted in increased TNF-α production by alveolar macrophages. These results are in accord with reports of augmented TNF-α production by alveolar macrophages after exposure of animals to asbestos, titanium dioxide, silica or endotoxin (Driscoll et al 1990; Perkins et al 1993; Pendino et al 1994) and suggest that TNF-α expression may be a sensitive marker of PM exposure. One mechanism by which TNF-α may contribute to PM-induced tissue injury is by amplifying the inflammatory response. This could occur through TNF-α activation of autocrine and paracrine pathways leading to the release of chemokines (eg, interleukin 8, monocyte chemotactic protein-1, macrophage inflammatory protein-1) as well as reactive oxygen and/or nitrogen intermediates (Driscoll et al 1997).

Reactive oxygen intermediates (eg, superoxide anion, H_2O_2, hydroxyl radical) are produced by neutrophils and macrophages to protect the body against inhaled pathogens and to destroy foreign material. Production of these intermediates represents one of the early phases in the inflammatory response to injury and is critical for nonspecific host defense. However, excess quantities of reactive oxygen intermediates can also cause damage to the surrounding tissue (Oosting et al 1990). Oxidant stress and the generation of reactive oxygen species have previously been correlated with the inflammatory response to inhaled PM (Li et al 1996; Donaldson et al 1997). Similarly, after exposure of rats to $(NH_4)_2SO_4$ + 20 ppb H_2O_2, we found that superoxide anion release by alveolar macrophages transiently increased. This may represent one early mechanism by which macrophages contribute to fine PM-induced injury.

The reaction of superoxide anion and nitric oxide leads to formation of peroxynitrite, a potent cytotoxic mediator (Koppenol et al 1992; Radi et al 1992; Rodenas et al 1995). Once formed, peroxynitrite can react with proteins, generating addition and substitution products that alter their function (Moncada et al 1991; Nathan 1992). Superoxide anion production after exposure of rats to $(NH_4)_2SO_4$ + 20 ppb H_2O_2 may drive the formation of peroxynitrite. Peroxynitrite formation might account for the decreases in nitric oxide and superoxide anion observed 24 hours after $(NH_4)_2SO_4$ + H_2O_2 exposure. Our detection of nitrotyrosine residues in tissue from rats 24 hours after exposure to $(NH_4)_2SO_4$ + H_2O_2 supports this idea. Our results suggest that peroxynitrite formation may also be a cytotoxic mechanism of $(NH_4)_2SO_4$ + H_2O_2–induced tissue injury.

Pulmonary injury and inflammation after exposure to fine PM involves altered gene expression and synthesis of the inflammatory proteins, TNF-α, interleukin 6, IFN-γ, and transforming growth factor-β, which are regulated by the transcription factor, nuclear factor κB (NFκB) (Shukla et al 2000). The finding that fine PM–induced gene expression is inhibited by catalase demonstrates that NFκB activation is oxidant-dependent (Shukla et al 2000). After exposure of rats to $(NH_4)_2SO_4$ + H_2O_2, we observed a lower expression of HO-1 protein in alveolar macrophages compared with cells from rats exposed to particle-free air. This suggests that oxidant levels are upregulated in the lung after PM exposure, which may contribute to generation of inflammatory cytokines via activation of NFκB. HO-1 protein expression increased when alveolar macrophages from $(NH_4)_2SO_4$ + H_2O_2–exposed animals, but not animals exposed to particle-free air, were incubated with LPS and IFN-γ. These findings support the concept that alveolar macrophages are primed to respond to inflammatory mediators after exposure to $(NH_4)_2SO_4$ + H_2O_2. Our results are consistent with reports of increased antioxidant enzyme expression, such as HO-1, by alveolar macrophages after in vitro exposure to diesel exhaust particles (Li et al 2000).

Injury and inflammation after exposure to fine PM may also involve production of prostaglandins. Pulmonary macrophages, as well as epithelial cells, are significant sources of these mediators (Mitchell et al 1994), and higher COX-2 gene expression has been observed after exposure of rats to residual oil fly ash (Samet et al 2000b). In contrast, we could not detect any significant differences in COX-2 expression in lung tissue from animals exposed to particle-free air or $(NH_4)_2SO_4$ + H_2O_2. Thus prostaglandins may not play a prominent role in the response to $(NH_4)_2SO_4$ + H_2O_2. Alternatively, these mediators may be generated via COX-1, but this remains to be determined.

An unexpected finding in our studies was that H_2O_2 alone exerted biological effects. Modeling studies have suggested that vapor-phase H_2O_2 should dissolve in the mucus membranes of the upper airways and not reach the lower lung or contribute to toxicity (Wexler and Sarangapani 1998). However, we observed a higher serum LDH and greater TNF-α staining of lung tissue after inhalation of vapor-phase H_2O_2 (20 ppb), and transmission electron microscopy showed an influx of neutrophils into the airways. These findings are in accord with published results indicating that oxidative injury stimulates macrophages to release TNF-α (reviewed in Driscoll 2000). Superoxide anion production by alveolar macrophages was also higher 24 hours after rats were exposed to 20 ppb H_2O_2, but nitric

oxide production by these cells was lower than production by cells from rats exposed to particle-free air. Nitrotyrosine residues were also detected in cells from H_2O_2-exposed rats. Taken together, these findings suggest that vapor-phase H_2O_2 does in fact penetrate the lower lung and exert biological effects. The significance of changes in alveolar macrophage functioning after H_2O_2 exposure remains to be determined. Of interest was our observation that some biological effects were observed with 10 or 20 ppb H_2O_2, but not with 100 ppb H_2O_2. This lack of response at the highest concentration may be due to development of tolerance as observed after exposure to high or repeated doses of other toxicants (Plopper et al 2001; Wesselkamper et al 2001).

A possible limitation of our studies is our choice of $(NH_4)_2SO_4$ as a model of fine PM. Because $(NH_4)_2SO_4$ was considered nontoxic (Loscutoff et al 1985), we did not anticipate pulmonary responses to this particle. Surprisingly, we observed a decrease in the number of cells in BAL fluid recovered immediately after exposure of animals to 430 $\mu g/m^3$ $(NH_4)_2SO_4$, but not to 215 $\mu g/m^3$ $(NH_4)_2SO_4$. In addition, nitrotyrosine staining was detected in lung tissue obtained 0 hours and 24 hours after exposure. Thus, at higher doses $(NH_4)_2SO_4$ induced a limited biological response. The lower cell number after exposure to $(NH_4)_2SO_4$ may be due to increased adherence of alveolar macrophages to the epithelium, making them more difficult to remove by lavage. This effect appears to be transient because the decrease in cell number was not observed 24 hours after exposure. Related previous studies have demonstrated that alveolar macrophages from rats exposed to ozone for 3 to 16 hours were more adherent to epithelial cells, both in vivo and in vitro, than cells from air-exposed rats (Pino et al 1992; Pearson and Bhalla 1997). Our findings are also consistent with studies demonstrating biological effects after prolonged exposure of animals to $(NH_4)_2SO_4$ (0.5 mg/m^3 for 4 to 8 months) (Smith et al 1989). Inhalation of $(NH_4)_2SO_4$ by rats and guinea pigs at concentrations 100 times greater than ambient fine PM levels (65 $\mu g/m^3$) were also reported to induce lung irritation (Chen et al 1992). $(NH_4)_2SO_4$ inhalation also induced minor reductions in ventilation volume of rats (Loscutoff et al 1995).

Partitioning of H_2O_2 between the vapor and particle phases depends on the concentration and composition of atmospheric PM. Atmospheric $PM_{2.5}$ is expected to be somewhat less hygroscopic than $(NH_4)_2SO_4$ (the model aerosol for this study) because it includes not only hygroscopic species (like polar organics, sulfate, and nitrate) but also nonhygroscopic organics and minerals. We would expect a freshly emitted combustion aerosol to be dominated by low polarity organic compounds that would take up little water. Because an aerosol such as this is transported through the atmosphere, clear-sky photochemical and in-cloud oxidation reactions form particulate sulfate, nitrate and organic species. These components either condense on existing particles, partition into existing particles, or form new particles. These hygroscopic species dominate the $PM_{2.5}$ mass in many locations across the United States. Thus, using $(NH_4)_2SO_4$ as a model in the present studies is reasonable. Interestingly, hygroscopic organic PM and H_2O_2 are also formed indoors through reactions between alkenes and ozone, providing suitable conditions for indoor as well as outdoor exposures (Appendix B).

In general, the biological differences after inhalation of $(NH_4)_2SO_4$ + H_2O_2 by rats as reported in this study are modest. Not every type of respirable particle elicits a strong inflammatory response, but subtle changes may be observed. For example, although no evidence of an inflammatory response was noted in lungs of mice acutely exposed to carbonaceous particles surface-coated with acid sulfate, alveolar macrophage Fc receptor-mediated phagocytosis was reportedly decreased (Clarke et al 2000). In another study, old mice with elastase-induced emphysema showed lymphocytic infiltration into connective tissue around airway blood vessels after inhalation of ultrafine carbon, platinum, and Teflon particles although no overt inflammatory response was evident in the lungs of healthy young or old animals (Oberdörster et al 2000). These differences in response may be attributed to particle size, age, and genetic factors, which are thought to determine severity of the inflammatory response to inhaled materials.

In many instances, respirable particles that are nontoxic in the micrometer size range exert toxicity in the nanometer range (reviewed in Donaldson et al 1998; Oberdörster 2001). For example, in studies comparing the inflammatory potential of inhaled or intratracheally instilled titanium dioxide (TiO_2) of two sizes (ultrafine, 20 nm, and fine, 250 nm), the ultrafine particles elicited a much greater inflammatory reaction in the lungs when compared to the larger particles (Ferin et al 1992; Oberdörster et al 1994). Similarly, Li and colleagues (1999) reported that ultrafine carbon black was more inflammogenic after instillation in the rat lung than fine carbon black of the same mass. The severity of an inflammatory response induced by particles may also strongly correlate with surface area (Oberdörster 1996; Cullen et al 2000; Tran et al 2000). Recent studies of ozone-induced airway inflammation have demonstrated that genetic factors affect individual responses to the environment (Holz et al 1999). Similar genetic variability may contribute to the susceptibility of individuals to injury induced by inhalation of fine PM and peroxides. Advances in functional genomics, which show linkage of chromosomal regions to various traits, have begun to provide new insights into the influence of genetics over the inflammatory responses of individuals (Leikauf et al 2000).

Recent studies suggest that atmospheric organic hydroperoxides may also contribute to PM-induced injury (Tobias and Ziemann 2000). To test this possibility, we adapted our system to generate particles consisting of cumene hydroperoxide. The mass median diameter and number concentration of this aerosol were similar to those of our $(NH_4)_2SO_4$ + H_2O_2–containing aerosol. Surprisingly, we found that cumene hydroperoxide particles exerted less of a biological effect than did $(NH_4)_2SO_4$ + H_2O_2. The most pronounced response was reduced expression of HO-1. Suppression of HO-1 gene expression by mediators such as angiotensin II, IFN-γ, transforming growth factor-β_1, and interleukin 10 has been described (reviewed by Immenschuh and Ramadori 2000). The mechanisms underlying these effects are unknown. Because HO-1 has been shown to provide cytoprotection in various models of injury (Immenschuh and Ramadori 2000), suppression of HO-1 protein expression after exposure of rats to inhaled peroxides may be an important response of the lung.

In summary, the present studies show that exposure of rats to $(NH_4)_2SO_4$ + H_2O_2 induces tissue damage and modulates the activity of alveolar macrophages. While additional research is needed to draw definitive conclusions, the results of these studies indicate that increased TNF-α production and peroxynitrite formation are two plausible mechanisms mediating the toxicity of $(NH_4)_2SO_4$ + H_2O_2. Our findings also suggest that vapor-phase H_2O_2 reaches the lower lung and modulates macrophage function. Further, alterations in macrophage functioning after inhalation of $(NH_4)_2SO_4$ + H_2O_2 may contribute to heightened individual susceptibility to infection after fine PM exposure.

ACKNOWLEDGMENTS

The authors acknowledge the technical assistance of Jennie Brittingham in conducting the animal experiments. Electron microscopy studies were conducted in collaboration with Dr Ronald Gordon of the Department of Pathology at Mt Sinai School of Medicine (New York NY). Studies using ^{18}O-labeled H_2O_2 were conducted in collaboration with Dr Gary Hatch of the EPA at Research Triangle Park (NC) and Dr Guobin Sun, formerly at the EPA and now at the University of North Carolina (Chapel Hill NC). Indoor H_2O_2 experiments were conducted through collaboration with Drs Charles Weschler and Helen Shields of Telcordia Technologies (Red Bank NJ) in two unoccupied Telcordia offices. The active involvement of our collaborators in this research and in the data interpretation is gratefully acknowledged.

REFERENCES

Barieux JJ, Schirmann JP. 1987. ^{17}O-enriched hydrogen peroxide and *t*-butyl hydroperoxide: Synthesis, characterization and some applications. Tetrahedron Lett 28:6443–6446.

Becker, KH, Bechara J, Brockmann KJ. 1993. Studies on the formation of H_2O_2 in the ozonolysis of alkenes. Atmos Environ 27A:57–61.

Becker KH, Brockmann KJ, Bechara J. 1990. Production of hydrogen peroxide in forest air by reaction of ozone with terpenes. Nature 346:256–258.

Becker S, Soukup JM. 1998. Decreased CD11b expression, phagocytosis, and oxidative burst in urban particulate pollution-exposed human monocytes and alveolar macrophages. J Toxicol Environ Health A 55:455–477.

Becker S, Soukup JM. 1999. Exposure to urban air particulates alters the macrophage-mediated inflammatory response to respiratory viral infection. J Toxicol Environ Health A 57:445–457.

Becker S, Soukup JM, Gilmour MI, Devlin RB. 1996. Stimulation of human and rat alveolar macrophages by urban air particulates: effects on oxidant radical generation and cytokine production. Toxicol Appl Pharmacol 141:637–48.

Bohlinger I, Leist M, Barsig J, Uhlig S, Tiegs G, Wendel A. 1995. Interleukin-1 and nitric oxide protect against tumor necrosis factor-a-induced liver injury through distinct pathways. Hepatology 22:1829–1837.

Brouckaert P, Fiers W. 1996. Tumor necrosis factor and the systemic inflammatory response syndrome. Curr Top Microbiol Immunol 216:167–187.

Brown SK, Sim MR, Abramson MJ, Gray CN. 1993. Concentration of volatile organic compounds in indoor air—a review. Indoor Air 4:123–134.

Bruch J, Rehn B, Song H, Gono E, Malkusch W. 1993. Toxicological investigations on silicon carbide. 1. Inhalation studies. Br J Ind Med 50:797–806.

Calvert JG, Lazrus A, Kok GL, Heikes BG, Lind J, Cantrell CA. 1985. Chemical mechanisms of acid generation in the troposphere. Nature 317:27–35.

Chan CK, Flagan RC, Seinfeld JH. 1992. Water activities of NH_4NO_3/$(NH_4)_2SO_4$ solutions. Atmos Environ 26A:1661–1673.

Chen LC, Fine JM, Qu QS, Amdur MO, Gordon T. 1992. Effects of fine and ultrafine sulfuric acid aerosols in guinea pigs: Alterations in alveolar macrophage function and intracellular pH. Toxicol Appl Pharmacol 113:109–117.

Chin BY, Choi ME, Burdick MD, Strieter RM, Risby TH, Choi AMK. 1998. Induction of apoptosis by particulate matter: role of TNF-α and MAPK. Am J Physiol 275:L942–L949.

Clarke RW, Antonini JM, Hemenway DR, Frank R, Kleeberger SR, Jakab GJ. 2000. Inhaled particle-bound sulfate: Effects on pulmonary inflammatory responses and alveolar macrophage function. Inhalation Toxicol 12:169–86.

Cullen RT, Tran CL, Buchanan D, Davis JMG, Searl A, Jones AD, Donaldson K. 2000. Inhalation of poorly soluble particles: I. Differences in inflammatory response and clearance during exposure. Inhalation Toxicol 12:1089–1111.

Das M, Aneja VP. 1994. Measurements and analysis of concentrations of gaseous hydrogen peroxide and related species in the rural central Piedmont region of North Carolina. Atmos Environ 28:2473–2483.

Dasgupta PK, Dong S, Hwang H. 1990. Diffusion scrubber-based field measurements of atmospheric formaldehyde and hydrogen peroxide. Aerosol Sci Technol 12:98–104.

Dasgupta PK, Dong S, Hwang H, Yang H, Genfa Z. 1988. Continuous liquid-phase fluorometry coupled to a diffusion scrubber for the real-time determination of atmospheric formaldehyde, hydrogen peroxide and sulfur dioxide. Atmos Environ 22:949–963.

Dockery DW, Schwartz J, Spengler JD. 1992. Air pollution and daily mortality: Associations with particulates and acid aerosols. Environ Res 59:362–373.

Donaldson K, Brown DM, Mitchell C, Dineva M, Beswick PH, Gilmour P, MacNee W. 1997. Free radical activity of PM_{10}; iron mediated generation of hydroxyl radicals. Environ Health Perspect 105(Suppl 5):1285–1289.

Donaldson K, Li XY, MacNee W. 1998. Ultrafine (nanometer) particle-mediated lung injury. J Aerosol Sci 29:553–560.

Dong W, Lewtas J, Luster MI. 1996. Role of endotoxin in tumor necrosis factor alpha expression from alveolar macrophages treated with urban air particles. Exp Lung Res 22:577–592.

Driscoll KE. 2000. TNF-alpha and MIP-2: Role in particle-induced inflammation and regulation by oxidative stress. Toxicol Lett 15:177–183.

Driscoll KE, Carter JM, Hassenbein DG, Howard B. 1997. Cytokines and particle-induced inflammatory cell recruitment. Environ Health Perspect 105(Suppl 5):1159–1164.

Driscoll KE, Carter JM, Howard BW, Hassenbein DG, Pepelko W, Baggs RB, Oberdörster G. 1996. Pulmonary inflammatory, chemokine, and mutagenic responses in rats after subchronic inhalation of carbon black. Toxicol Appl Pharmacol 136:372–380.

Driscoll KE, Lindenschmidt RC, Maurer JK, Higgens JM, and Ridder G. 1990. Pulmonary response to silica or titanium dioxide: Inflammatory cells, alveolar macrophage derived cytokines and histopathology. Am J Respir Cell Mol Biol 2:381–390.

Environmental Protection Agency (US). 1996a. Toxicological studies of particulate matter. In: Air Quality Criteria for Particulate Matter. National Center for Environmental Assessment, Research Triangle Park NC.

Environmental Protection Agency (US). 1996b. Integrative synthesis of key points: Particulate matter exposure, dosimetry, and health risks. In: Air Quality Criteria for Particulate Matter. National Center for Environmental Assessment, Washington DC.

Feng L, Xia Y, Garcia GE, Hwang D, Wilson CB. 1995. Involvement of reactive oxygen intermediates in cyclooxygenase-2 expression by interleukin-1, tumor necrosis factor-α, and lipopolysaccharide. J Clin Invest 95:1669–1675.

Ferin J, Oberdörster G, Penney DP. 1992. Pulmonary retention of ultrafine and fine particles in rats. Am J Respir Cell Mol Biol 6:535–542.

Finlayson-Pitts BJ, Pitts JN Jr (eds). 1986. Atmospheric Chemistry: Fundamental and Experimental Techniques. John Wiley & Sons, New York NY.

Friedlander SK, Yeh EK. 1998. The submicron atmospheric aerosol as a carrier of reactive chemical species; case of peroxides. Appl Occup Environ Hyg 13:416–420.

Fuchs NA, Sutugin AG. 1971. High dispersed aerosols. In: Topics in Current Aerosol Research (Part 2) (Hidy GM, Brock JR, eds). Pergamon Press, New York NY.

Glasius M, Lahaniati M, Calogirou A, Bella DD, Jensen NR, Hjorth J, Kotzias D, Larsen BR. 2000. Carboxylic acids in

secondary aerosols from oxidations of cyclic monoterpenes by ozone. Environ Sci Technol 34:1001–1010.

Goldsmith CA, Imrich A, Danaee H, Ning YY, Kobzik L. 1998. Analysis of air pollution particulate-mediated oxidant stress in alveolar macrophages. J Toxicol Environ Health A 54:529–545.

Goldsmith CA, Kobzik L. 1999. Particulate air pollution and asthma: A review of epidemiological and biological studies. Rev Environ Health 14:121–134.

Gouveia N, Fletcher T. 2000. Time series analysis of air pollution and mortality: Effects by cause, age and socioeconomic status. J Epidemiol Community Health 54:750–755.

Green LC, Wagner DA, Glogowski J, Skipper PL, Wishnok JS, Tannenbaum SR. 1982. Analysis of nitrate, nitrite, and [^{15}N]nitrate in biological fluids. Anal Biochem 126:131–138.

Grosjean D, Williams EL II, Seinfeld JH. 1992. Atmospheric oxidation of selected terpenes and related carbonyls: Gas-phase carbonyl products. Environ Sci Technol 26:1526–1533.

Gunz DW, Hoffman MR. 1990. Atmospheric chemistry of peroxides: A review. Atmos Environ 24A:1601–1633.

Hadwen GE, McCarthy JF, Womble SE, Girman JR, Brightman HS. 1997. Volatile organic compound concentrations in 41 office buildings in the continental United States. In: Proceedings of Healthy Buildings/IAQ '97 (Woods JE, Grimsrud DT, Boschi N, eds). US Environmental Protection Agency, Washington DC.

Hatch GE, Slade R, Harris LP, McDonnell WF, Devlin RB, Koren HS, Costa DL, McKee J. 1994. Ozone dose and effect in humans and rats: A comparison using oxygen-19 labeling and bronchoalveolar lavage. Am J Respir Crit Care Med 150:676–683.

Hewitt CN, Kok GL. 1991. Formation and occurrence of organic hydroperoxides in the troposphere: Laboratory and field observations. J Atmos Chem 12:181–194.

Holz O, Jorres RA, Timm P, Mucke M, Richter K, Koschyk S, Magnussen H. 1999. Ozone-induced airway inflammation changes differ between individuals and are reproducible. Am J Respir Crit Care Med 159:776–784.

Hyslop PA, Hinshaw DB, Halsey WA Jr. 1988. Mechanisms of oxidant-mediated cell injury. J Biol Chem 263:1665–1675.

Immenschuh S, Ramadori G. 2000. Gene regulation of heme oxygenase-1 as a therapeutic target. Biochem Pharmacol 60:1121–1128.

Ischiropoulos H, Gow A, Thorn SR, Kooy NW, Royall JA, Crow JP. 1999. Detection of reactive nitrogen species using 2,7-dichlorodihydrofluorescein and dihydrorhodamine 123. Methods Enzymol 301:367–373.

Ischiropoulos H, Zhu L, Beckman JS. 1992. Peroxynitrite formation from macrophage-derived nitric oxide. Arch Biochem Biophys 298:446–451.

Kaplan J. 1981. Lung macrophages. In: Pathophysiology of the Reticuloendothelial System (Altura B, Saba T, eds). Raven Press, New York NY.

Kim KJ, Suh DJ. 1993. Asymmetric effects of H_2O_2 on alveolar epithelial barrier properties. Am J Physiol 264:L308–L315.

Kirk RE, Othmer DF. 1983. Kirk-Othmer Encylopedia of Chemical Technology, 3rd ed, Vol 22. John Wiley & Sons, New York NY.

Kleeberger SR, Hudak BB. 1992. Acute ozone induced changes in airway permeability: Role of infiltrating leukocytes. J Appl Physiol 72:670–676.

Kleindienst TE, Shepson PB, Hodges DN, Nero CM, Amts RR, Dasgupta PK, Hwang H, Kok GL, Lind JA, Lazrus AL, MacKay GI, Mayne LK, Schiff HI. 1988. Comparison of techniques for measurement of ambient levels of hydrogen peroxide. Environ Sci Technol 22:53–61.

Klemm RJ, Mason RM, Heilig CM, Neas LM, Dockery DW. 2000. Is daily mortality associated specifically with fine particles? Data reconstruction and replication of analyses. J Air Waste Manag Assoc 50:1215–1222.

Kok GL, Holler TP, Lopez MB, Nachtrieb HA, Yuan M. 1978. Chemiluminescent method for determination of hydrogen peroxide in the ambient atmosphere. Environ Sci Technol 12:1072–1076.

Kok GL, Walega JG, Heikes BG, Lind JA, Lazrus AL. 1990. Measurements of hydrogen peroxide and formaldehyde in Glendora, California. Aerosol Sci Technol 12:49–55.

Koppenol WH, Moreno JJ, Pryor WA, Ischiropoulos H, Beckman JS. 1992. Peroxynitrite, a cloaked oxidant formed by nitric oxide and superoxide. Chem Res Toxicol 5:834–842.

Kreyling WG. 1992. Intracellular particle dissolution in alveolar macrophages. Environ Health Perspect 97:121–126.

LaCagnin LB, Browman L, Ma JYC, Miles PR. 1990. Metabolic changes in alveolar type II cells after exposure to hydrogen peroxide. Am J Physiol 259:L57–L65.

Laskin DL, Heck DE, Gardner CR, Feder LS, Laskin JD. 1994. Distinct patterns of nitric oxide production in hepatic macrophages and endothelial cells following acute exposure of rats to endotoxin. J Leukocyte Biol 56:751–758.

Laskin DL, Pendino KJ. 1995. Macrophages and inflammatory mediators in tissue injury. Annu Rev Pharmacol Toxicol 35:655–677.

Lazrus AL, Kok GL, Lind JA, Gitlin SN, Heikes BG, Shetter RE. 1986. Automated fluorometric method for hydrogen peroxide in air. Anal Chem 58:594–597.

Lee JH, Leahy DF, Tang IN, Newman L. 1993. Measurement and speciation of gas phase peroxides in the atmosphere. J Geophys Res 98:2911–2915.

Lee JH, Tang IN. 1990. Nonenzymatic method for determination of hydrogen peroxide in atmospheric samples. Anal Chem 62:2381–2384.

Lee K, Vallarino J, Dumyahn T Ozkaynak H, Spengler JD. 1999. Ozone decay rates in residences. J Air Waste Manag Assoc 49:1238–1244.

Lee M, Heikes BG, O'Sullivan DW. 2000. Hydrogen peroxide and organic hydroperoxide in the troposphere: A review. Atmos Environ 34:3475–3494.

Leikauf GD, McDowell SA, Gammon K, Wesselkamper SC, Bachurski CJ, Puga A, Wiest JS, Leikauf JE, Prows DR. 2000. Functional genomics of particle-induced lung injury. Inhalation Toxicol 12(Suppl 3):59–73.

Li N, Venkatesan MI, Miguel A, Kaplan R, Gujuluva C, Alam J, Nel A. 2000. Induction of heme oxygenase-1 expression in macrophages by diesel exhaust particle chemicals and quinones via the antioxidant-responsive element. J Immunol 165:3393–3401.

Li XY, Brown D, Smith S, MacNee W, Donaldson K. 1999. Short-term inflammatory responses following intratracheal instillation of fine and ultrafine carbon black in rats. Inhalation Toxicol 11:709–731.

Li XY, Gilmour PS, Donaldson K, MacNee W. 1996. Free radical activity and pro-inflammatory effects of particulate air pollution (PM10) in vivo and in vitro. Thorax 51:1216–1222.

Liang C, Pankow JF, Odum JR, Seinfeld JH. 1997. Gas/particle partitioning of semivolatile organic compounds to model inorganic, organic, and ambient smog aerosols. Environ Sci Technol 31:3086–3092.

Lind JA, Kok GL. 1986. Henry's law determination for aqueous solutions of hydrogen peroxide, methylhydroperoxide and peroxyacetic acid. J Geophys Res 91:7889–7895. Correction: J Geophys Res 1994; 99:119.

Loscutoff SM, Cannon WC, Buschbom RL, Busch RH, Killand BW. 1985. Pulmonary function in elastase-treated guinea pigs and rats exposed to ammonium sulfate or ammonium nitrate aerosols. Environ Res 36:170–180.

Mackay GI, Mayne LK, Schiff HI. 1990. Measurements of H_2O_2 and HCHO by tunable diode laser absorption spectroscopy during the 1986 carbonaceous species methods comparison study in Glendora, California. Aerosol Sci Technol 12:56–63.

Mitchell JA, Belvisi MG, Akarasereenont P, Robbins RA, Kwon OJ, Croxtall J, Barnes PJ, Vane JR. 1994. Induction of cyclo-oxygenase-2 by cytokines in human pulmonary epithelial cells: Regulation by dexamethasone. Br J Pharmacol 113:1008–1014.

Moolgavkar SH. 2000. Air pollution and daily mortality in three US counties. Environ Health Perspect 108:777–784.

Moolgavkar SH, Luebeck EG. 1996. A critical review of the evidence on particulate air pollution and mortality. Epidemiology 7:420–428.

Moncada S, Palmer RMJ, Higgs EA. 1991. Nitric oxide: Physiology, pathophysiology, and pharmacology. Pharmacol Rev 43:109–142.

Nadadur SS, Schladweiler MGJ, Kodavanti UP. 2000. A pulmonary rat gene array for screening altered expression profiles in air pollutant-induced lung injury. Inhalation Toxicol 12:1239–1254.

Nathan C. 1992. Nitric oxide as a secretory product of mammalian cells. FASEB J 6:3051–3064.

Nazaroff WW, Gadgil AJ, Weschler CJ. 1993. Critique of the use of deposition velocity in modeling indoor air quality. In: Modeling of Indoor Air Quality and Exposure, ASTM STP 1205 (Niren L, Nagda ED, eds). American Society for Testing and Materials, Philadelphia PA.

Oberdörster G. 1996. Significance of particle parameters in the evaluation of exposure-dose–response relationships of inhaled particles. Inhalation Toxicol 8(Suppl):73–89.

Oberdörster G. 2001. Pulmonary effects of inhaled ultrafine particles. Int Arch Occup Environ Health 74:1–8.

Oberdörster G, Ferin J, Lehnert BE. 1994. Correlation between particle size, in vivo particle persistence, and lung injury. Environ Health Perspect 102(Suppl 5):173–179.

Oberdörster G, Finklestein JN, Johnston C, Gelein R, Cox C, Baggs R, Elder ACP. 2000. Acute Pulmonary Effects of Ultrafine Particles in Rats and Mice. Research Report 96. Health Effects Institute, Cambridge MA.

Oosting RS, van Bree L, van Iwaarden JF, van Golde LM, Verhoef J. 1990. Impairment of phagocytic functions of alveolar macrophages by hydrogen peroxide. Am J Physiol 259:L87–L94.

Pankow JF. 1994. An absorption model of the gas/aerosol partitioning involved in the formation of secondary organic aerosol. Atmos Environ 28:189–193.

Pearson AC, Bhalla DK. 1997. Effects of ozone on macrophage adhesion in vitro and epithelial and inflammatory responses in vivo: The role of cytokines. J Toxicol Environ Health 50:143–157.

Pendino KJ, Laskin JD, Shuler RL, Punjabi CJ, Laskin DL. 1993. Enhanced production of nitric oxide by rat alveolar macrophages after inhalation of a pulmonary irritant is associated with increased expression of nitric oxide synthase. J Immunol 151:7196–7205.

Pendino KJ, Meidhof TM, Heck DE, Laskin JD, Laskin DL. 1995. Inhibition of macrophages with gadolinium chloride abrogates ozone-induced pulmonary injury and inflammatory mediator production. Am J Respir Cell Mol Biol 13:125–132.

Pendino KJ, Shuler RL, Laskin JD, Laskin DL. 1994. Enhanced production of interleukin-1, tumor necrosis factor-α, and fibronectin by rat lung phagocytes following inhalation of a pulmonary irritant. Am J Respir Cell Mol Biol 11:279–286.

Perkins P, Scheule RK, Hamilton R, Gomes G, Friedman G, Holian A. 1993. Human alveolar macrophage cytokine release in response to in vitro and in vivo asbestos exposure. Exp Lung Res 19:55–65.

Pilaro AM, Laskin DL. 1986. Accumulation of activated mononuclear phagocytes in the liver following lipopolysaccharide treatment of rats. J Leukocyte Biol 40:29–41.

Pino MV, Levin JR, Stovall MY, Hyde DM. 1992. Pulmonary inflammation and epithelial injury in response to acute ozone exposure in the rat. Toxicol Appl Pharmacol 112:64–72.

Plopper CG, Buckpitt A, Evans M, Van Winkle L, Fanucchi M, Smiley-Jewell S, Lakritz J, West J, Lawson G, Paige R, Miller L, Hyde D. 2001. Factors modulating the epithelial response to toxicants in tracheobronchial airways. Toxicology 160:173–180.

Pope CA III. 2000. Epidemiology of fine particulate air pollution and human health: Biological mechanisms and who's at risk? Environ Health Perspect 108(Suppl 4):713–723.

Pope CA III, Schwartz J, Ransom MR. Daily mortality and PM10 pollution in Utah Valley. 1992. Arch Environ Health 47:211–217.

Prokhorova S, Lavnikova N, Laskin, DL. 1994. Functional characterization of interstitial macrophages and subpopulations of alveolar macrophages from rat lung. J Leukocyte Biol 55:141–146.

Raabe, OG. 1976. The generation of aerosols of fine particles. In: Fine Particles—Aerosol Generation, Measurement, Sampling and Analysis (Liu BYH, ed). Academic Press, Orlando FL.

Radi R, Beckman JS, Bush KM, Freeman BA. 1992. Peroxynitrite-induced lipid peroxidation: The cytotoxic potential of superoxide and nitric oxide. Arch Biochem Biophys 288:481–487.

Robbins RA, Hadeli K, Nelson D, Sato E, Hoyt JC. 2000. Nitric oxide, peroxynitrite, and lower respiratory tract inflammation. Immunopharmacology 48:217–221.

Rodenas J, Mitjavila MY, Carbonell T. 1995. Simultaneous generation of nitric oxide and superoxide by inflammatory cells in rats. Free Radic Biol Med 18:869–875.

Romieu I, Lugo MC, Colome S, Garcia AM, Avila MH, Geyh A, Velasco SR, Rendon EP. 1998. Evaluation of indoor ozone concentration and predictors of indoor-outdoor ratio in Mexico City. J Air Waste Manag Assoc 48:327–335.

Sakugawa H, Kaplan IR. 1989. H_2O_2 and O_3 in the atmosphere of Los Angeles and its vicinity: Factors controlling their formation and their role as oxidants of SO_2. J Geophys Res 94:12957–12973.

Samet JM, Dominici F, Curriero FC, Coursac I, Zeger SL. 2000a. Fine particulate air pollution and mortality in 20 US cities, 1987–1994. N Engl J Med 343:1742–1749.

Samet JM, Ghio AJ, Costa DL, Madden MC. 2000b. Increased expression of cyclooxygenase 2 mediates oil fly ash-induced lung injury. Exp Lung Res 26:57–69.

Santrock J, Hayes J. 1987. Adaptation of the Unterzaucher procedure for determination of oxygen-18 in organic substances. Anal Chem 591:19–27.

Sauer F, Schafer C, Neeb P, Horie O, Moortgat GK. 1999. Formation of hydrogen peroxide in the ozonolysis of isoprene and simple alkenes under humid conditions. Atmos Environ 33:229–241.

Schiff HI, Hastie DR, Mackay GI, Iguchi T, Ridley BA. 1983. Tunable diode laser systems for measuring trace gases in tropospheric air. Environ Sci Technol 17:352A–364A.

Schraufstatter IU, Cochrane CG. 1991. Types, sources, and mechanisms of injury. In: The Lung: Scientific Foundations (Crystal RG, West JB, eds). Raven Press, New York NY.

Seifert B, Mailahn W, Schulz C, Ullrich D. 1993. Seasonal variation of concentrations of volatile organic compounds in selected German homes. Environ Int 15:397–408.

Seinfeld JH, Pandis SN (eds). 1998. Atmospheric Chemistry and Physics: From Air Pollution to Climate Change. John Wiley & Sons, New York NY.

Shibayama Y, Hashimoto K, Nakata K. 1991. Relation of the reticuloendothelial function to endotoxin hepatotoxicity. Exp Pathol 43:173–179.

Shields HC, Fleischer DM, Weschler CJ. 1996. Comparisons among VOCs measured in three types of US commercial buildings with different occupant density. Indoor Air 6:2–17.

Shukla A, Timblin C, BeruBe K, Gordon T, McKinney W, Driscoll K, Vacek P, Mossman BT. 2000. Inhaled particulate matter causes expression of nuclear factor (NF)-kappaB-related genes and oxidant-dependent NF-kappaB activation in vitro. Am J Respir Cell Mol Biol 23:182–187.

Simonaities R, Olszyna KJ, Meagher JF. 1991. Production of hydrogen peroxide and organic peroxides in the gas phase reactions of ozone with natural alkenes. Geophys Res Lett 18:9–12.

Slemr F, Harris GW, Hastie DR, Mackay GI, Schiff HI. 1986. Measurement of gas phase hydrogen peroxide in air by tunable diode laser absorption spectroscopy. J Geophys Res 91:5371–5378.

Smith LG, Busch RH, Buschbom RL, Cannon WC, Loscutoff SM, Morris JE.1989. Effects of sulfur dioxide or ammonium sulfate exposure, alone or combined, for 4 or 8 months on normal and elastase-impaired rats. Environ Res 49:60–78.

Smith WL, Garavito RM, De Witt DL. 1996. Prostaglandin endoperoxide H synthases (cyclooxygenases)-1 and -2. J Biol Chem 271:33157–33160.

Sredni-Kenigsbuch D, Kambayashi T, Strassmann G. 2000. Neutrophils augment the release of TNF-alpha from LPS-stimulated macrophages via hydrogen peroxide. Immunol Lett 71:97–102.

Tanner RL, Markovits GY, Ferreri EM, Kelly TJ. 1986. Sampling and determination of gas-phase peroxide following removal of ozone by gas-phase reaction with nitric oxide. Anal Chem 58:1857–1865.

Tanner RL, Schorran DE. 1995. Measurements of gaseous peroxides near the Grand Canyon-implication for summertime visibility impairment from aqueous-phase secondary sulfate formation. Atmos Environ 29:1113–1122.

Tobias HJ, Ziemann PJ. 2000. Thermal desorption mass spectrometric analysis of organic aerosol formed from reactions of 1-tetradecene and O_3 in the presence of alcohols and carboxylic acids. Environ Sci Technol 34:2105–2115.

Tran CL, Buchanan D, Cullen RT, Searl A, Jones AD, Donaldson K. 2000. Inhalation of poorly soluble particles: II. Influence of particle surface area on inflammation and clearance. Inhalation Toxicol 12:1113–1126.

Traynor GW, Anthon DW, Hollowell CD. 1982. Technique for determining pollutant emissions from a gas-fired range. Atmos Environ 16:2979–2987.

Wainman T. 1999. Use of a Two Tiered Dynamic Chamber to Investigate Indoor Air Chemistry [dissertation]. Rutgers University, Piscataway NJ.

Wang JH, Redmond HP, Watson RWG, Bouchier-Hayes D. 1995. Role of lipopolysaccharide and tumor necrosis factor-a in induction of hepatocyte necrosis. Am J Physiol 269:G297–G304.

Watkins BA, Parrish DD, Buhr S, Norton RB, Trainer M, Yee JE, Fehsenfeld FC. 1995. Factors influencing the concentration of gas phase hydrogen peroxide during the summer at Kinterbish, Alabama. J Geophys Res 100:22841–22851.

Weschler CJ. 2000. Ozone in indoor environments: Concentration and chemistry. Indoor Air 10:269–288.

Weschler CJ, Hodgson A, Wooley JD. 1992. Indoor chemistry: Ozone, volatile organic compounds, and carpets. Environ Sci Technol 26:2371–2377.

Weschler CJ, Shields HC. 1996. Production of the hydroxyl radical in indoor air. Environ Sci Technol 30:3250–3258.

Weschler CJ, Shields HC. 1999. Indoor ozone/terpene reactions as a source of indoor particles. Atmos Environ 33:2301–2312.

Wesselkamper SC, Chen LC, Kleeberger SR, Gordon T. 2001. Genetic variability in the development of pulmonary tolerance to inhaled pollutants in inbred mice. Am J Physiol 281:L1200–L1209.

Wexler AS, Sarangapani R. 1998. Particles do not increase vapor deposition in human airways. J Aerosol Sci 29:197–204.

Williams CS, Mann M, DuBois RN. 1999. The role of cyclooxygenases in inflammation, cancer, and development. Oncogene 18:7908–7916.

Wilson WE, Suh HH. 1997. Fine and coarse particles: Concentration relationships relevant to epidemiological studies. J Air Waste Manag Assoc 47:1238–1249.

Wizemann TM, Gardner CR, Laskin JD, Quinones S, Durham SK, Goller NL, Ohnishi ST, Laskin DL. 1994. Production of nitric oxide and peroxynitrite in the lung during endotoxemia. J Leukocyte Biol 56:759–68.

Wolkoff P. 1995. Volatile organic compounds: Sources, measurements, emissions, and the impact on indoor air quality. Indoor Air Suppl 3:1–73.

Zhang J, Lioy PJ. 1994. Ozone in residential air: Concentrations, I/O ratios, indoor chemistry, and exposure. Indoor Air 4:95–105.

Zhang X, Turpin BJ, McMurry PH, Hering SV, Stolzenburg MR. 1994. Mie theory evaluation of species contributions to 1990 wintertime visibility reduction in the Grand Canyon. J Air Waste Manag Assoc 44:153–162.

APPENDIX A. PULMONARY DEPOSITION OF PARTICLE-PHASE AND VAPOR-PHASE H_2O_2

INTRODUCTION

These studies were designed to validate the transport of H_2O_2 into the lower lung when associated with $(NH_4)_2SO_4$, using oxygen-18 (^{18}O)-labeled H_2O_2. They were conducted in collaboration with Dr Gary Hatch (EPA, Research Triangle Park NC) and Dr Guobin Sun (formerly at EPA, now at Curriculum in Toxicology, University of North Carolina, Chapel Hill NC).

METHODS

Preparation of ^{18}O-Labeled H_2O_2

The method for preparing ^{18}O-labeled H_2O_2 was modified from Barieux and Schirmann (1987). Briefly, 2-ethylanthraquinone (0.375 g, 1.5 mmol) was added to a solution of toluene/*n*-octanol (1:1, 24 mL) containing 20 mg of palladium black. This mixture was hydrogenated at 40°C for 2.5 hours under 1 atm. Subsequent filtration of the reaction mixture removed palladium black. The solution was oxidized by $^{18}O_2$ (96%) at room temperature for 2 hours under 1 atm. The product, $H_2{}^{18}O_2$, was obtained by extraction with water (4.2 mL) with a yield of 70% (based on the consumption of $^{18}O_2$ added to the reaction).

Sample Collection and Measurement of ^{18}O Incorporation

Exposures for these experiments were conducted as described earlier in this report, except that ^{18}O-labeled H_2O_2 was introduced into the nebulizer (particle-phase experiments) or bubbler (vapor-phase experiments) in place of H_2O_2. After the exposures, the animals were anesthetized and killed by exsanguination. The trachea and lungs were removed en bloc and lavaged. BAL cells and fluid were collected and snap frozen on dry ice. The nasopharynx was dissected and snap frozen. The trachea and lungs were gently inflated with compressed air. While continuing to stream compressed air, the inflated lungs were frozen in sample jars by exposure to liquid nitrogen vapor. The frozen lobes were wrapped in aluminum foil, lyophilized to absolute dryness, and stored at 4°C prior to ^{18}O analyses.

A blood sample collected prior to exsanguination was used to create an internal plasma control for background levels of ^{18}O. The assay for excess ^{18}O was accomplished using a modification of the method of Santrock and Hayes (1987). An elemental analyzer converted oxygen in the dried samples to CO and measured oxygen contents of the samples. Then the CO passed through a column filled with I_2O_5 and was converted to CO_2. Finally, an isotope ratio mass spectrometer measured the fractional abundance of ^{18}O in the resulting CO_2. This procedure was further modified using an online injection system between the elemental analyzer and the mass spectrometer as described by Hatch and associates (1994). The CO_2 mass ratios (46/44 D) were initially expressed as a delta value with respect to a known CO_2 standard. This delta value was corrected for time-dependent drift within a sample run. Statistical analyses were performed on these drift-corrected samples. The delta values were then converted to $^{18}O/^{16}O$ ratios using a standard curve generated with standards

included in each sample run. To determine the excess ^{18}O in the exposed tissue, the mean ^{18}O /^{16}O ratios of plasma samples were subtracted from those for the $H_2{}^{18}O_2$-exposed tissue. The plasma samples were included in each mass spectrometer run with tissues from exposed animals. Data were expressed as microgram ^{18}O per gram dry weight (µg/g). Each experiment used 4 animals per exposure group.

RESULTS AND DISCUSSION

^{18}O content in samples collected from animals exposed to $(NH_4)_2SO_4$ + $H_2{}^{18}O_2$ are summarized in Figure A.1. In our initial set of experiments, we found that excess ^{18}O ranged from undetectable levels in BAL cells to 5.3 µg/g dry weight in BAL fluid obtained 24 hours after the animals were exposed to $(NH_4)_2SO_4$ + 20 ppb $H_2{}^{18}O_2$. These measurements were close to the lower limits of detection for the assay. In subsequent experiments, animals were exposed to higher concentrations of $H_2{}^{18}O_2$ in both the vapor phase (200 ppb $H_2{}^{18}O_2$) and particle phase $(NH_4)_2SO_4$ + 70 ppb $H_2{}^{18}O_2$. The animals were killed immediately (0 hour) after the 2-hour exposure. We found that exposure to vapor-phase 200 ppb $H_2{}^{18}O_2$ resulted in excess ^{18}O in BAL fluid (Figure B.1). The increase, compared to plasma levels, was larger in rats exposed to $(NH_4)_2SO_4$ + 70 ppb $H_2{}^{18}O_2$. In contrast, excess ^{18}O was present in BAL cells from rats exposed to $(NH_4)_2SO_4$ + 70 ppb $H_2{}^{18}O_2$ compared to plasma, but no significant differences were observed in BAL cells from rats exposed to 200 ppb $H_2{}^{18}O_2$ alone. Plasma from rats exposed to 200 ppb $H_2{}^{18}O_2$ was also enriched with ^{18}O over plasma from rats exposed to $(NH_4)_2SO_4$ + 70 ppb $H_2{}^{18}O_2$, demonstrating some variability in the controls. No ^{18}O enrichment was evident in scrapings from the nasal passage, trachea, small airways, or lung parenchyma from these animals or from animals exposed to room air.

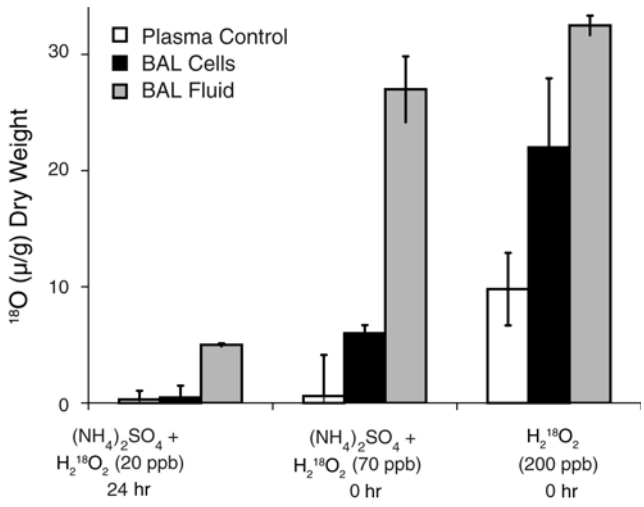

Figure A.1. ^{18}O incorporation measured by mass spectrometry. Cells and fluids were collected immediately or 24 hours after exposure of rats to the indicated test atmosphere. Each value represents the average ± SEM (n = 4 animals per group).

Animals exposed to $(NH_4)_2SO_4$ + $H_2{}^{18}O_2$ exhibited the greatest enrichment of ^{18}O in the BAL fluid and in BAL cells compared to plasma, which is interesting because only 3% of H_2O_2 is thought to be associated with the $(NH_4)_2SO_4$ particles. This finding suggests that $(NH_4)_2SO_4$ particles are involved in the transport of H_2O_2 to the lower lung and may prevent its diffusion into and/or reaction with other chemical or cellular components.

APPENDIX B. ASSESSMENT OF INDOOR H_2O_2 FORMATION

INTRODUCTION

The indoor environment is well known to contain various vapors and particles. These arise from emissions from indoor sources (Shields et al 1996), formation via indoor reactions, and penetration from outdoors. These materials are removed by deposition to surfaces and by ventilation (Nazaroff et al 1993). Vapor-phase reactions of ozone (penetrating from outdoors) with volatile organic compounds (emitted indoors) produce secondary pollutants, some of which can be irritating (Weschler et al 1992). For example, formaldehyde, acetaldehyde, and other aldehydes are formed from the reactions of selected carpet emissions (eg, 4-phenylcyclohexene, 4-vinylcyclohexene, and styrene) with ozone (Weschler et al 1992). Weschler and Shields (1999) have also shown that reactions of ozone with certain alkenes (such as *d*-limonene and α-terpinene) might be a significant source of submicron particles in indoor environments. Because hydroperoxyl radicals are formed through the reaction of ozone with organic compounds, it is likely that H_2O_2 is also formed in the indoor environment through self-reactions of hydroperoxyl radicals and reactions of water vapor with Criegee biradicals. This is important because H_2O_2 carried by submicron aerosols has been identified as a possible contributor to PM-induced toxicity (Friedlander and Yeh 1996).

Hewitt and Kok (1991) showed that H_2O_2 is a product of the ozonolysis of α-pinene, β-pinene, and *d*-limonene in the presence of water vapor. Unsaturated hydrocarbons such as *d*-limonene and α-terpinene are commonly found in indoor odorants and cleaners (Kirk and Othmer 1983; Weschler and Shields 1996); *d*-limonene is commonly detected indoors (Brown et al 1993; Wolkoff 1995; Shields et al 1996; Hadwen et al 1997). Commercial dipentene and

pine oil are sources of *d*-limonene (Weschler and Shields 1996). Indoor *d*-limonene and α-pinene concentrations of 6.2 ± 2.7 and 0.3 ± 3 ppb, respectively, have been measured in 11 administrative offices (Shields et al 1996). Brown and coworkers (1993) and Seifert and colleagues (1993) have reported indoor *d*-limonene concentrations over 80 ppb. Wainman (1999) measured *d*-limonene concentrations as high as 175 ppb after applying spray wax to a coffee table for 15 seconds. The 5-hour integrated indoor ozone residential concentration averaged 60 ± 30 ppb (window open), and the mean indoor to outdoor (I/O) ratio of ozone concentrations ranged from 0.22 ± 0.09 to 0.62 ± 0.11 during the summer for 6 homes in New Jersey (Zhang and Lioy 1994). Lee and associates (1999) measured a residential I/O ratio of 0.68 ± 0.18 (window open) during summer for 20 homes in California. Given that the 1-hour average outdoor ozone concentration can reach 300 ppb (Romieu et al 1998) and using an I/O ratio of 0.68, we estimate that indoor ozone could reach concentrations as high as 200 ppb (worst case) during ozone episodes in some locations (eg, Mexico City).

In addition to the photochemical formation of H_2O_2, the ozonolysis of a variety of naturally occurring alkenes can lead to the formation of H_2O_2 via a route not involving hydroperoxyl radicals. Becker and coworkers (1990, 1993) measured H_2O_2 yields from the reaction of ozone with terpenes in a 130-L glass cylinder reactor (297 K, 760 mm Hg, 2–60 ppmv ozone, 5–35 ppmv alkene, and 0–15 mm water). The molar yield of H_2O_2, defined as the ratio of the H_2O_2 concentration to the concentration of the reacted alkene, was 1.8% for reactions of ozone with *d*-limonene at 11 mm H_2O (~ 50% relative humidity) compared to 0.3% without water vapor. Becker and coworkers (1993) concluded that the direct reaction of water vapor with the Criegee biradical, the main intermediate in reactions of ozone with alkenes, is an important pathway for H_2O_2 formation. Simonaities and colleagues (1991) measured the molar yields of H_2O_2 from reactions of ozone and α-pinene, β-pinene and *d*-limonene of 9%, 19%, and 9%, respectively (58–406 ppb ozone, 40–900 ppb alkene, 6–13 × 10^3 ppm water). Tobias and Ziemann (2000) suggested that organic peroxides also form as a result of alkene–ozone reactions in the presence of alcohols and carboxylic acids and that formation is likely to be a direct result of reaction with Criegee biradicals.

Other organic compounds are also formed in ozone-alkene reactions. For example, limonic acid, limononic acid, limononaldehyde, and limonaketone have all been identified as products of ozone and *d*-limonene reactions (Grosjean et al 1992; Glasius et al 2000). Some of these compounds (eg, limonic acid and limononic acid) are highly polar, have low vapor pressures, and will condense or absorb into preexisting airborne particles (ie, form secondary organic aerosol).

We hypothesized that H_2O_2 is present indoors as a result of the outdoor-to-indoor transport of H_2O_2 into residential environments as well as the formation of H_2O_2 indoors. We speculate that concentrations of H_2O_2 indoors could be as high as 0.3% to 2.0% of the indoor *d*-limonene concentration at low and high relative humidity if sufficient ozone is present. Assuming a 2% yield (Becker et al 1990, 1993), an indoor ozone concentration of 200 ppb (300 ppb outdoors; an I/O ratio of 0.68), and a *d*-limonene concentration of 175 ppb (Wainman 1999), an upper limit of 3.5 ppb of indoor H_2O_2 concentration would be expected to form from the ozone/*d*-limonene reactions. The presence of other reactive organic gases, frequently higher indoors than outdoors, is likely to further increase indoor H_2O_2 concentrations. Indoor H_2O_2 levels will vary with time of day, season, and precursor emission strength. For example, the ozone concentration indoors is higher during summer in the mid afternoon (Weschler 2000) and indoor *d*-limonene is higher during cleaner applications. Thus, we predict that peak indoor H_2O_2 concentrations will be at least comparable and likely greater than peak outdoor concentrations.

We measured the formation of H_2O_2 through reactions of ozone and *d*-limonene at low and moderate relative humidity in a series of experiments performed in a manipulated but realistic indoor environment. This work increases awareness regarding the impact of ozone chemistry on the residential indoor environment and the potential for consumer products to yield secondary products with altered, perhaps adverse, toxicologic properties. This work also contributes to an improved understanding of H_2O_2 exposure.

METHODS

Comparable unoccupied offices (3.1 m × 3.1 m × 3.0 m) were used as experimental (ozone and/or *d*-limonene) and control (room air only) rooms. These rooms were located on the second floor of a three story building in suburban New Jersey. The rooms were carpeted, had acoustic ceiling tiles and standard office furniture, and maintained a rate of 12 to 18 air exchanges per hour when the air handling system was operating. In each room, the door and window were closed during the experiments. Ozone and *d*-limonene were introduced into the experimental room; another room served as a control. An ozone generator (Quantum series 300) was used to emit ozone at a rate of 330 to 2000 µg/min, producing an ozone concentration of 80 to 175 ppb. *d*-Limonene was

introduced by diffusion by placing 20 mL of 100% *d*-limonene in an open 50 mL beaker, which produced *d*-limonene concentrations of 100 to 360 ppb. We used a commercial humidifier to increase the relative humidity in some experiments. A reduced air exchange rate (2–4/hour) was achieved by turning off the air supply to the rooms. Experiments were conducted with deliberate introduction of ozone alone ($n = 1$), *d*-limonene alone ($n = 1$), and ozone with *d*-limonene ($n = 7$) at low (< 10%) and moderate (25–35%) relative humidity and at low (2–4/hour) and high (12–18/hour) air exchange rates.

The air exchange rate was measured by releasing SF_6 (sulfur hexafluoride) into the control room and recording its decay. SF_6 was measured by a photoacoustic infrared detection method (Bruel & Kjaer multi-gas monitor, type 1302). The ozone concentration was monitored using a UV photometric analyzer (Dasibi model 1003-AH) with a wavelength of 254 nm and a concentration range of 0 to 500 ppb. The precision of the ozone analyzer is within 1% or 1 ppb, whichever is greater.

d-Limonene was measured with a passive sampler (OVM 3500, 3M Corp) that collects volatile organic compounds by diffusion to a charcoal sorbent. One passive sampler was placed near the H_2O_2 collection device and the other on the windowsill. An internal standard (*d*-xylene) was added to the sorbent prior to extraction with 1.5 mL of carbon disulfide. The extract was then analyzed using a gas chromatograph/mass spectrometer (ion trap; Varian Saturn II) with a 30 m × 0.25 mm (0.25 µm film thickness) capillary column (DB5, J & W Scientific). The spectrometer was calibrated with four *d*-limonene standards (0.32–4.0 ng/µL). The recovery was over 95%.

Total H_2O_2 was measured by pulling 3 L/min of air through two 125-mL gaswashing bottles in series; each contained 50 mL of deionized water. The second gaswashing bottle was used to check for breakthrough. A dynamic blank (water) and a positive control (standard 2 µM of H_2O_2) were transported, stored, and analyzed with the collected samples. H_2O_2 samples were stored on ice and analyzed by the automated H_2O_2 analyzer.

Particle number concentrations in both rooms were measured by two eight-channel laser particle counters (Particle Measuring Systems, LASAIR model 1002). The relative humidity and temperature were measured continuously using a data logger (HOBO, Onset, Pocasset MA). The logger measures temperatures from −20°C to 70°C with an accuracy of 0.7°C at 21°C and relative humidity with an accuracy of 5%.

RESULTS AND DISCUSSION

Table B.1 summarizes the experimental conditions and results. Particle number concentrations at low air-exchange rates exceeded the measurement limits of the laser particle counter. The coefficient of determination (R^2) for the H_2O_2 calibration curve was typically greater than 99%. The detection limit of H_2O_2 was 0.08 µM (0.2 ppb; for an average sampling time of 183 minutes) expressed as 3 times the standard deviation of the dynamic blank ($n = 6$). H_2O_2 was below detection limits in the dynamic water blank, and the positive control (eg, a 2-µM standard) was 2.07 ± 0.05 µM. No H_2O_2 was lost during transport according to a paired test at the 95% confidence level. The concentration of H_2O_2 in the second bubbler was below detection limits for all experiments.

Table B.2 presents H_2O_2 concentrations and yields (not adjusted for depositional loss) in the experimental room at low and moderate relative humidity and at low and high air exchange. The yield of H_2O_2 is defined as the ratio of H_2O_2 concentration to the concentration of limiting reagent, *d*-limonene or ozone, whichever is smaller. The yield of H_2O_2 ranged from 0.6% to 1.9% for all experimental conditions. Three experiments with ozone and *d*-limonene and one experiment with ozone alone were conducted at elevated air exchange, while four experiments with ozone and *d*-limonene and one experiment with *d*-limonene alone were conducted at reduced air exchange. In all nine experiments, H_2O_2 concentrations in the control room (absent ozone and *d*-limonene) were below detection limits. At an elevated air exchange, when ozone and *d*-limonene were both present, the H_2O_2 concentration ranged from 0.58 to 0.80 ppb; when only ozone was present, the H_2O_2 concentration was below detection limits. At a reduced air exchange, when ozone and *d*-limonene were both present, the H_2O_2 concentration ranged from 1.00 to 1.50 ppb; when only *d*-limonene was present, the H_2O_2 concentration was below detection limits.

Effects of Air Exchange Rate on H_2O_2

The concentration of H_2O_2 was significantly higher at a low air exchange rate ($n = 4$; 2–4/hour) when compared to the elevated air exchange rate ($n = 3$; 12–18/hour) according to a paired test at the 95% confidence level (Table B.1). The reduced air exchange provided additional time for reactions of ozone and *d*-limonene, secondary reactions, and reduced dilution by ventilation, thus increasing H_2O_2 concentrations. At the low air exchange, particle number concentrations increased by as much as 40-fold, and the H_2O_2 concentration increased by 2-fold when compared with concentrations at an elevated air exchange rate. This observation may indicate that secondary PM is a primary

Table B.1. Summary of Experimental Conditions and Results[a]

Sampling Date	Room	Ozone (ppb)	*d*-limonene (ppb)	Temp (°C)	RH (%)	H_2O_2 (ppb)	Total Particle Number (particles/cm^3)	Total Particle Mass (μg/m^3)
High Air Exchange Rate (12–18 per hour)								
12/16/99	A	125	160	23	<10	0.71 ± 0.02	7,640 ± 4040	14.5 ± 7.6
	B		NM	27	<10	ND	1,640 ± 930	3.5 ± 1.8
12/29/99	A	100	0	NM	9	0.2	120 ± 5	0.2 ± 0.01
	B		ND	NM	<10	ND	NM	NM
1/13/2000[b]	A	100	240	22	28	0.80 ± 0.01	21,230 ± 5840	114 ± 33
	B		30	23	NM	ND	3,100 ± 1070	11.9 ± 4.1
1/19/2000	A	100	210	23	5	0.58 ± 0.01	4,460 ± 2370	15.7 ± 8.4
	B		14	26	<10	ND	400 ± 130	1.4 ± 0.5
Low Air Exchange Rate (2–4 per hour)								
1/27/2000	A	80	205	37	6	1.2 ± 0.05	OL	OL
	B		13	32	<10	ND	13,600 ± 6150	171 ± 72
2/4/2000[b]	A	80	359	28	35	1.5 ± 0.06	OL	OL
	B		9	27	NM	ND	10,800 ± 6650	76.3 ± 59.8
2/11/2000	C	0	270	27	20	0	1,040 ± 90	3.7 ± 0.3
	B		ND	28	20	ND	2,420 ± 230	8.5 ± 0.8
2/15/2000	C	175	123	32	11	1.0 ± 0.04	OL	OL
	B		ND	NM	NM	ND	1,570 ± 190	6.6 ± 0.4
2/16/2000[b]	C	125	100	30	30	1.3 ± 0.05	OL	OL
	B		ND	NM	NM	ND	2,020 ± 190	9.6 ± 1.1

[a] Average sampling time = 183 minutes. A = experimental room, B = control room, C = experimental room. ND = not detected; NM = not measured; OL = out of particle counter limits; RH = relative humidity.

[b] Humidifier operated inside the experimental room.

Table B.2. H_2O_2 Concentrations (ppb) in a Manipulated But Realistic Indoor Office[a]

	Low RH (< 10%)	Moderate RH (28%–35%)
Low air exchange rate (2–4/hr)	1.20 ± 0.05 (1.2%)	1.50 ± 0.06 (1.9%)
	1.00 ± 0.04 (0.8%)[b]	1.30 ± 0.05 (1.3%)[b]
High air exchange rate (12–18/hr)	0.71 ± 0.02 (0.57%)	0.80 ± 0.01 (0.8%)
	0.58 ± 0.01 (0.58%)	

[a] 80–175 ppb ozone; 100–359 ppb *d*-limonene; 22–37°C; 5% < RH < 35%; 2–18/hr air exchange rate. Values inside the parentheses are the H_2O_2 yields. The yield is defined as the ratio of the concentration of H_2O_2 to the concentration of *d*-limonene or ozone, whichever is less as a limiting reagent. RH = relative humidity.

[b] Indicates experiments where *d*-limonene concentrations were less than ozone concentrations.

product and that H_2O_2 is formed later in the reaction sequence. Alternatively, this difference might reflect differences in surface removal rates between the two species (PM and H_2O_2).

Effects of Relative Humidity on H_2O_2

We expected that H_2O_2 concentrations would increase with increasing water vapor concentrations if the addition of water vapor to the Criegee biradical is an important pathway for H_2O_2 formation. Figure B.1 suggests that the concentration of H_2O_2 is slightly but not significantly higher at moderate relative humidity (28%–35%) than that at low relative humidity (< 10%) according to a paired test at the 95% confidence level. Additional studies at higher humidity are necessary to more fully characterize the dependence of H_2O_2 formation on the water content of the air.

The yields without considering deposition loss were 0.6% to 1.9%. These findings are consistent with studies of Becker and coworkers (1990), who measured yields in the

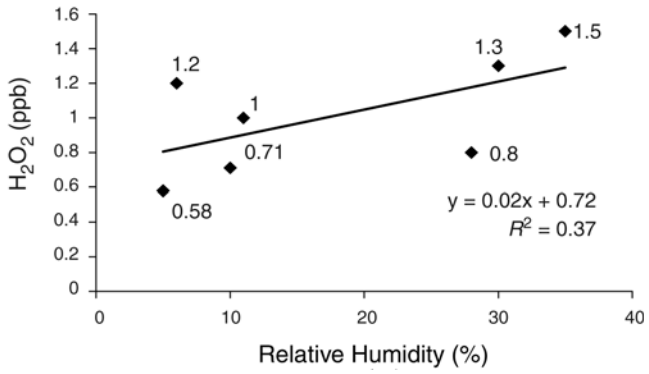

Figure B.1. Concentration of H_2O_2 at varied relative humidity in experimental room. Data labels are H_2O_2 concentration in parts per billion.

range of 0.3% to 1.8% from low to high relative humidity. Becker and coworkers (1990) measured H_2O_2 yields from the reaction of ozone with terpenes in a 130-L glass cylinder reactor (297 K, 760 mm Hg, 2–60 ppmv ozone, 5–35 ppmv alkene, and 0–15 mm H_2O). The yield of H_2O_2 was 1.8% for reactions of ozone with *d*-limonene at approximately 50% relative humidity compared to 0.3% without water vapor.

Particle Observations

Figure B.2 shows the particle number concentrations measured in experimental and control rooms. Prior to ozone and *d*-limonene introduction, particle number concentrations and size distributions were similar in the rooms. Shortly after contact of *d*-limonene with ozone, a particle burst occurred. This burst is evidence of secondary organic aerosol formation (Glasius et al 2000), probably due to addition of secondary organic PM to preexisting particles (< 0.1 µm). These particles grow into a size that can be measured by the laser particle counter. The particle number concentration reached a maximum in the 0.1 to 0.2 µm channel first, followed by a maximum in the 0.2 to 0.3 µm channel about 15 minutes later. Number concentrations were highest in the 0.1 to 0.2 µm diameter range. Total particle number concentrations increased by as much as 40 fold in the experimental room when ozone and *d*-limonene were introduced. Particle number concentrations did not increase significantly when only ozone or only *d*-limonene was introduced to in the experimental room (not shown).

A similar phenomenon in which the particle number concentration reaches a maximum in the 0.1 to 0.2 µm channel first, followed by a maximum in the 0.2 to 0.3 µm channel about 15 minutes later, was observed in the adjacent control room. However, the particle number concentrations were one tenth of the number in the experimental room (Figure A.3). This difference suggests that particles were transported from the experimental room to the control room, primarily across the drop ceiling.

Interestingly, the H_2O_2 measurements in the experimental and neighboring control rooms suggest a negligible transport of H_2O_2 between the rooms. Presumably, this implies a very low inter-room penetration factor for H_2O_2 compared to fine particles, because of greater deposition and reaction during transport from the experimental and control room. These data also suggest that transport of outdoor H_2O_2 into indoor environments is very small.

Figure B.3 shows the number concentrations of 0.1 to 0.2 µm particles in the experimental room at a high air exchange rate and low relative humidity, and at a high air exchange rate and high relative humidity, respectively. At a low air exchange rate, particle number concentrations were beyond the measurement limits of the particle counter.

A typical evolution of particle number and mass concentration is shown in Figure B.4. The initial increase in

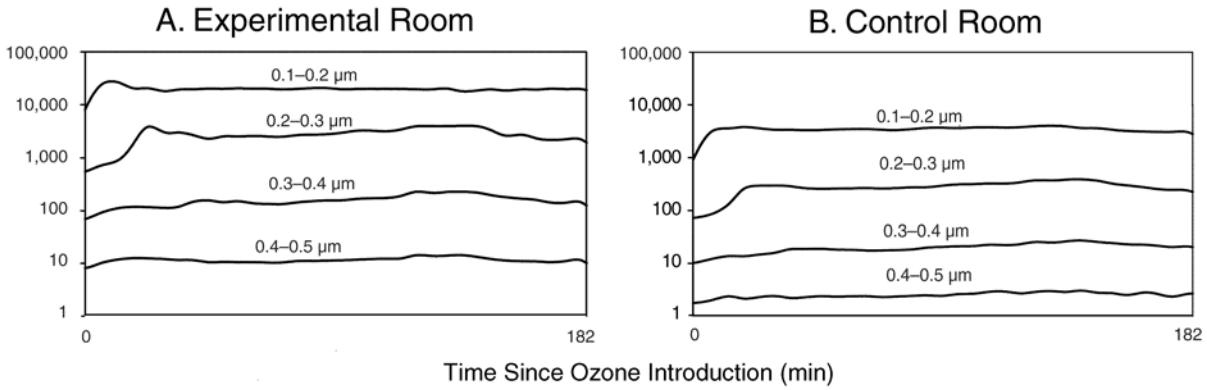

Figure B.2. Particle number concentrations. ***A***. In the experimental room after introduction of ozone and *d*-limonene to the experimental room. ***B***. In the control room after ozone and *d*-limonene introduction into the experimental room. Number concentrations for particles > 0.5 µm in diameter are too small to be seen in these figures.

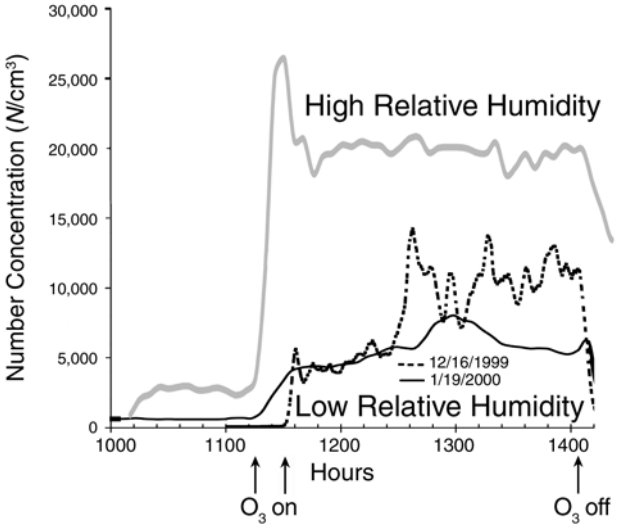

Figure B.3. Number concentrations of 0.1 to 0.2 µm particles. In the presence of ozone (100–125 ppb) and *d*-limonene (160–210 ppb) at low relative humidity (< 10%) and elevated air exchange rate (12–18/hour) on two separate days. In the presence of ozone (100 ppb) and *d*-limonene (215–265 ppb) at high relative humidity (28%) and elevated air exchange rate (12–18/hour).

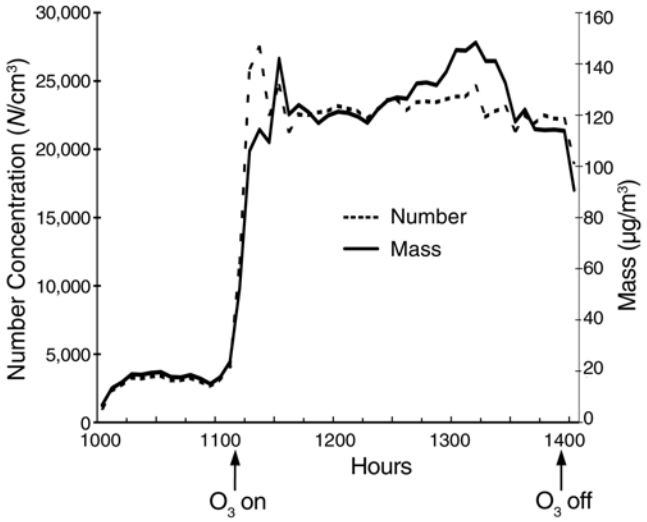

Figure B.4. Particle number and mass concentrations in presence of ozone (100 ppb) and *d*-limonene (215–265 ppb). Particle number and mass concentrations decreased immediately after turning off the ozone generator.

number and mass concentration is probably due to addition of secondary organic PM to preexisting particles (< 0.1 µm) that grow into the measurement range of the laser particle counter. Particle deposition and coagulation explain the decrease in number concentrations from 1115 to 1135 hours. An increase in mass concentration with stable number concentration was observed from 1215 to 1330 hours. This suggests continued particle growth by absorption, adsorption or condensation of low or semivolatile secondary products.

CONCLUSIONS

The analytic methods developed for the animal studies were used to measure H_2O_2 concentrations in a realistic but manipulated indoor environment. This appended study revealed that peak indoor H_2O_2 concentrations can be comparable to outdoor peak concentrations. H_2O_2 will form indoors during photochemical smog episodes or when indoor ozone generators are used and reactive organics (ie, *d*-limonene) are emitted indoors (eg, through the use of cleaners and deodorizers). In addition to H_2O_2 formation, secondary organic aerosol in excess of 10 µg/m^3 to greater than 100 µg/m^3 was generated by reactions of ozone and *d*-limonene. It seems likely that indoor particle concentrations would exceed the $PM_{2.5}$ standard under high indoor ozone concentration with use of *d*-limonene-containing cleaners. Because people spend approximately 80% to 90% of their time indoors, human exposure to H_2O_2 in indoor environments could be substantial. The same reactions that form H_2O_2 also form substantial quantities of secondary organic aerosols. Secondary organic aerosol formed from reactions of *d*-limonene and other alkenes with ozone comprises polar, hygroscopic compounds. Such an aerosol will take up water [like $(NH_4)_2SO_4$] and enable H_2O_2 to partition into the particle phase. Particle-associated H_2O_2 appears to be more readily transported to the lower lung where it can cause the tissue damage identified in the toxicologic assessments.

ABOUT THE AUTHORS

Debra L Laskin is a professor II (distinguished professor) and chair of the Department of Pharmacology and Toxicology at Rutgers University and a member of the Toxicology Division of the Environmental and Occupational Health Sciences Institute at Rutgers University and University of Medicine and Dentistry of New Jersey–Robert Wood Johnson Medical School. She received her PhD in pharmacology and toxicology in 1980 from the Medical College of Virginia (Richmond VA). After postdoctoral training in immunology at the Wistar Institute of the University of Pennsylvania (Philadelphia PA), she became a faculty member at Rutgers University in 1982. Her research interests are in immunotoxicology, specifically in the role of macrophages and inflammatory mediators in chemically induced tissue injury.

Lisa A Morio is currently a postdoctoral researcher at Johnson and Johnson Pharmaceuticals. She received her PhD in toxicology in 1999 from Rutgers University and the University of Medicine and Dentistry of New Jersey. Her research interests focus on cytokine regulation of matrix metalloproteinase expression in tissue injury and repair.

Kimberly A Hooper received her PhD in chemistry in 1997 from Rutgers University and was a postdoctoral fellow in the Department of Pharmacology and Toxicology at Rutgers University from 1997 to 1999. Her research interests focus on understanding the interaction between foreign materials introduced into the body either through implantation or inhalation and the immune system.

Tsung-Hung Li received his PhD in environmental sciences in 2001 from Rutgers University and currently holds the position of scientist at Transave (Monmouth Junction NJ). His research interests are developing aerosol generation and delivery systems for inhalation studies, characterizing chemical and physical properties of aerosols, and studying the partitioning of water-soluble gases on aerosols.

Brian Buckley is currently executive director of laboratories and facilities at the Environmental and Occupational Health Sciences Institute and is a member of the graduate faculty at Rutgers University. He received a PhD in analytic chemistry from North Carolina State University in 1989 and did postdoctoral training at the Oak Ridge National Laboratory. His work has focused on methods development for the analysis of environmental contaminants at their biological interface.

Barbara J Turpin is an associate professor in the Department of Environmental Sciences at Rutgers University and a member of the Exposure Assessment Group at the Environmental and Occupational Health Sciences Institute. She received her PhD in Environmental Science and Engineering in 1990 from the Oregon Graduate Institute at Oregon Health Sciences University. After postdoctoral training at the Particle Technology Laboratory in the Department of Mechanical Engineering at the University of Minnesota, she joined the faculty of Rutgers University in 1994. Her research focuses on understanding the atmospheric transformations of aerosols, which is essential for the development of effective pollution control strategies. Related areas of interest include the development of more rapid and more sensitive instrumentation for sampling and analysis of atmospheric organic aerosols; microscopic mixing characteristics of ambient aerosols, secondary formation of organic aerosols; partitioning of organic compounds between gas and particulate phases; exposure assessment; collaborative aerosol health studies.

OTHER PUBLICATIONS RESULTING FROM THIS RESEARCH

Li TH, Turpin BJ, Shields HC, Weschler CJ. 2002. Indoor hydrogen peroxide derived from ozone/*d*-limonene reactions. Environ Sci Technol 36:3295–3302.

Morio LA, Hooper KA, Brittingham J, Li TH, Gordon RE, Turpin BJ, Laskin DL. 2001. Tissue injury following inhalation of fine particulate matter and hydrogen peroxide is associated with altered production of inflammatory mediators and antioxidants by alveolar macrophages. Toxicol Appl Pharmacol 177:188–199.

Li TH, Hooper KA, Fischer E, Laskin DL, Buckley B, Turpin BJ. 2000. An exposure system to study the effects of water-soluble gases of PM-induced injury. Inhalation Toxicol 12:563–576

ABBREVIATIONS AND OTHER TERMS

ACH	air exchange rate
ANOVA	analysis of variance
atm	standard atmosphere
BAL	bronchoalveolar lavage
$C_6H_5C(CH_3)_2OOH$	cumene hydroperoxide
CO	carbon monoxide
COX	cyclooxygenase (COX-1, COX-2)
DMEM	Dulbecco modified Eagle medium
DS	diffusion scrubber
EDTA	ethylenediaminetetraacetic acid
EPA	Environmental Protection Agency (US)
FBS	fetal bovine serum
$GdCl_3$	gadolinium chloride
H_2O_2	hydrogen peroxide
HBSS	Hank balanced salt solution
HO-1	heme oxygenase-1
HRP	horseradish peroxide
HSP	heat shock protein (HSP60, HSP70)

IFN-γ	interferon-γ
I/O	indoor to outdoor ratio
K	Kelvin
kd	kilodalton
LDH	lactate dehydrogenase
LPS	lipopolysaccharide
NFκB	nuclear factor κB
$(NH_4)_2SO_4$	ammonium sulfate
NOS II	inducible nitric oxide synthase
^{18}O	oxygen-18
PBS	phosphate-buffered saline
PHPA	*p*-hydroxyphenylacetic acid
PM	particulate matter
$PM_{2.5}$	PM < 2.5 μm in aerodynamic diameter
PM_{10}	PM < 10 μm in aerodynamic diameter
ppb	parts per billion
ppbv	ppb by volume
ppm	parts per million
ppmv	ppm by volume
PTFE	polytetrafluoroethylene (Teflon)
R^2	coefficient of determination
SDS	sodium dodecyl sulfate
SF_6	sulfur hexafluoride
TDLAS	tunable diode laser absorption spectroscopy
TNF-α	tumor necrosis factor α
TPA	12-O-tetradecanolyphorbol-13-acetate

Epidemiologic studies have established an association between short-term increases in ambient levels of particulate matter (PM*) and increases in morbidity and mortality, especially in individuals with preexisting cardiovascular or respiratory disease (Dockery and Pope 1994; Goldberg et al 2000; Klemm et al 2000; Samet et al 2000). Despite the consistency of the epidemiologic findings, however, the biological mechanisms underlying these associations are not well understood. One set of research questions has focused on the role of particle attributes (such as size, surface properties, and composition) in causing adverse health effects. In 1996, the Health Effects Institute issued Request for Applications (RFA) 96-1, *Mechanisms of Particle Toxicity: Fate and Bioreactivity of Particle-Associated Compounds*, for studies that would improve our understanding of the characteristics of ambient particles that may be toxicologically relevant. Specifically, HEI was interested in research investigating the biologic role of compounds associated with inhaled particles (that is, their bioavailability and fate) and how they interact with cell components across species. Determining which attributes of PM are most toxic is important in order to focus efforts to control ambient PM concentrations on the most toxic components.

In response to this RFA, Dr Debra Laskin of Rutgers University and colleagues proposed to investigate the role of hydrogen peroxide (H_2O_2) associated with fine $PM_{2.5}$ (less than 2.5 µm in aerodynamic diameter) in causing lung inflammation in rats. They hypothesized that fine PM would transport hydrogen peroxide into the lower lung, where this compound could contribute to lung tissue injury. They proposed to use ammonium sulfate [$(NH_4)_2SO_4$] as a model particle of fine PM because of its prevalence in the eastern United States and its low reported toxicity (Loscutoff et al 1985; US Environmental Protection Agency [EPA] 2001). Rats would be exposed to hydrogen peroxide, ammonium sulfate, or combinations thereof. Health endpoints would include assessment of lung tissue injury, inflammatory markers, and activation of alveolar macrophages, which are involved in the first line of defense against foreign objects that enter the lung. The HEI Research Committee decided to fund this study because they thought that the project would provide valuable insight into particulate transport of gaseous compounds into the lung and would provide important information on the health effects of peroxides.†

This Commentary is intended to aid the sponsors of HEI and the public by highlighting both the strengths and limitations of the study and by placing the Investigators' Report into scientific and regulatory perspective.

SCIENTIFIC BACKGROUND

PM is a complex, heterogeneous mixture of solid and liquid components, also called *aerosols*. Primary particles originating from combustion sources usually consist of a carbonaceous core with chemicals (such as sulfates, metals, and polycyclic aromatic hydrocarbons) adsorbed to their surfaces. In addition, secondary particles form by chemical reactions in the atmosphere of primary particles with gases, (such as nitric oxides, ozone, and sulfur oxides, which are strong oxidants), leading to formation of nitrates and ammonia. The specific composition and size distribution of PM varies by region, time of year, time of day, weather conditions, and other factors. For example, sulfates dominate the $PM_{2.5}$ mixture in the eastern United States (EPA 2001; Zheng et al 2002), whereas nitrates are more abundant in the western United States (EPA 2001).

Hydroperoxides, compounds with the chemical formula ROOH (in which R represents a group of carbon and hydrogen atoms), are oxidants found in the atmosphere. Hydrogen peroxide (formula HOOH) is the simplest hydroperoxide. Its ambient concentrations show seasonal and diurnal variation and also vary in response to weather conditions, such as humidity (Jackson and Hewitt 1999; Largiuni et al 2002; Moortgat et al 2002), and atmospheric levels of nitrogen oxides (Lee et al 2000). Gas phase concentrations of atmospheric hydrogen peroxide have been reported to range from 0.1 to 6.3 ppb by volume (Jackson and Hewitt 1999). Ground level concentrations are typically lower than concentrations at higher altitudes (Heikes et al 1987; Lee et al 2000), with the possible exception of heavy smog conditions (Kok et al 1978). Hydrogen peroxide gas is soluble and can be adsorbed onto the organic or water fraction of PM in a process termed *gas-particle*

* A list of abbreviations and other terms appears at the end of the Investigators' Report.

This document has not been reviewed by public or private party institutions, including those that support the Health Effects Institute; therefore, it may not reflect the views of these parties, and no endorsements by them should be inferred.

† Dr Laskin's 3-year study, *Role of Peroxides and Macrophages in Fine Particulate Matter Toxicity,* began in January 1997. Total expenditures were $448,319. The draft Investigators' Report from Laskin and colleagues was received for review in May 2001. A revised report, received in January 2002, was accepted for publication in February 2002. During the review process, the HEI Health Review Committee and the investigators had the opportunity to exchange comments and to clarify issues in both the Investigators' Report and in the Review Committee's Commentary.

partitioning (Liang et al 1997; Choi and Chan 2002). Hydrogen peroxide is much more readily adsorbed onto PM than other peroxides although the majority of hydrogen peroxide molecules in the atmosphere remain in the gas phase (Friedlander and Yeh 1998; Wexler and Sarangapani 1998).

Increasing evidence suggests that specific components of PM (eg, metals) are associated with adverse health effects (Pope 1996; Ghio and Devlin 2001). Long-term exposure to airborne sulfates, a major component of PM, has been associated with premature mortality (Krewski et al 2000; Pope et al 2002). Additionally, an increase in sulfate levels has been associated with an increase in hospital admissions for respiratory and cardiac disease the following day (Burnett et al 1995). However, sulfate levels often correlate closely with $PM_{2.5}$ levels and acidity, which are also associated with adverse health effects and are more likely causal factors (Lippmann and Thurston 1996). In addition, toxicologic evidence generally has not found adverse effects of ammonium sulfate, even at high exposure concentrations (Schlesinger and Cassee 2003).

Inhalation of high concentrations of hydrogen peroxide, which is widely used in industrial settings, irritates the nose and throat (Hathaway et al 1996). Occupational exposure limits have been set at 1 ppm, or 1.4 mg/m^3, averaged over an 8 hour workday (US Occupational Safety and Health Association 2002), but ambient levels of hydrogen peroxide are in the ppb range, about a hundredfold to a thousand fold less than this standard (Jackson and Hewitt 1999). Hydrogen peroxide also is produced in the body by alveolar macrophages as part of the respiratory burst that occurs during early stages of the inflammatory response (Kinnula et al 1991). Activated macrophages consume increased amounts of oxygen (hence, respiratory burst) and convert it to superoxide (O_2^-). Superoxide is then rapidly converted to hydrogen peroxide by superoxide dismutase (Murphy et al 1995). The hydrogen peroxide produced kills bacteria and other foreign bodies, but accumulated amounts may become toxic to the body's own cells. For example, hydrogen peroxide causes cytotoxicity in human airway epithelial cells and rat alveolar type II epithelial cells (Rice et al 1992; Gabrielson et al 1994) and inhibits alveolar macrophage proliferation (Patton et al 1997). In addition, hydrogen peroxide exposure reportedly increases capillary permeability in isolated perfused rat lungs (Habib and Clements 1995), damages the plasma membrane of pulmonary arterial cells (Block 1991), and increases permeability of the alveolar cell monolayer and alveolar type II cells (Kim and Suh 1993; Gardner et al 1997). Another study showed that hydrogen peroxide inhibited phagocytosis and superoxide anion production by alveolar macrophages while cell viability was unaffected (Oosting et al 1990). In guinea pigs, instillation of 0.1 to 1 M hydrogen peroxide solution caused an increase in vascular permeability (a sign of inflammation) as well as bronchoconstriction (Misawa and Arai 1993).

Based on limited evidence of hydrogen peroxide's ability to associate with particles, some researchers have hypothesized that hydrogen peroxide transported by PM into the lower lung may contribute to the adverse health effects of PM (Friedlander and Yeh 1998). To address this hypothesis, Laskin and colleagues—who had previously explored alveolar macrophage responses to ozone (Pendino et al 1994, 1995; Laskin and Pendino 1995; Laskin and Laskin 2001)—proposed to investigate the effects of inhaled hydrogen peroxide in combination with fine PM on rat lung. They chose ammonium sulfate particles because of their abundance in ambient air and their relatively low toxicity in toxicologic assays.

TECHNICAL EVALUATION

SPECIFIC AIMS

Laskin and colleagues addressed two major specific aims in their study:

- To determine whether inhaled hydrogen peroxide contributes to PM-induced lung tissue injury;
- To determine whether a mixture of ammonium sulfate and hydrogen peroxide activates alveolar macrophages, which then contribute to lung injury.

To accomplish these aims, they built an exposure system and a hydrogen peroxide detector. The investigators also performed several studies using hydrogen peroxide labeled with oxygen-18 (^{18}O), an organic hydro-peroxide (cumene hydroperoxide), and an inhibitor of ozone-induced pulmonary injury (gadolinium chloride). They also monitored formation of hydrogen peroxide in an indoor environment.

The investigators accomplished their objectives, with exception of the gadolinium chloride experiments, which were not completed due to a suspected infection in the rat colony. The experiments evaluating the formation of hydrogen peroxide in an indoor environment were outside the scope of the original research proposal.

APPROACH

The investigators built an exposure system to generate aerosols (ammonium sulfate, or ammonium sulfate with

hydrogen peroxide) and gases (hydrogen peroxide alone or filtered air) (section 1). They also built a detector to provide continuous measurements of hydrogen peroxide during animal exposures (section 2). Groups of female Sprague Dawley rats weighing 150 to 175 g were exposed for 2 hours to ammonium sulfate particles, gas-phase hydrogen peroxide, a combination of ammonium sulfate particles and hydrogen peroxide, or filtered air (section 3). Additional groups remained unexposed. The investigators obtained bronchoalveolar lavage (BAL) fluid and lung tissue immediately and 24 hours after exposure to evaluate markers of inflammation, macrophage activation, and cell stress. Identical experimental conditions were used for ^{18}O-labeled hydrogen peroxide (Appendix A) and cumene hydroperoxide exposures (section 3). To assess indoor hydrogen peroxide formation, the investigators introduced ozone with or without the cleaning agent *d*-limonene into indoor offices (Appendix B). *d*-Limonene is commonly found in indoor environments and contributes to chemical reactions and hydrogen peroxide formation (Hoffmann et al 1997).

METHODS

Aerosol Generation

Solutions of ammonium sulfate, ammonium sulfate + hydrogen peroxide, or cumene hydroperoxide were placed into a nebulizer to create aerosol atmospheres. Cumene hydroperoxide was chosen because it forms particles when aerosolized. The ammonium sulfate particle size was 0.45 ± 0.15 µm in mass median diameter. Particle number, mass concentrations, and relative humidity were adjusted by diluting the solution in the nebulizer; dilution did not alter the particle diameter. The cumene hydroperoxide particle size was also 0.45 ± 0.1 µm. Hydrogen peroxide gas and filtered air were created by bubbling compressed air through hydrogen peroxide liquid or water, respectively. The concentration of hydrogen peroxide gas was linearly related to the concentration of hydrogen peroxide in the solution. Relative humidity was adjusted to 85% for all exposure atmospheres except cumene hydroperoxide, which was kept at 45% relative humidity. The investigators created a solvent control atmosphere for the cumene hydroperoxide experiments by filtering out all cumene hydroperoxide particles after they left the nebulizer.

Exposure Procedures

The investigators designed and tested a six-port, nose-only rat exposure system (Li et al 2000). Exposure conditions were monitored continuously in two empty exposure ports using an online hydrogen peroxide detector. The total flow rate was 3.2 L/min, with individual exposure ports receiving approximately 0.5 L/min. Two to four rats were exposed simultaneously. For some experiments the animals were acclimated to the exposure chamber for 1 hour on 2 days preceding experimental exposures.

Exposure concentrations were 430 µg/m^3 ammonium sulfate; 10, 20 and 100 ppb gas-phase hydrogen peroxide gas; and all combinations of ammonium sulfate and hydrogen peroxide. Exposure concentrations measured in ports containing rats were 30% lower than in empty ports (ie, 290 µg/m^3 ammonium sulfate, and 7, 14 and 72 ppb hydrogen peroxide). Additional experiments used 430 µg/m^3 ammonium sulfate + 20 ppb ^{18}O-hydrogen peroxide, 430 µg/m^3 ammonium sulfate + 70 ppb ^{18}O-hydrogen peroxide, 200 ppb ^{18}O-hydrogen peroxide, and 100 µg/m^3 cumene hydroperoxide.

Markers of Lung Inflammation

The researchers examined a variety of inflammatory markers and indicators of macrophage activation (Commentary Table 1). Some endpoints were evaluated with a limited number of exposure atmospheres or at only one of the timepoints (0, 24, 48 or 72 hours after exposure). The investigators obtained BAL fluid to determine cell counts, cell viability, and content of protein and lactate dehydrogenase (LDH). The presence of white blood cells other than alveolar macrophages (or protein) in BAL fluid is recognized as a general marker of an inflammatory response; LDH is generally considered to be a sensitive marker for cytotoxicity. Macrophages were isolated and cultured for further testing.

Subsequently, lungs were removed, preserved and sectioned for histologic examination by light and electron microscopy. The investigators examined lung tissue for signs of inflammation, such as neutrophil influx and adherence. Additional lung sections were stained with antibodies for the inflammatory cytokine tumor necrosis factor α (TNF-α) and for nitrotyrosine, a marker for production of reactive nitrogen oxide intermediates.

Activation of Alveolar Macrophages

Macrophages were isolated from BAL fluid collected 0, 24, 48 or 72 hours after rats were exposed to experimental atmospheres. Macrophages were cultured in vitro and tested for production of superoxide anion, nitric oxide, peroxynitrite anion ($ONOO^-$), and inducible nitric oxide synthase (known as *iNOS* or *NOS II*). Increased levels of these compounds indicate formation of reactive oxygen and nitrogen intermediates during the respiratory burst that occurs when macrophages are activated. Thus, NOS II mediates nitric oxide production by macrophages; superoxide anion and nitric oxide combine to form peroxynitrite. In turn, peroxynitrite is involved in formation of nitrotyrosine (Ischiropoulos et al 1992).

Commentary Table 1. Measurement of Inflammatory Endpoints and Macrophage Activation

Endpoint	Method	Time (hr)	Exposure Concentration
Inflammation			
Cell number, viability Total protein content LDH content	In BAL In BAL In BAL and serum	0, 24	Ammonium sulfate; 10, 20, or 100 ppb hydrogen peroxide; combinations; filtered air
Gross morphology	Electron microscopy of lung tissue slices	0, 24	Ammonium sulfate; 20 ppb hydrogen peroxide; combination; filtered air
TNF-α and nitrotyrosine	Immunohistochemistry of macrophages in lung tissue slices	24	Ammonium sulfate; 10 or 20 ppb hydrogen peroxide; combinations; filtered air
Macrophage Activation			
Superoxide anion[a] and nitric oxide[b]	In culture medium	0, 24	Ammonium sulfate; 10, 20, or 100 ppb hydrogen peroxide; combinations; filtered air
Peroxynitrite[a,b]	In culture medium	0, 24	Ammonium sulfate + 10 ppb hydrogen peroxide; filtered air
NOS II, HO-1, HSP 60, HSP 70, and COX-2	Protein expression[b] via Western blot	0, 24, 48, 72	Ammonium sulfate + 20 ppb hydrogen peroxide; filtered air

[a] Stimulated with TPA.

[b] Stimulated with LPS and/or IFN-γ.

Macrophages were also tested for production of three heat shock proteins or HSPs (HSP60, HSP70, and heme oxygenase-1 or HO-1, also known as *HSP32*) as well as the protein cyclooxygenase-2 (COX-2). HSPs are general markers of cell stress produced in response to inflammation, tissue injury, or other stressors. Research has shown that exposure to hydrogen peroxide in vitro increases HSP expression (Kerendian et al 1992). Macrophage production of COX-2 is induced by proinflammatory cytokines such as TNF-α and interleukin 1 (Feng et al 1995). HSPs and COX-2 were measured in macrophages collected after exposure to ammonium sulfate + 20 ppb hydrogen peroxide only. Macrophage assays were performed in unstimulated macrophages as well as macrophages stimulated by adding 12-O-tetradecanolyphorbol-13-acetate (TPA), lipopolysaccharide (LPS), and/or interferon-γ (IFN-γ) to the culture medium. Stimulated macrophages produce higher levels of proteins, facilitating detection.

Statistical Analyses of Section 3

The investigators used one-way analyses of variance (ANOVAs) followed by multiple comparisons (section 3). A P value ≤ 0.05 was considered statistically significant. Endpoints were compared in the following ways: unexposed versus filtered air at 0 and 24 hours; filtered air versus other atmospheres at 0 and 24 hours; and each atmosphere at 0 hours versus the same atmosphere at 24 hours. For comparisons of two or more atmospheres, the Dunnett t test was used; for comparison of one atmosphere at two times, independent two-sample t tests were conducted. Data from protein expression measurements using Western blots were not analyzed quantitatively.

Peroxide Deposition

To quantify transport of hydrogen peroxide to the lower lung, the investigators exposed rats to inhaled hydrogen peroxide labeled with ^{18}O alone or in combination with ammonium sulfate (Appendix A). They measured ^{18}O in BAL cells and fluid as well as in scrapings from the nasal passage, trachea, small airways, and lung parenchyma immediately or 24 hours after exposure. Measurements were compared with background ^{18}O levels in plasma. Higher concentrations of hydrogen peroxide (70 ppb and 200 ppb) were used in these experiments than in the main study because ^{18}O levels after 20 ppb hydrogen peroxide were close to the detection limit. Four animals were used per treatment group.

Indoor Hydrogen Peroxide Formation

In furnished, unoccupied indoor offices, the investigators evaluated formation of hydrogen peroxide arising from 80 to 175 ppb ozone reacting with 100 to 360 ppb *d*-limonene (Appendix B). Experiments were performed in one office; another office was used as a control environment. The

investigators introduced ozone and/or *d*-limonene into the office at low (< 10%) or moderate (25%–35%) relative humidity and low (2–4/hour) or high (12–18/hour) air exchange rates. Hydrogen peroxide levels were measured continuously for 2 hours after introduction of the compounds into the room. Air exchange rate, relative humidity, temperature, concentrations of ozone and *d*-limonene, and particle numbers were also monitored continuously.

RESULTS AND INTERPRETATION

Exposure to Ammonium Sulfate and Hydrogen Peroxide

An overview of key results is presented in Commentary Table 2 and summarized here. (All results are compared to filtered air exposure.) A decrease in cell number and an increase in cell viability (but no other changes in inflammatory endpoints) were observed after exposure to ammonium sulfate alone. Exposure to gas-phase hydrogen peroxide alone caused several changes in inflammatory endpoints. In some cases, exposure to combinations of ammonium sulfate and hydrogen peroxide aerosol produced larger effects than exposure to hydrogen peroxide alone.

Commentary Table 2. Signs of Inflammation and Macrophage Activation[a]

Endpoint	Ammonium Sulfate	Hydrogen Peroxide	Ammonium Sulfate + Hydrogen Peroxide
Inflammation			
Neutrophils	⇔	⇧	⇧
TNF-α	⇔	⇧	⇧
Nitrotyrosine	⇧	⇔	⇧
Macrophage Activation			
Superoxide anion	⇔	⇧(24)[b]	⇧(0)[b]
Nitric oxide (stimulated)	⇩	⇩	⇩(24)
Peroxynitrite (stimulated)	NM	NM	⇩
HO-1 and HSP 60	NM	NM	⇩(unstimulated) ⇧(stimulated)

[a] ⇔, no change compared to filtered air; ⇧/⇩, higher / lower than with filtered air; (0)/(24), effect occurred at 0/24 hours after exposure only; NM, not measured.

[b] Effects only seen with 20 ppb hydrogen peroxide, not with 10 or 200 ppb.

Additional results: cell number and viability were higher after exposure to ammonium sulfate alone but were unchanged with the other exposure atmospheres. Serum LDH was higher after exposure to 20 ppb hydrogen peroxide but unchanged with the other exposure atmospheres.

After exposure to 20 ppb hydrogen peroxide, a larger number of neutrophils was identified in capillary spaces adjacent to the terminal respiratory bronchioles as well as in alveolar ducts. In addition, greater adherence of neutrophils to vascular endothelium was observed. These effects were more pronounced after exposure to a combination of ammonium sulfate and 20 ppb hydrogen peroxide. No other hydrogen peroxide concentrations were tested, however.

Staining for the inflammatory cytokine TNF-α was greater in macrophages collected after exposure to 20 ppb hydrogen peroxide. TNF-α staining was even greater in macrophages collected after exposure to a combination of ammonium sulfate and 20 ppb hydrogen peroxide. Exposure to 10 ppb hydrogen peroxide alone or in combination with ammonium sulfate did not lead to increased TNF-α staining. No measurements were made using 100 ppb hydrogen peroxide.

Production of superoxide anion, a reactive oxygen intermediate, was higher in macrophages collected immediately after exposure to combined ammonium sulfate and 20 ppb hydrogen peroxide or 24 hours after exposure to 20 ppb hydrogen peroxide alone. However, exposure to 10 or 100 ppb hydrogen peroxide alone or combined with ammonium sulfate did not cause significantly different superoxide anion production at 0 or 24 hours.

Nitric oxide production from stimulated macrophages collected at 24 hours was lower after exposure to all concentrations of hydrogen peroxide as well as after exposure to 10 or 100 ppb hydrogen peroxide combined with ammonium sulfate. In contrast, more nitric oxide was produced by unstimulated macrophages. Nitrotyrosine staining was also greater in macrophages collected after exposure to ammonium sulfate alone or after exposure to 10 or 20 ppb hydrogen peroxide in combination with ammonium sulfate. Not all exposure concentrations were tested.

Serum LDH was higher after exposure to 20 ppb hydrogen peroxide but unchanged for all other exposure atmospheres. Other endpoints were not significantly different.

Exposure to Cumene Hydroperoxide

An overview of key results is presented in Commentary Table 3. Exposure to cumene hydroperoxide aerosol induced differences in fewer endpoints than did exposure to hydrogen peroxide in combination with ammonium sulfate. More NOS II was produced by macrophages from rats exposed to cumene hydroperoxide than by macrophages from unexposed rats, but a similar NOS II level was produced by macrophages from rats exposed to the solvent control. More HO-1 and nitric oxide were produced by macrophages from rats exposed to the solvent control than by unexposed rats and rats exposed to cumene hydroperoxide.

Commentary Table 3. Key Findings After Cumene Hydroperoxide and Solvent Control Exposures[a]

Endpoint	Solvent Control	Cumene Hydroperoxide
Superoxide anion (stimulated)	⇔	⇔
Nitric oxide	⇧(24)	⇔
NOS II	⇧	⇧
HO-1	⇧	⇔,⇩[b]

a ⇔, no change compared with unexposed animals; ⇧/⇩, increased/decreased compared with unexposed animals; (0)/(24), effect observed at 0/24 hours exposure only.

b Decreased compared with rats exposed to solvent control but no significant difference compared with unexposed rats.

Deposition of ^{18}O-Labeled Hydrogen Peroxide

The investigators did not detect ^{18}O in scrapings from the nasal passage, trachea, small airways, or lung parenchyma after the animals were exposed to 70 ppb ^{18}O-hydrogen peroxide with ammonium sulfate. Exposure to 200 ppb ^{18}O-hydrogen peroxide gas or a combination of ammonium sulfate and 70 ppb ^{18}O-hydrogen peroxide yielded higher ^{18}O levels in BAL fluid and BAL cells. ^{18}O levels in BAL fluid were greater after the combined exposure, compared with hydrogen peroxide alone, indicating that sulfate particles facilitated transport of hydrogen peroxide to the lower lung.

Indoor Hydrogen Peroxide Formation

Between 0.58 and 1.5 ppb hydrogen peroxide was produced after introduction of *d*-limonene and ozone into an indoor office environment. Introduction of either substance alone did not lead to formation of hydrogen peroxide. Air exchange rates and relative humidity also affected the formation of hydrogen peroxide: Particle numbers and hydrogen peroxide concentrations were higher with a low air exchange rate than with a high exchange rate. The hydrogen peroxide concentration tended to be higher with 28% to 35% relative humidity than with 10% relative humidity, but this difference was not significant. Particle bursts (sudden large increases in particle number) were observed after contact of *d*-limonene with ozone. Initially, the largest number of particles was in the 0.1 to 0.2 µm size range. Subsequently, the size distribution showed a peak at the 0.2 to 0.3 µm size range, indicating that the particles rapidly aggregated into larger particles upon formation. Particle numbers did not increase significantly after introduction of either ozone or *d*-limonene into the room.

DISCUSSION

The investigators designed this study to investigate the effects of exposure to hydrogen peroxide alone or in combination with particles on rat lungs. In order to carry out their goal, they successfully built a system to generate and monitor exposure atmospheres of hydrogen peroxide gas, ammonium sulfate as a model of fine PM, hydrogen peroxide in combination with ammonium sulfate particles, and a cumene hydroperoxide aerosol.

INFLAMMATORY EFFECTS OF AMMONIUM SULFATE ALONE

The investigators observed that exposure to ammonium sulfate alone modestly affected BAL cell number and viability and yielded a higher number of macrophages staining positive for nitrotyrosine. This finding is consistent with other animal inhalation studies, which found some effects of exposure to sulfates but usually only after prolonged exposure or at concentrations above ambient levels (Loscutoff et al 1985; Smith et al 1989; Schlesinger et al 1990; Heyder et al 1999; Maier et al 1999). A human study using ammonium sulfate, ammonium bisulfate, and sulfuric acid showed no adverse effects on lung function after controlled exposure for 2 hours per day for several days at concentrations intended to simulate worst case exposures during Los Angeles smog episodes (Avol et al 1979). These studies confirm that ammonium sulfate is unlikely to cause lung injury at the concentrations used in the current study.

INFLAMMATORY EFFECTS OF HYDROGEN PEROXIDE WITH AMMONIUM SULFATE

The study provided evidence of lung injury 24 hours after exposure to hydrogen peroxide or a combination of hydrogen peroxide and ammonium sulfate. Lung injury was most clearly manifested by induction of the inflammatory cytokine TNF-α in lung epithelium and macrophages. In addition, lung capillaries showed increased numbers of neutrophils as well as enhanced endothelial adhesion of these neutrophils. Other changes were observed in macrophage production of superoxide anion (a reactive oxygen intermediate) and in lung staining for nitrotyrosine, a marker for reactive nitrogen intermediates. Many other inflammatory endpoints were not changed, however.

Although these observations suggest lung injury and macrophage activation, interpretation of the results is complicated by several factors. For example, there was no evidence for clear dose-response relations; many effects were observed after exposure to 20 ppb but not 100 ppb hydrogen

peroxide. This lack of a consistent dose-response relation (ie, fewer effects observed at the highest dose) weakens the evidence for an association between hydrogen peroxide exposure and lung injury. The reasons for the lack of a dose-response relation are unclear. The investigators hypothesized that tolerance may have occurred at higher concentrations. In pharmacologic experiments, a diminished effect may be observed when concentrations increase above an apparent optimum, resulting in an inverted U-shape to the dose-response curve. For example, alveolar macrophages exposed to higher doses of hydrogen peroxide (75–100 pmol/10^6 cells) produced less superoxide anion than macrophages exposed to lower doses (10–25 pmol/10^6 cells) (Murphy et al 1995), but whether such a phenomenon explains the patterns observed in the current study remains unclear. The fact that several endpoints were assessed at only one concentration of hydrogen peroxide also complicates generalization of the results.

The ^{18}O in BAL fluid and cells observed after exposure to ^{18}O-hydrogen peroxide gas demonstrated that hydrogen peroxide can reach the lower lung and cause inflammatory changes. This finding was unexpected because hydrogen peroxide has been hypothesized to dissolve in the upper airways and not reach the lower lung (Wexler and Sarangapani 1998). Evidence for deposition was obtained with concentrations of 200 ppb hydrogen peroxide gas and 70 ppb hydrogen peroxide with ammonium sulfate. Some uncertainty remains regarding deposition of lower concentrations (10 and 20 ppb) of hydrogen peroxide in the lower lung because ^{18}O was near the detection limit at those concentrations. In addition, the equilibrium between peroxide gas and peroxide particles may depend on the concentration.

The investigators observed larger amounts of ^{18}O in BAL fluid and cells after exposure to hydrogen peroxide and ammonium sulfate combined than after hydrogen peroxide alone. They also observed larger increases in neutrophil numbers and TNF-α expression after exposure to hydrogen peroxide with ammonium sulfate than after exposure to hydrogen peroxide gas. Both observations support the hypothesis that peroxides are transported into the lung. The results of histology assessments such as neutrophil influx and adherence are not easily quantifiable, however. Therefore it is difficult to assess objectively whether one exposure condition caused a larger change than another.

Interpretation of macrophage activation by hydrogen peroxide is complicated by the fact that the investigators evaluated the effects of hydrogen peroxide in stimulated as well as unstimulated macrophages. Adding stimulating agents, such as TPA, LPS and/or IFN-γ, is often done to increase background levels of inflammatory proteins. In the current study, effects of hydrogen peroxide in unstimulated macrophages were sometimes different from effects observed in stimulated macrophages. For example, the release of superoxide anion was not changed in unstimulated macrophages whereas it was higher in stimulated macrophages obtained from exposed rats. Because TPA, LPS and IFN-γ are much more potent stimulators of macrophages than air pollutants, the effects of hydrogen peroxide and ammonium sulfate in stimulated macrophages may be obscured or difficult to interpret.

INFLAMMATORY EFFECTS OF CUMENE HYDROPEROXIDE

The fact that the investigators found more changes after exposure of animals to the solvent than after cumene peroxide makes these results inconsistent with some in vitro studies that have reported changes after exposure to cumene hydroperoxide. For example, exposure of perfused rat lungs to either cumene hydroperoxide or hydrogen peroxide reportedly decreased lung compliance, conductance, and perfusate flow rate (Olafsdottir et al 1991). In another study, cumene hydroperoxide caused a dose-dependent decrease in the ability of rat alveolar macrophages to phagocytose foreign matter (Hempenius et al 1992). The comparison between cumene hydroperoxide and hydrogen peroxide in the current study remains incomplete because the two endpoints that were most affected by hydrogen peroxide exposure, TNF-α expression and neutrophil influx into the lung, were not assessed with cumene hydroperoxide.

Cumene hydroperoxide was chosen for this study because it forms particles and is commercially available (it is used in phenol production and as a polymerization catalyst: Tice and Brevard 1998). It may not be the most suitable organic peroxide for such comparative experiments, however. Organic peroxides consist of the chemical form ROOR, with *R* representing a group of carbon and hydrogen atoms, the simplest being a methyl group (CH_3). Several organic peroxides have been identified in ambient air, including methyl hydroperoxide (CH_3OOH), hydroxymethyl hydroperoxide ($HOCH_2OOH$), and ethyl hydroperoxide (CH_3CH_2OOH) (Lee et al 2000). Organic peroxides are usually measured in the atmosphere as a group because of their many different forms and difficulty in quantifying them individually (Lee et al 2000; Moortgat et al 2002). Concentrations of organic peroxides are highest in areas with low levels of nitric oxides, but even in these conditions levels are generally much lower than levels of hydrogen peroxide in ambient air (Lee et al 2000). To date, cumene peroxide has not been detected in the ambient atmosphere. Therefore, the results with cumene peroxide may not be generalizable to organic peroxides that are present in the atmosphere.

AMMONIUM SULFATE AS A MODEL FOR $PM_{2.5}$

Because sulfate is a major component of $PM_{2.5}$, especially in the eastern United States (EPA 2001), the choice of the relatively inert ammonium sulfate as a particle seems valid. $PM_{2.5}$ also contains metals, organic compounds and other substances, however. Because organic and mineral compounds are nonhygroscopic, most ambient PM is less hygroscopic than ammonium sulfate. Therefore, ambient PM would be likely to transport less hydrogen peroxide into the lung than the model particle ammonium sulfate in the current study. In addition, it remains unclear whether the hydrogen peroxide used in the study was adsorbed onto the ammonium sulfate particles or whether it remained a separate component within the mixed atmosphere. A study by Jakab and colleagues (1992) showed that carbon black particles were not effective transporters of formaldehyde gas, which is soluble, to the lower respiratory tract. Those results suggest that soluble gases may not necessarily be readily adsorbed onto particles. In a study modeling the human airway, Wexler and Sarangapani (1998) predicted that only compounds with high water solubility and high Henry's law constant (which indicates gas/water partitioning), such as hydrogen peroxide, would be sufficiently adsorbed onto PM to be carried into the respiratory regions of the lung. However, their models showed that these compounds would be diluted by a factor of 20 before reaching the lower lung due to the high humidity in the respiratory tract. Whether dilution due to humidity would have consequences for the final concentration of hydrogen peroxide delivered to the lung epithelium in this study remains to be determined.

STATISTICAL ANALYSES

The statistical design was appropriate for this study. However, the quality of the analysis could have been improved by increasing and balancing the sample size of exposure groups and collecting data for all exposure atmospheres and concentrations. The number of experiments per exposure category ranged from 4 to 21 with 2 to 4 rats per experiment, creating large disparities among the number of data entries for each group. These disparities reduced statistical power and thereby the likelihood of finding significant differences. In addition, some endpoints (such as neutrophil influx and tissue staining for TNF-α and nitrotyrosine) are hard to quantify. Whether one exposure condition produces greater staining than another remains largely subjective, complicating interpretation of the results. Importantly, ANOVAs assume that statistical variation follows a normal distribution with constant variance. The validity of these assumptions is suspect and is not addressed in the report.

SUMMARY AND CONCLUSIONS

Laskin and colleagues found evidence for lung inflammation and activation of alveolar macrophages in rats exposed to hydrogen peroxide gas as well as in rats exposed to hydrogen peroxide in association with ammonium sulfate at concentrations that are one to two orders of magnitude greater than concentrations in ambient air. The most consistent effects were increased neutrophil influx, neutrophil adherence, and TNF-α expression in lung tissue. The presence of ^{18}O in BAL cells and fluid confirmed that hydrogen peroxide alone penetrated the lower lung and, to a greater extent, in combination with ammonium sulfate. These results suggest that ammonium sulfate particles can transport hydrogen peroxide into the lower airways and induce inflammation. Some evidence suggested that the effects of combined exposure were greater than exposure to hydrogen peroxide alone. Caution is needed in interpreting these data, however, due to a lack of dose-response relations for some endpoints (eg, superoxide anion and nitric oxide production by alveolar macrophages) and a lack of quantification of other endpoints (eg, neutrophil influx and HSP expression by alveolar macrophages). In addition, many other inflammatory endpoints did not change after exposure to hydrogen peroxide with or without ammonium sulfate. Whether ammonium sulfate or other particles indeed promote transport of peroxides and other oxidants into the lung at ambient concentrations, thereby increasing the possibility for adverse effects, is still uncertain and remains to be investigated further.

Exposure to cumene peroxide had less of an effect than hydrogen peroxide exposure, but these results may not be generalizable to other organic peroxides. Finally, the investigators demonstrated that low levels of hydrogen peroxide may form in indoor environments under highly polluted conditions. Potential health effects of indoor exposure to peroxides remains subject to further investigation.

ACKNOWLEDGMENTS

The Health Review Committee thanks the ad hoc reviewers for their help in evaluating the scientific merit of the Investigators' Report. The Committee is also grateful to Maria Costantini for her oversight of the study, to Annemoon van Erp and Ellen Wells for their assistance in preparing its Commentary, and to Sally Edwards, Jenny Lamont, Melissa Harke, and Quentin Sullivan for their roles in publishing this Research Report.

REFERENCES

Avol EL, Jones MP, Bailey RM, Chang NM, Kleinman MT, Linn WS, Bell KA, Hackney JD. 1979. Controlled exposures of human volunteers to sulfate aerosols. Health effects and aerosol characterization. Am Rev Respir Dis 120:319–327.

Block ER. 1991. Hydrogen peroxide alters the physical state and function of the plasma membrane of pulmonary artery endothelial cells. J Cell Physiol 146:362–369.

Burnett RT, Dales R, Krewski D, Vincent R, Dann T, Brook JR. 1995. Associations between ambient particulate sulfate and admissions to Ontario hospitals for cardiac and respiratory diseases. Am J Epidemiol 142:15–22.

Choi MY, Chan CK. 2002. The effects of organic species on the hygroscopic behaviors of inorganic aerosols. Environ Sci Technol 36:2422–2428.

Dockery DW, Pope CA III. 1994. Acute respiratory effects of particulate air pollution. Annu Rev Public Health 15:107–132.

Environmental Protection Agency (US). 2001. Latest Findings on National Air Quality: 2000 Status and Trends. EPA 454/K-01-002. Office of Air Quality Planning and Standards, Research Triangle Park NC.

Feng L, Xia Y, Garcia GE, Hwang D, Wilson CB. 1995. Involvement of reactive oxygen intermediates in cyclooxygenase-2 expression induced by interleukin-1, tumor necrosis factor-alpha, and lipopolysaccharide. J Clin Invest 95:1669–1675.

Friedlander SK, Yeh EK. 1998. The submicron atmospheric aerosol as a carrier of reactive chemical species: Case of peroxides. Appl Occup Environ Hyg 13:416–420.

Gabrielson EW, Yu X-Y, Spannhake EW. 1994. Comparison of the toxic effects of hydrogen peroxide and ozone on cultured human bronchial epithelial cells. Environ Health Perspect 102:972–974.

Gardner SY, Brody AR, Mangum JB, Everitt JI. 1997. Chrysotile asbestos and H2O2 increase the permeability of alveolar epithelium. Exp Lung Res 23:1–16.

Ghio AJ, Devlin RB. 2001. Inflammatory lung injury after bronchial instillation of air pollution particles. Am J Respir Crit Care Med 164:704–708.

Goldberg MS, Bailar JC III, Burnett RT, Brook JR, Tamblyn R, Bonvalot Y, Ernst P, Flegel KM, Singh RK, Valois M-F. 2000. Identifying Subgroups of the General Population That May Be Susceptible to Short-Term Increases in Particulate Air Pollution: A Time-Series Study in Montreal, Quebec. Research Report 97. Health Effects Institute, Cambridge MA.

Habib MP, Clements NC. 1995. Effects of low-dose hydrogen peroxide in the isolated perfused rat lung. Exp Lung Res 21:95–112.

Hathaway GJ (ed), Proctor NH, Hughes JP. 1996. Proctor and Hughes's Chemical Hazards of the Workplace, 4th edition. Van Nostrand Reinhold, New York NY.

Heikes BG, Kok GL, Walega JG, Lazrus AL. 1987. H_2O_2, O_3 and SO_2 measurements in the lower troposphere over the eastern United States during fall. J Geophys Res 92:915–931.

Hempenius RA, Rietjans IM, Grooten HN, de Vries J. 1992. Comparative study on the toxicity of methyl linoleate-9, 10-ozonide and cumene hydroperoxide to alveolar macrophages. Toxicology 73:23–34.

Heyder J, Beck-Speier I, Busch B, Dirscherl P, Heilmann P, Ferron GA, Josten M, Karg E, Kreyling WG, Lenz AG, Maier KL, Miaskowski U, Platz S, Reitmeir P, Schulz H, Takenaka S, Ziesenis A. 1999. Health effects of sulfur-related environmental air pollution. I. Executive summary. Inhalation Toxicol 11:343–359.

Hoffmann T, Odum JR, Bowman F, Collins D, Klockow D, Flagan RC, Seinfeld JH. 1997. Formation of organic aerosols from the oxidation of biogenic hydrocarbons. J Atmos Chem 26:189–222.

Ischiropoulos H, Zhu L, Beckman JS. 1992. Peroxynitrite formation from macrophage-derived nitric oxide. Arch Biochem Biophys 298:446–451.

Jackson AV, Hewitt CN. 1999. Atmosphere hydrogen peroxide and organic hydroperoxides: A review. Crit Rev Environ Sci Tech 28:175–228.

Jakab GJ, Risby TH, Hemenway DR. 1992. Use of Physical Chemistry and in Vivo Exposure to Investigate the Toxicity of Formaldehyde Bound to Carbonaceous Particles in the Murine Lung. Research Report 53. Health Effects Institute, Cambridge MA.

Kerendian J, Enomoto H, Wong CG. 1992. Induction of stress proteins in SV-40 transformed human RPE-derived cells by organic oxidants. Curr Eye Res 11:385–396.

Kim KJ, Suh DJ. 1993. Asymmetric effects of H2O2 on alveolar epithelial barrier properties. Am J Physiol 264:L308–L315.

Kinnula VL, Everitt JI, Whorton AR, Crapo JD. 1991. Hydrogen-peroxide production by alveolar type-II cells,

alveolar macrophages, and endothelial-cells. Am J Physiol 261:L84–L91.

Klemm RJ, Mason RM Jr, Heilig CM, Neas LM, Dockery DW. 2000. Is daily mortality associated specifically with fine particles? Data reconstruction and replication of analyses. J Air Waste Manage Assoc 50:1215–1222.

Krewski D, Burnett RT, Goldberg MS, Hoover K, Siemiatycki J, Jerrett M, Abrahamowicz M, White WH. 2000. Reanalysis of the Harvard Six Cities Study and the American Cancer Society Study of Particulate Air Pollution and Mortality. A Special Report of the Institute's Particle Epidemiology Reanalysis Project. Health Effects Institute, Cambridge MA.

Kok GL, Darnall KR, Winer AM, Pitts JN Jr, Gay BW. 1978. Ambient measurements of hydrogen peroxide in the California south coast air basin. Environ Sci Technol 12:1077–1080.

Largiuni O, Giacomelli MC, Piccardi G. 2002. Concentration of peroxides and formaldehyde in air and rain and gas-rain partitioning. J Atmos Chem 41:1–20.

Laskin DL, Pendino KJ. 1995. Macrophages and inflammatory mediators in tissue injury. Annu Rev Pharmacol Toxicol 35:655–677.

Laskin DL, Laskin JD. 2001. Role of macrophages and inflammatory mediators in chemically induced toxicity. Toxicology 160:111–118.

Lee M, Heikes BG, O'Sullivan DW. 2000. Hydrogen peroxide and organic hydroperoxide in the troposphere: A review. Atmos Environ 34:3475–3494.

Li TH, Hooper KA, Fischer E, Laskin DL, Buckley B, Turpin BJ. 2000. An exposure system to study the effects of water-soluble gases on PM-induced toxicity. Inhalation Toxicol 12:563–576.

Liang C, Pankow JF, Odum JR, Seinfeld JH. 1997. Gas/particle partitioning of semivolatile organic compounds to model inorganic, organic and ambient smog aerosols. Environ Sci Technol 31:3086–3092.

Lippmann M, Thurston GD. 1996. Sulfate concentrations as an indicator of ambient particulate matter air pollution for health risk evaluations. J Expo Anal Environ Epidemiol 6:123–146.

Loscutoff SM, Cannon WC, Buschbom RL, Busch RH, Killand BW. 1985. Pulmonary function in elastase-treated guinea pigs and rats exposed to ammonium sulfate or ammonium nitrate aerosols. Environ Res 36:170–180.

Maier KL, Beck-Speier I, Dayal N, Dirscherl P, Griese M, Heilmann P, Hinze H, Josten M, Karg E, Keryling WG, Lenz A-G, Leuschel L, Meyer B, Miaskowski U, Reitmeir P, Ruprecht L, Schumann G, Ziesenis A, Heyder J. 1999. Health effects of sulfur-related environmental air pollution. II. Cellular and molecular parameters of injury. Inhalation Toxicol 11:361–389.

Misawa M, Arai H. 1993. Airway inflammatory effect of hydrogen peroxide in guinea pigs. J Toxicol Environ Health 38:435–448.

Moortgat GK, Grossmann D, Boddenberg A, Dallmann G, Ligon AP, Turner WV, Gäb S, Slemr F, Wieprecht W, Acker K, Kibler M, Schlomski S, Bächmann K. 2002. Hydrogen peroxide, organic peroxides and higher carbonyl compounds determined during the BERLIOZ campaign. J Atmos Chem 42:443–463.

Murphy JK, Hoyal CR, Livingston FR, Forman HJ. 1995. Modulation of the alveolar macrophage respiratory burst by hydroperoxides. Free Radic Biol Med 18:37–45.

Occupational Safety & Health Administration (US). 2002. Occupational Safety and Health Guideline for Hydrogen Peroxide (last updated 4/27/99). *www.osha-slc.gov/SLTC/healthguidelines/hydrogenperoxide/recognition.html*. Accessed 2/7/03.

Olafsdottir K, Ryrfeldt A, Atzori L, Berggren M, Moldeus P. 1991. Hydroperoxide-induced broncho- and vasoconstriction in the isolated rat lung. Exp Lung Res 17:615–627.

Oosting RS, van Bree L, van Iwaarden JF, van Golde LM, Verhoef J. 1990. Impairment of phagocytic functions of alveolar macrophages by hydrogen peroxide. Am J Physiol 259:L87–L94.

Patton GW, Paciga JE, Shelley SA. 1997. NR8383 alveolar macrophage toxic growth arrest by hydrogen peroxide is associated with induction of growth-arrest and DNA damage-inducible genes *GADD45* and *GADD153*. Toxicol Appl Pharmacol 147:126–134.

Pendino KJ, Shuler RL, Laskin JD, Laskin DL. 1994. Enhanced production of interleukin-1, tumor necrosis factor-α, and fibronectin by rat lung phagocytes following inhalation of a pulmonary irritant. Am J Respir Cell Mol Biol 11:279–286.

Pendino KJ, Meidhof TM, Heck DE, Laskin JD, Laskin DL. 1995. Inhibition of macrophages with gadolinium chloride abrogates ozone-induced pulmonary injury and inflammatory mediator production. Am J Respir Cell Mol Biol 13:125–132.

Pope CA III. 1996. Particulate pollution and health: A review of the Utah valley experience. J Expo Anal Environ Epidemiol 6:23–34.

Pope CA III, Burnett RT, Thun MJ, Calle EE, Krewski D, Ito K, Thurston GD. 2002. Lung cancer, cardiopulmonary mortality, and long-term exposure to fine particulate air pollution. JAMA 287:1132–1141.

Rice KL, Duane PG, Archer SL, Gilboe DP, Niewoehner DE. 1992. H_2O_2 injury causes Ca^{2+}-dependent and -independent hydrolysis of phosphatidylcholine in alveolar epithelial cells. Am J Physiol 263:L430–L438.

Samet JM, Zeger SL, Dominici F, Curriero F, Coursac I, Dockery DW, Schwartz J, Zanobetti A. 2000. The National Morbidity, Mortality, and Air Pollution Study, Part II: Morbidity and Mortality from Air Pollution in the United States. Research Report 94. Health Effects Institute, Cambridge MA.

Schlesinger RB, Cassee F. 2003. Atmospheric secondary inorganic particulate matter: the toxicological perspective as a basis for health effects risk assessment. Inhalation Toxicol 15:197–235.

Schlesinger RB, Chen LC, Finkelstein I, Zelikoff JT. 1990. Comparative potency of inhaled acidic sulfates: Speciation and the role of hydrogen ion. Environ Res 52:210–224.

Smith LG, Busch RH, Buschbom RL, Cannon WC, Loscutoff SM, Morris JE. 1989. Effects of sulfur dioxide or ammonium sulfate exposure, alone or combined, for 4 or 8 months on normal and elastase-impaired rats. Environ Res 49:60–78.

Tice R, Brevard B. 1998. Cumene Hydroperoxide [80-15-9]: Review of Toxicological Literature. National Institute of Environmental Health Sciences, Research Triangle Park NC. Available from *ntp-server.niehs.nih.gov/htdocs/Chem_Background/ExSumPdf/CumeneHydroperoxide.pdf.*

Wexler AS, Sarangapani R. 1998. Particles do not increase vapor deposition in human airways. J Aerosol Sci 29:197–204.

Zheng M, Cass GR, Schauer JJ, Edgerton ES. 2002. Source apportionment of $PM_{2.5}$ in the southeastern United States using solvent-extractable organic compounds as tracers. Environ Sci Technol 36:2361–2371.

RELATED HEI PUBLICATIONS: PARTICULATE MATTER

Report Number	Title	Principal Investigator	Date*
Research Reports			
118	Controlled Exposures of Healthy and Asthmatic Volunteers to Concentrated Ambient Particles in Metropolitan Los Angeles	H Gong	2003
112	Health Effects of Acute Exposure to Air Pollution	ST Holgate	2003
	Part I. Healthy and Asthmatic Subjects Exposed to Diesel Exhaust		
	Part II. Healthy Subjects Exposed to Concentrated Ambient Particles		
111	Effect of Concentrated Ambient Particulate Matter on Blood Coagulation Parameters in Rats	C Nadziejko	2002
110	Particle Characteristics Responsible for Effects on Human Lung Epithelial Cells	AE Aust	2002
107	Emissions from Diesel and Gasoline Engines Measured in Highway Tunnels		
	Part I. Real-World Particulate Matter and Gaseous Emissions from Motor Vehicles in a Highway Tunnel	AW Gertler	2002
	Part II. Airborne Carbonyls from Motor Vehicle Emissions in Two Highway Tunnels	D Grosjean	2002
106	Effects of Combined Ozone and Air Pollution Particle Exposure in Mice	L Kobzik	2001
105	Pathogenomic Mechanisms for Particulate Matter Induction of Acute Lung Injury and Inflammation in Mice	GD Leikauf	2001
104	Inhalation Toxicology of Urban Ambient Particulate Matter: Acute Cardiovascular Effects in Rats	R Vincent	2001
101	Epithelial Penetration and Clearance of Particle-Borne Benzo[*a*]pyrene	P Gerde	2001
99	A Case-Crossover Analysis of Fine Particulate Matter Air Pollution and Out-of-Hospital Sudden Cardiac Arrest	H Checkoway	2000
98	Daily Mortality and Fine and Ultrafine Particles in Erfurt, Germany	H-E Wichmann	2000
	Part I. Role of Particle Number and Particle Mass		
97	Identifying Subgroups of the General Population That May Be Susceptible to Short-Term Increases in Particulate Air Pollution: A Time-Series Study in Montreal, Quebec	MS Goldberg	2000
96	Acute Pulmonary Effects of Ultrafine Particles in Rats and Mice	G Oberdörster	2000
95	Association of Particulate Matter Components with Daily Mortality and Morbidity in Urban Populations	M Lippmann	2000
91	Mechanisms of Morbidity and Mortality from Exposure to Ambient Air Particles	JJ Godleski	2000
68	Pulmonary Toxicity of Inhaled Diesel Exhaust and Carbon Black in Chronically Exposed Rats		
	Part I. Neoplastic and Nonneoplastic Lung Lesions	JL Mauderly	1994
	Part II. DNA Damage	K Randerath	1995
	Part III. Examination of Possible Target Genes	SA Belinsky	1995

Continued

** Reports published since 1990, with exceptions.*
Copies of these reports can be obtained from the Health Effects Institute and many are available at www.healtheffects.org.

RELATED HEI PUBLICATIONS: PARTICULATE MATTER

Report Number	Title	Date*
Special Reports		
	Revised Analyses of Time-Series Studies of Air Pollution and Health	2003
	Reanalysis of the Harvard Six Cities Study and the American Cancer Society Study of Particulate Air Pollution and Mortality: A Special Report of the Institute's Particle Epidemiology Reanalysis Project	2000
	Particulate Air Pollution and Daily Mortality: The Phase I Report of the Particle Epidemiology Evaluation Project	
	Phase I.A. Replication and Validation of Selected Studies	1995
	Phase I.B. Analyses of the Effects of Weather and Multiple Air Pollutants	1997
HEI Communications		
9	Evaluation of Human Health Risk from Cerium Added to Diesel Fuel	2001
8	The Health Effects of Fine Particles: Key Questions and the 2003 Review (Report of the Joint Meeting of the EC and HEI)	1999
5	Formation and Characterization of Particles: Report of the 1996 HEI Workshop	1996
HEI Research Program Summaries		
	Research on Diesel Exhaust and Other Particles	2003
	Research on Particulate Matter	1999
HEI Perspectives		
	Understanding the Health Effects of Components of the Particulate Matter Mix: Progress and Next Steps	2002
	Airborne Particles and Health: HEI Epidemiologic Evidence	2001

** Reports published since 1990, with exceptions.*
Copies of these reports can be obtained from the Health Effects Institute and many are available at www.healtheffects.org.

HEALTH
EFFECTS
INSTITUTE

Charlestown Navy Yard
120 Second Avenue
Boston MA 02129-4533 USA
+1-617-886-9330
www.healtheffects.org

RESEARCH
REPORT

Number 117
December 2003